QATAR UNIVERSITY

COLLEGE OF ARTS AND SCIENCES

CARBON BASED CONDUCTIVE FIBERS FOR FUEL CELL APPLICATION

BY

BUKR GHAZI AHMED BUDWAN

A Thesis Submitted to the Faculty of

the Faculty of the College of Arts and

Sciences

in Partial Fulfillment

of the Requirements

for the Degree of

Masters of Science

in

Material Science and Technology

June 2018

COMMITTEE PAGE

The members of the Committee approve the Thesis of Bukr Ghazi Budwan

defended on 20/05/2018.

_____

Dr. Ahmed Elzatahry
Thesis/Dissertation Supervisor

_____

Dr. Aboubakr M. Abdullah
Committee Member

_____

Prof. Yonghui Deng
Committee Member

_____

Dr. Mohammed Hassan
Committee Member

Approved:

_____

Rashid Al-Kuwari, Dean, College of College of Arts and Sciences

ABSTRACT

BUDWAN, BUKR, GHAZI., Masters : January : [2018], Material Science and Technology

Title: Carbon Based Conductive Fibers for Fuel cell Application

Supervisor of Thesis: Dr. Ahmed, Abdelfattah, Elzatahry.

A novel catalyst consists of a group of metals (Ni, Co and Cu) deposited on carbon fiber support and was prepared for oxidation using methanol and ethanol in alkaline medium. The carbon fiber support was fabricated by carbonization of electrospun composite made with an average diameter of 0.2 μm and 0.3 μm respectively and prepared by using electrospinning a mixture of polyacrylonitrile (PAN), polyaniline (PANi) and graphene. Moreover, the composites fibers were characterized with transmission electron microscopy (TEM), scanning electron microscopy (SEM), Energy dispersive X-ray spectroscopy (EDX), X-ray photoelectron spectroscopy (XPS) and X-ray diffraction (XRD). We believe it to be a promising material in the near future.

This work focused on the structure of polymeric fibers, which are produced from polymer materials by using electrospinning, such as polyacrylonitrile (PAN), and then verified the conversion of the electrospun fibers to carbon fibers (CFs). This study is divided into several sections:

Section 1, Summarized introduction and literature review on theory of electrospinning, parameters and factors affecting the process of electrospinning, applications of this technique, the support materials used and the use of electro-oxidation as a primary factor in fuel cell applications.

Section 2, Mainly concerned with the various materials and techniques of the experiments, which were used to study and to reach the target of this thesis.

Section 3, Discussion on the results of this thesis, which is separated into three main parts (A, B, and C).

- Part A, focuses on the preparation of electrospun fibers. It covers the investigation on the effect of various processing parameters and fiber composition preparation and improving a novel approach to fabricate nanocomposite mats.
- Part B, focuses mainly on the characterization of polymer fibers and carbon fibers composites, based on polyacrylonitrile (PAN).
- Part C, this part will focus on electrochemical characterization which was used to show the effectiveness of the prepared catalysts represented in (nickel, cobalt and copper) which are deposited by electrochemical technique with chronoamperometry process on carbon fiber ink (cast over glass carbon electrode).

Section 4, Includes the conclusion derived from this study followed by References.

Section 5, Includes discussion on future work.

LIST OF ABBREVIATIONS

Abbreviations	Meaning
AgNPs	Silver nanoparticles
AN	Acrylonitrile
CEs	Counter electrodes
CFs	Carbon fibers
CFE	Carbon fiber electrode
CFP	Carbon fiber powder
CNFs	Carbon nanofibers
CTAB	Cetyltrimethylammonium bromide
DMF	N,N-dimethylformamide
DMFCs	Direct methanol fuel cells
DMSO	Dimethylsulfoxide
DSC	Differential scanning calorimetry
DSSCs	Dye-sensitized solar cells
EC	Ethyl cellulose
ECSA	Electrochemical active surface area
EDX	Energy dispersive X-ray spectroscopy
ESNFs	Electrospun nanofibers
FCs	Fuel cells
GDLs	Gas diffusion layers

GEC	Glass carbon electrode
GO	Graphene oxide
GPP	Graphene (PAN) (PVDF)
HP	Hot-pressed
HPMCAS	Hydroxypropyl methylcellulose acetate succinate
IA	Itaconic acid
IT	Current time **or** Current transients
KET	Ketoprofen
LIBs	Lithium-ion batteries
LPs	Large pore size
MADO	Poly (dopamine methacrylamide-co-methyl methacrylate)
MEA	Membrane electrode assembly
MOR	Methanol oxidation reaction
MSP	Multiscale porous
NFs	Nanofibers
NPs	Nanoparticles
PAA	Polyamic acid
PAI	Poly(acrylonitrile-co-itaconic acid)
PAN	Polyacrylonitrile
PANi	Polyaniline
PEMFCs	Proton exchange membrane fuel cells

PEO	Polyethylene oxide
PMA	Polymethylacrylate
Poly (AN-co-MMA)	Poly (acrylonitrile-co-methacrylate)
Pt	Platinum
Pt/C	Platinum catalyst
Pt NPs	Platinum nanoparticles
PVA	Polyvinyl alcohol
PVDF	Polyvinylidene fluoride
PVP	Polyvinylpyrrolidone
SDBS	Sodium dodecylbenzenesulfonate
SEM	Scanning electron microscopy
SLE	Soursop leaves extract
TEM	Transmission electron microscopy
XPS	X-ray photoelectron spectroscopy
XRD	X-ray diffraction

ACKNOWLEDGMENT

I am thankful to the Almighty Allah, Most Gracious Most Compassionate; His infinite mercy has guided me to complete this Master degree thesis. May Peace and Blessings of Allah be upon His Prophet Muhammad.

Also I am grateful to Allah Almighty's blessings which allowed me to achieve my father's dream as his wish was for me was to be a Master Degree holder, I will not forget my family's continuous support in overcoming all the obstacles from beginning to end, and my mother's prayers day and night to achieve my goals. Needless to say, my wife's support made a big difference.

I would like to thank my advisor and my supervisor, Dr. Ahmed El-Zatahry for his guidance and encouragement throughout my Master study and support during my research work at the Material Science and Technology Program, Qatar University.

I am extending my gratefulness to Dr. Aboubakr Abdullah, and Dr. Mohammed Hassan for their advice and guidance throughout the experiment design, setup and result analysis.

I would like to also express my sincere appreciation to Qatar University, the College of Arts and Science and all faculty members and colleagues in the Chemistry Department, represented by Prof. Hala Al-Easa and Dr. Khalid Al-Saad. Of course I am also grateful to all of the faculty members in Material Science and Technology Program represented by Dr. Talal Altahtamouni, Dr.

Khaled Youssef and Mr. Mustafa Zagho, as well as my colleagues in the program, I wish them all continuous success.

I would like to thank the Center for Advanced Materials (CAM) in Qatar University, which supported my research thus leading to the completion of this thesis, my sincere thanks to Mr. Mustafa Salim. Furthermore, I would like to thank the Gas Processing Center (GPC) in Qatar University for helping me with numerous measurements and analysis of the samples for my thesis.

Finally and yet just as importantly, I am sincerely thankful to the Central Laboratory Unit (CLU) at Qatar University for their cooperation in providing continuous assistance represented by Dr. Saeed Al-Meer, Mr. Moaz Arar, Mr. Essam and Dr. Mohammed Yousif.

All my thanks and appreciation to everyone who aided and supported me practically and morally, whom I may not have included in my appreciation.

TABLE OF CONTENTS

LIST OF TABLES

LIST OF FIGURES

SECTION 1: INTRODUCTION AND LITERATURE REVIEW

1. Introduction and Literature Review

1.1. Electrospinning Definition

Electrospinning is defined as a highly effective and simple multilateral technique for producing ultrathin fibers (mainly polymers) with diameters ranging from a few microns to tens of nanometers. This technique has attracted tremendous interest recently in both academia and industry due to the easeof lab-scale set-up and its versatility in generating nanofibers from a vast range of materials in various fibrous assemblies [1], [2].

1.2. History of Electrospinning

This technique was discovered during the last century and the primary licenses were issued in the USA to JF Cooley (in 1900) and WJ Morton (in 1902) [3]–[7]. Over the course of ≈10 years (1934-1944), eleven patents were registered in the US- by Formhals- at the beginning of electrospinning development to generate fine filaments of polymer [8]–[18]. There are several examples of Formhals' patents that are worthy of mention here. In the year 1934, Formhals registered patent (No. 1975504). Certain embodiments of the process and apparatus for preparing artificial fibers will be characterized with reference to the below patterns in (Figures. 1, 2 and 3), wherein: Figure 1(1) is a diagram of a front view of apparatus describing the electrical field caused to disperse of the spinning fluid. Figure 1(2) is a side view of comparable apparatus but incarnating a sidetracking tool for the threads. Figures 1(3) and 1(4) are side views of devices

in which the wheel of spinning and filament-receiving tool are organized together with their axes at correct angles and parallel to each other respectively. Figure 1(5) displays an amendment of the devices shown in Figure 1(1) for damp spinning. Figure 2(6) is a diagrammatic view of different adjustments, one appears in Figures 2(7) and 2(8) in a view of foreground and side respectively. Figure 2(9) is a graphical longitudinal part. Figure 2(10) is a cross section of a portion of the device shown in Figure 2(6). However, Figures 3(11) and 3(12) graphically show amendments of the devices [8]. Another innovation in 1937 (No. 2077373) by Formhals for the fabrication of synthetic filaments, and particularly, it is linked to passing of a spinning solution through a nozzle or spinneret structure. For further explanation of the present innovation, refer to (Figure. 4), consisting of three figures. Figure 4(1) shows a syllabic image of a spinneret in accordance with the current innovation. Moreover, Figure 4(2) shows a magnified sectional image of a nozzle orifice plate part. While, Figure 4(3) shows a magnified sectional image of part of an adjusted shape of a nozzle orifice plate [9]. Geoffrey Taylor, in 1964, wrote an article which clarified the distortion of water droplets in the presence of an electrical field [19], and published another research paper in 1969 centering on the formation and ejection of smooth fibers from viscous solution. Annis et al. investigated in the late 1970s the electrospun polyurethane for potential vascular prostheses [20]. Overall, electrospinning technique was not considered to have many beneficial applications and languished for several years until the early 1990s, when the need arose significantly to fabricate fibers on a nanometer scales. For this purpose, Reneker,

Yarin, and other scientists closely studied the fibers that were fabricated by this process and examined the physical parameters of their formation [21]–[29].

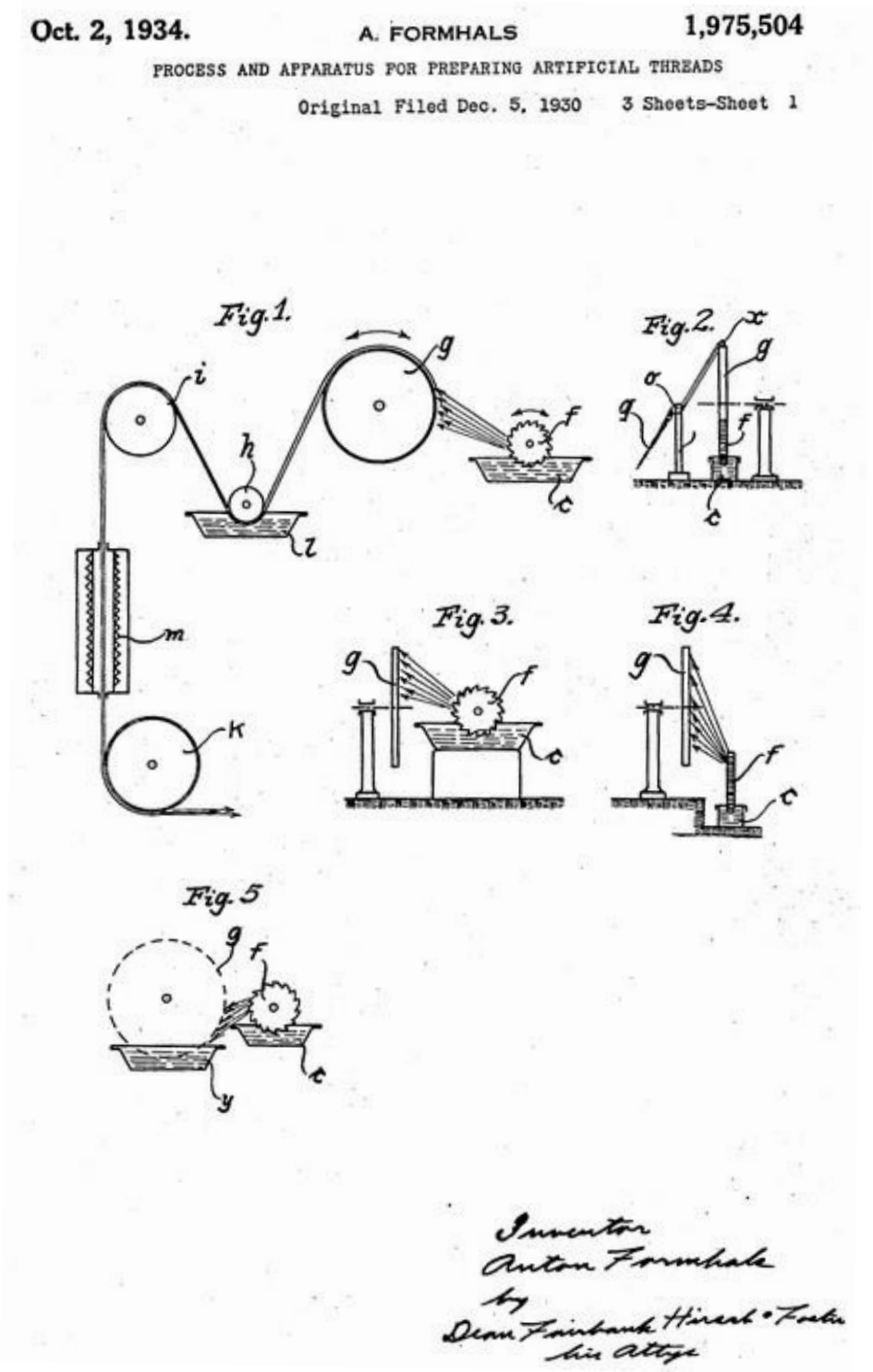

Figure 1. “Operation and devices for fabricating artificial fibers” [8]**.**

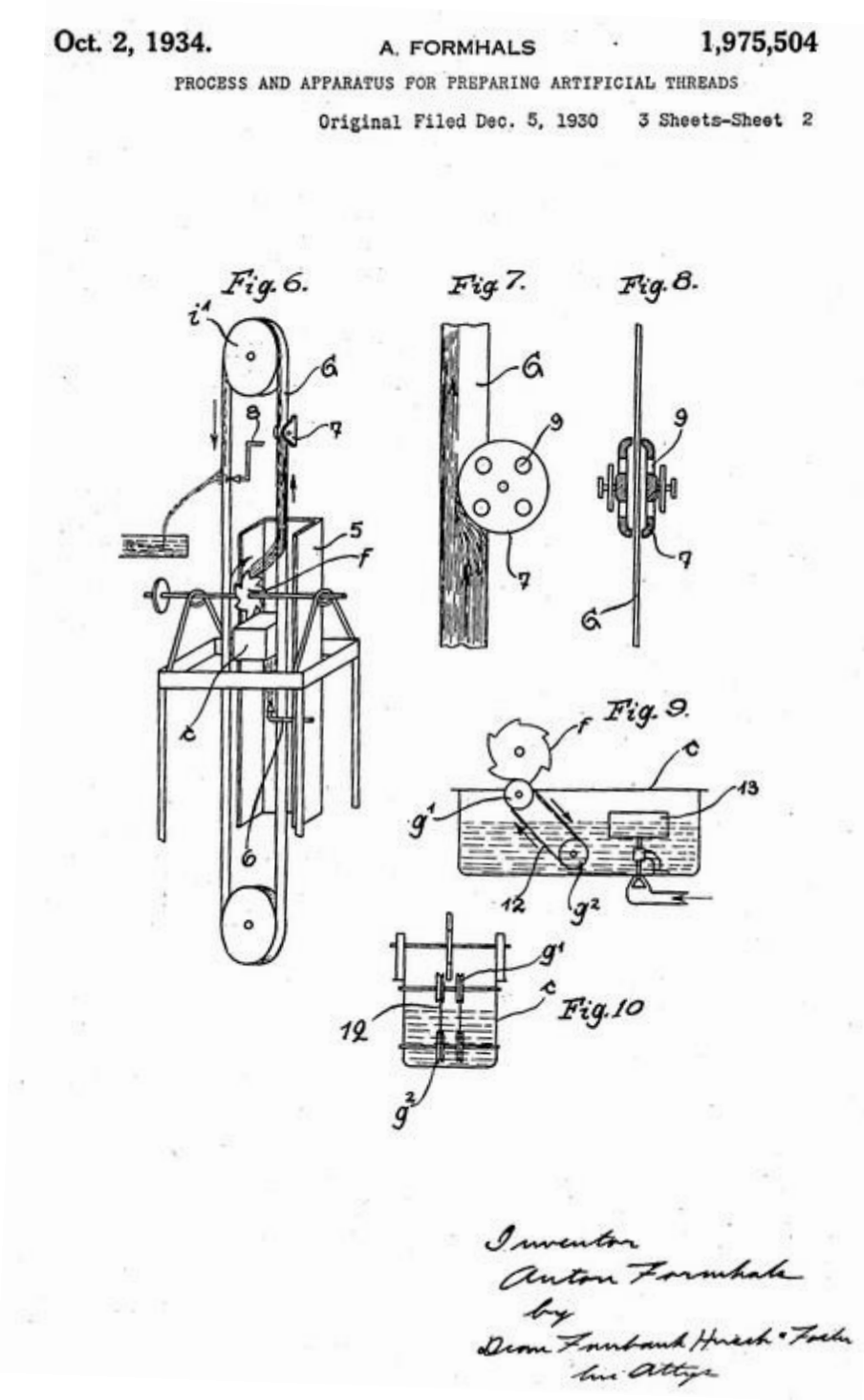

Figure 2. “Operation and devices for fabricating artificial fibers” [8].

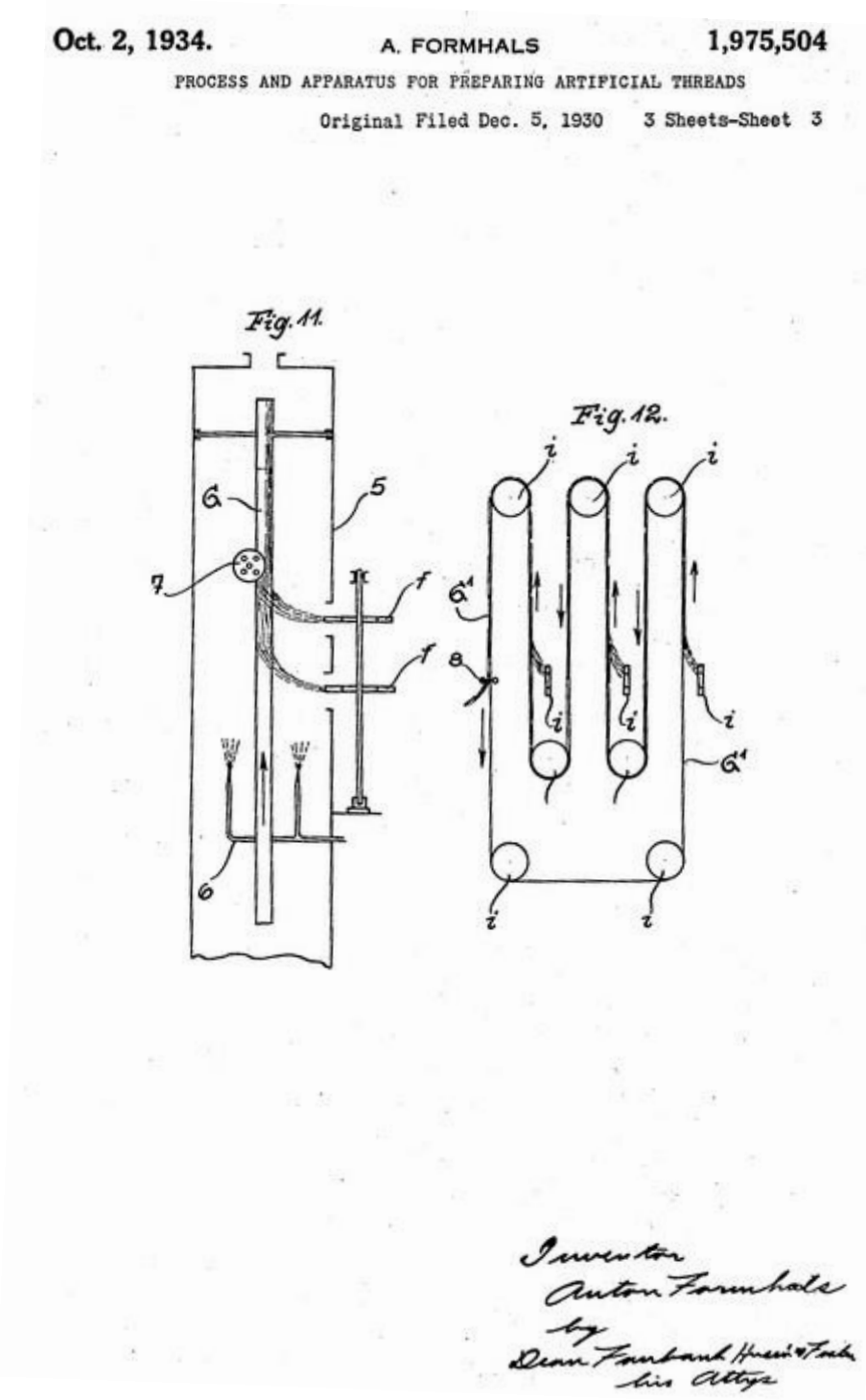

Figure 3. “Operation and devices for fabricating artificial fibers” [8].

April 13, 1937. A. FORMHALS 2,077,373

PRODUCTION OF ARTIFICIAL FIBERS

Filed Aug. 15, 1936

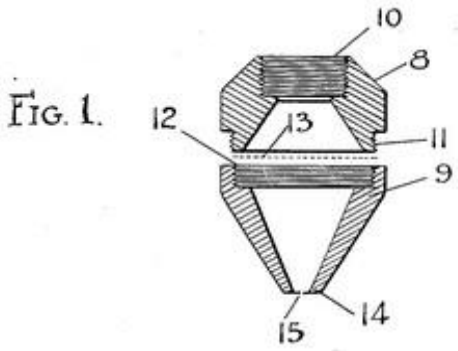

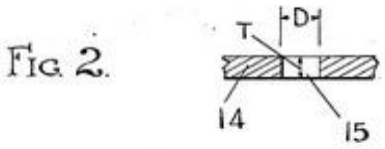

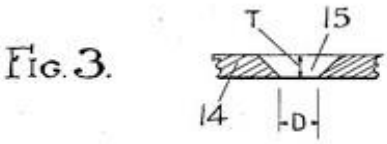

INVENTOR.
Anton Formhals
BY Louis Allis
ATTORNEYS.

Figure 4. “Production of artificial fibers” [9].

1.3. Electrospinning Process

The setup of electrospinning consists of three main ingredients, a power supply with a high voltage, spinneret (e.g. pipette tip or nozzle) and collector (rotating plate). Initially before applying electrospinning the polymer must be dissolved and then inserted into a capillary tube at room temperature. By applying a high voltage the polymer liquid is charged, then accelerated towards the collector, with an opposite polarity [30]–[33]. At critical voltage, the surface tension of the utilized polymer solution is eliminated by the electrostatic force, the charged jet ejected and produces the Tylor cone from the tip then the solvent will be vaporized and polymer fiber or nanofiber will be produced [34]–[36]. Generally, there are two famous and standard types of electrospinning setups; vertical and horizontal. (Figure. 5) shows the vertical setup [37], [38].

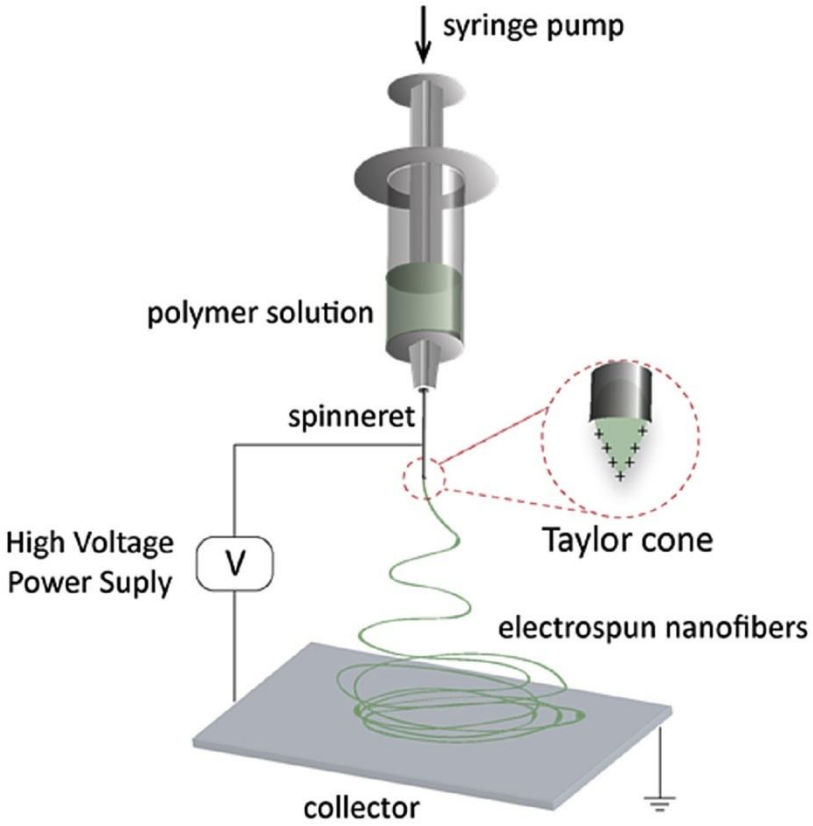

Figure 5. “A diagram setup for ideal electrospinning apparatus.”

1.4. Electrospinning Parameters

Three categories summarize the parameters of the electrospinning technique to control the process; solution preparation parameters, process controlled variables and ambient parameters [39]. These categories are shown in (Figure. 6).

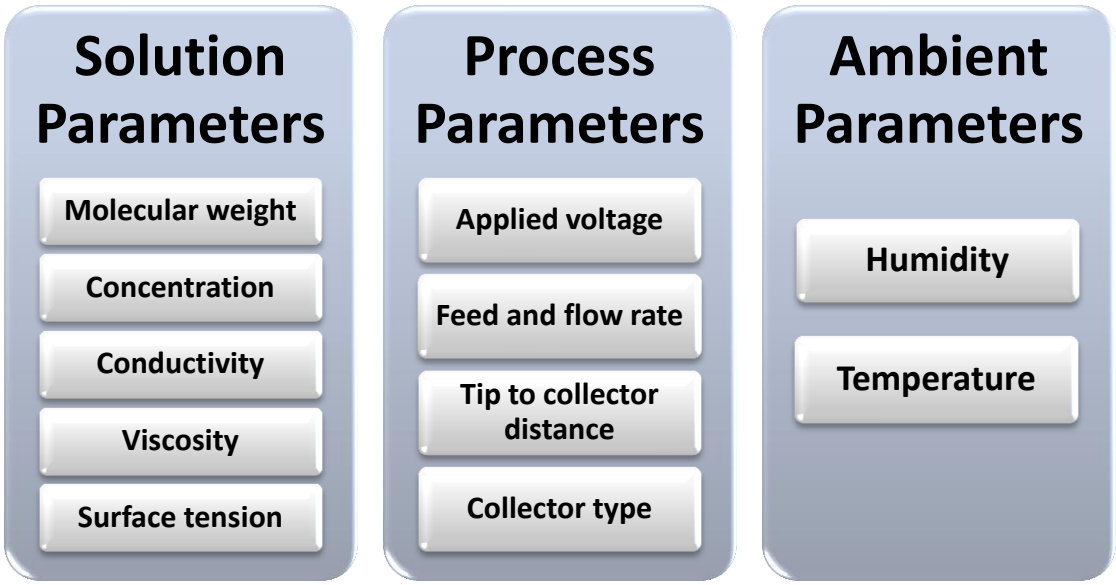

Figure 6. "Categories affecting on electrospinning technique."

1.5. Application of Electrospinning

Lately, scientists have begun to look at various applications, for electrospinning mats and fibers. As these provide various features such as high porosity, high surface area to volume ratio and improve the physio-mechanical properties through manipulation of the polymer solution and the process parameters and easily obtaining the required fibers with specific mechanical strength [39], [40]. Hence, this technique began to spread with its wide variety of applications in many different fields, perhaps the most prominent applications are in sectors such as filtration (membranes), sensors, protective clothing, drug delivery and wound healing. (Figure. 7) illustrates the different sectors of electrospinning

applications.

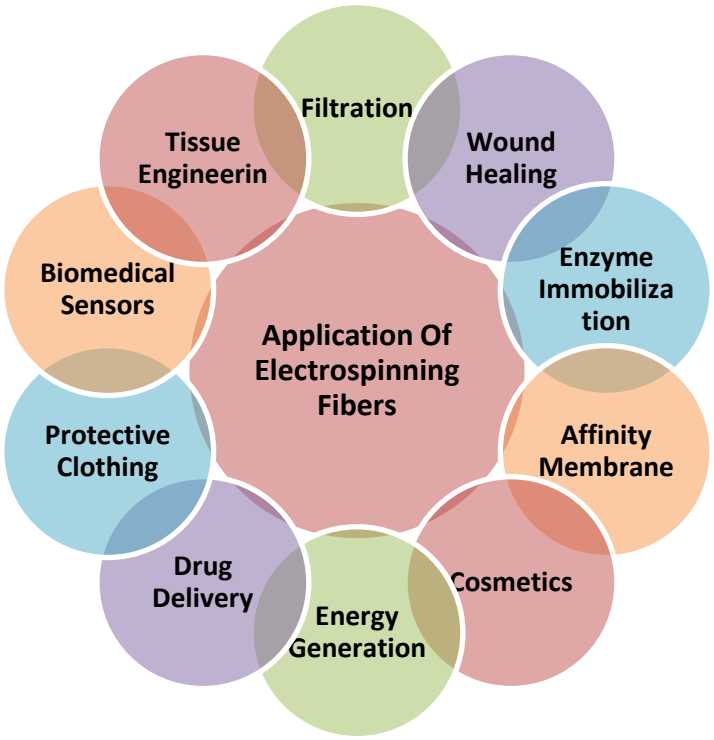

Figure 7. "Electrospinning applications in different sectors."

1.5.1. Biomedical Application

Biomedical applications of electrospinning are important through as some research highlights. The reason is their unique features, such as high surface-area-to-volume ratio, morphology and porosity. It also demonstrates a high ability to stimulate cell growth and protein absorption [41]. In addition, after studying the biomedical fibers widely, it is considered to be promising for its unique properties

in the field of environmental protection and purified materials [42]. It also demonstrated a vast range of applications in both biomedical engineering and environmental fields [43], [44].

1.5.1.1. Tissue Engineering

A domain process has been reported in the article for the fabrication of scaffolds for tissue engineering. Nevertheless, nanofiber methods have been based on the fabrication of tissue engineering scaffolds in the past decade [45]. For tissue renovation, biodegradable and biocompatible fibrous scaffolds are mostly distinguished over traditional scaffolds, due to their distinctive nature and ability to supply the targeted cells/tissues with a native medium through mimicking the extracellular matrix. Consequently, with each passing day it is logical that the electrospun nanofibers technique is being increasingly used in tissue engineering. Fiber scaffolds have shown an affect not only on cell interaction in the cell but also on increased cell interaction with the matrix [46]. Nevertheless, there are a few restrictions on the use of electrospinning nanofiber scaffolds in tissue engineering. One of the obstacles is due to the smaller intra-fiber pore size is the permeation of the cells inside the scaffolds. To overcome this obstacle, a lot of effort has gone into synthesizing fabricated scaffolds with greater intra-fiber pore size to allow the scaffolds to provide a 3D environment rather than a 2D environment. 3D scaffolds have revealed greater pore size and internal surface area compared with traditional 2D electrospinning scaffold thus showing an enhanced cell permeation. Therefore, the biocompatibility is excellent, spatial geometries and physical properties of 3D electrospinning

scaffolds are significant in tissue engineering such as vascular grafts, bone and nerve regeneration [47]. Consequently, scientists are trying to research several options in the manufacture 3D scaffolds. A single process would be blending multiple polymers and could result in the fabrication of nanofibers scaffolds to fabricate 3D scaffolds. As a result of the various expansions and soluble properties of the polymers in the space between the spinneret and collector, fibers will be formed with different diameters, which will affect a planned intra-fiber pore size. The planned large intra-fiber pore size will affect the permeation of cells into the electrospun mixed nanofibers scaffold. Beside the porosity, an encouraging construct could be prepared to use the moisturization of the polymer mixture, which would enhance cells adhesion and infiltration [48].

1.5.1.2. Drug Delivery

Drug delivery is applied in the medical field through the most appropriate physiological way. Equipping a drug with a minimal size and appropriate coating material promotes its ability to be absorbed or digested by the proposed location. Targeted drug delivery using electrospun nanofibers leads to increasing the surface area of the transporter and increasing the drug solubility rate. Numerous published papers highlight the feasibility of using electrospun nanofibers as a carrier of drug delivery [49].

For instance, Tipduangta et al. [50] studied a detailed investigation of the phase separation in polyvinylpyrrolidone (PVPK90) and hydroxypropyl methylcellulose acetate succinate (HPMCAS) nanofibers and the influence of phase separation on drug release. The study found that the electrospinning fibers were formed in

nanoscale phase separation in dissimilarity to the micron-scale phase separation by traditional blending methods including spin coating and film casting. This approach leads to variable rates of solvent evaporation. In addition, the potential idea of utilizing in situ-phase separation of the polymers was demonstrated to tune the rate of drug release, which can potentially be adopted for transferring two drugs in one formula that has various desirable targeted areas in the gut. More interestingly, the behavior of the phase separation of polymer fiber blends brings new insights for drug delivery, which can be used as active controlled drug carriers. On the other hand, there are considerable efforts devoted in the technology of drug delivery to fabricate electrospun nanofibers to avoid undesirable highly oral doses repeatedly during frequent times to bypass the risk of side effects and also to reduce effort of patient healing [51]–[53]. Wherefore, Deng-Guang et al. [54] synthesized a novel triaxial electrospun nanofiber for biomedical applications by adding different functional ingredients to ethyl cellulose (EC) polymer solution for new class of medication nanofibers with active components. They realized that the fabricated 3D electrospun nanofibers were highly smooth and continuously performed in inner, middle, and outer layers with constant concentration of EC with different concentrations of ketoprofen (KET). Moreover, the polymer fluids structurally resulted in smooth surface, linear morphology, and clear three-layer structures. The KET content was used to gradually increase the mobility from fibers exterior to inward, leading to enhancing the gradient distribution of drugs. Furthermore, Li et al. [55] designed new hydrophobic and hydrophilic drug carriers. They prepared

electrospun polyethylene oxide (PEO) nanofibers membrane with vesicles to be loaded with selected model drugs such as 5-fluoro-2.4(1H.3H) pyrimidinedione (5-Fu), hydrophilic/hydrophobic drugs, and paeonolum. This novel process enables us to easily and conveniently control the different drug amount in the vesicles. As a result, the new system of drug delivery was developed and loaded into the electrospun PEO nanofibers membranes by dissolving the model drugs in a mixture of cetyltrimethylammonium bromide (CTAB) and sodium dodecylbenzenesulfonate (SDBS) vesicle solution. In addition, the behavior of the new dual drug delivery layout can be monitored and controlled by changing the CTAB/SDBS molar ratio. Besides, this system has superior applications in medication, pharmaceuticals, material and food.

1.5.1.3. Wound Dressing

Healing of wound is a dynamic operation that follows a complex series of events, including hemostasis, proliferation, inflammation, and remodeling. This series was controlled through signaling molecules, various factors, and cells [56]. Accordingly, electrospinning was used to fabricate wound dressings because of the numerous characteristics that will provide agent preparation rather than utilizing conventional methods. Thus, the potential of electrospun nanofibers led us to prepare a skin-healing mask. (Figure. 8). illustrates several strategies used to fabricate a suitable dressing of awound with antibacterial properties [57].

For instance, Ghavami Nejad et al. [58] synthesized electrospun mussel-inspired copolymer of poly(dopamine methacrylamide-co-methyl methacrylate) (MADO), for amended antibacterial activity with silver nanoparticles (AgNPs) as a wound

dressing material. They developed antibacterial electrospun nanofibers to contain AgNPs in situ-formed without reducing agent to minimize tissue toxicity. In addition, they observed that composite nanofibers of MADO-AgNPs containing 1% NPs achieved eligible antibacterial activity versus bacteria, while they did not significantly affect mammalian cells. Moreover, they spotted within 24 h a rapid liberation of the silver nanoparticles and a sustained liberation for 5 days afterwards. Furthermore, in vitro and vivo studies approved the antimicrobial and bioavailability activity of MADO-AgNPs as effective materials for wound dressings.

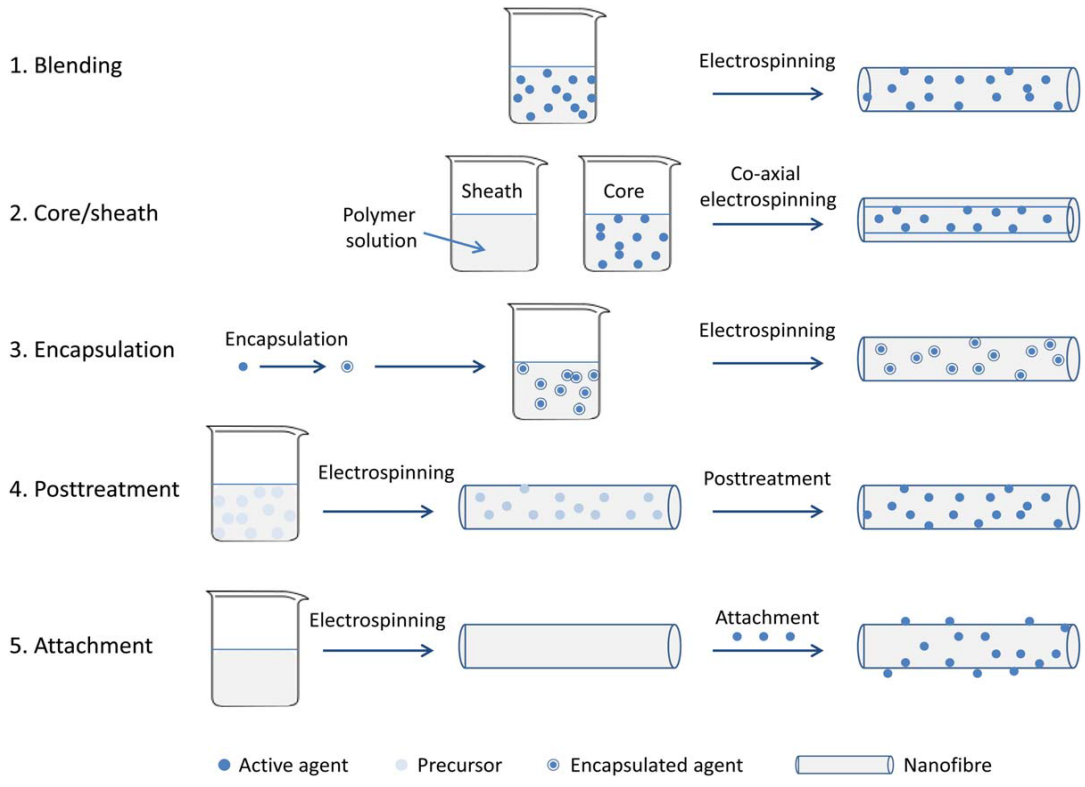

Figure 8. “Several strategies used to fabricate a suitable dressing of wound” [57].

On the other hand, Aruan et al. [59] produced an electrospun nanofiber composite with polyvinyl alcohol (PVA) loaded by soursop leaves extract (SLE) for wound dressings with an antibacterial activity. They believed that loading of SLE for polymeric matrix would compose an excellent layer on the surface with adhesive and emulsive characteristics that can be appropriate for the application of wound dressing. They successfully produced PVA/SLE composite fiber by using electrospinning technique. Due to, FTIR spectrum analyzer conclusively manifested the existence of flavonoid and alkaloid groups on membrane. Moreover, increasing PVA/SLE concentration in composite nanofibers resulted in increased activity of the antibacterial composite fiber.

1.5.1.4. Enzyme Immobilization

During the last 100 years, humankind has been dealing with the concept of immobilization of enzymes. However, over the last five decades, a wide range of applications have expanded for enzyme immobilization [60]. For this reason, immobilization of enzymes has attracted continuous attention in many different fields such as chemistry, biomedicine, and biosensors. The immobilized enzyme performance hugely depends on support structures. Wang et al. [61] believed that the nanostructured supports can keep the catalytic activity as well as ensure the efficiency of immobilization enzyme at high amplitude. Furthermore, electrospinning provides the fabrication of nanofiber supports in versatile and simple methods. The illustration shows in (Figure. 9) the idea of loading enzyme immobilization on to electrospun nanofibers.

From another perspective, El-Aassar [62] studied the immobilized β-galactosidase using copolymer nanofibers of poly (acrylonitrile-co-methacrylate)

poly (AN-co-MMA). He studied several variables which occur in the stability and activity accomplished when immobilizing enzymes on glutaraldehyde stimulated supports. He further determined pH and thermal stability of both immobilized and free enzymes. In addition, he compared and examined the storage stability system, free enzyme, and reusable stability of the immobilized enzyme. Interestingly he fabricated electrospun nanofibers of poly (AN-co-MMA) and nanofibers with glutaraldehyde bound with the enzyme molecules. In addition, the resistance to temperature and pH inactivation were better in immobilized β-galactosidase than the free form. In addition to the above, Tang et al [63]. Prepared a model of chemically cross-linked polyvinyl alcohol (PVA) nanofibers and immobilized hyperthermophilic enzyme solution by electrospinning. After confirming the impact of the reagents utilized in the cross-linking reaction, they minimized mat thickness and ameliorated the evident activity of immobilized enzyme by effective methods. For the understanding of the cross-linking, they applied effective process to progress the obvious activity of the immobilized enzyme as well as to minimize the thickness of the polymer fiber mats. They found that the hyperthermophilic enzymes immobilization within chemically cross-linked PVA nanofibers is vigorous and efficient at high temperatures. Notably, apparent activity was observed and exposed after immobilization and retained the hyperthermophilic nature with improving the thermal stability by 5.5-fold at 90 °C upon immobilization. Therefore, they studied potential reasons for decreasing the apparent mass transfer limitation, as well as cross-linking reaction. Notably, they improved the immobilizing enzyme performance by minimizing the mat

thickness to reduce the diffusion of the interfiber.

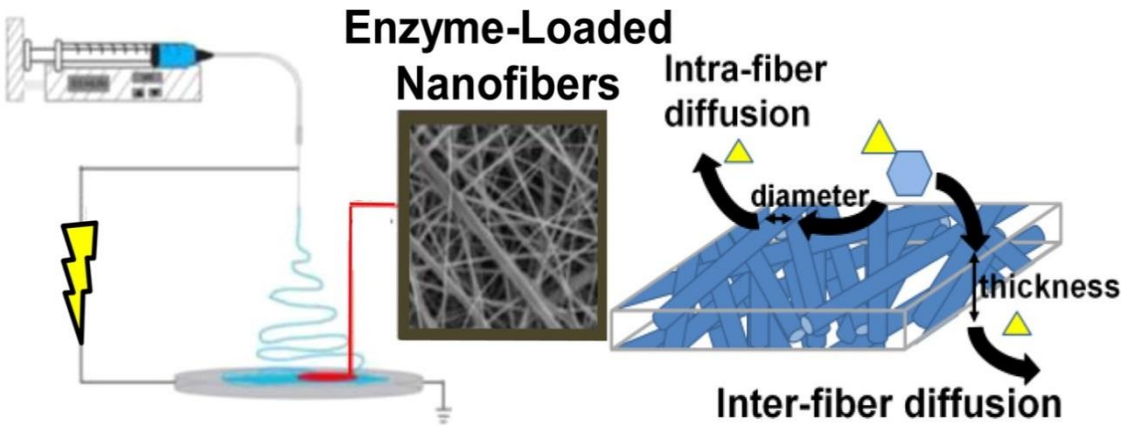

Figure 9. “The immobilization enzyme loaded onto electrospun nanofibers” [63].

1.5.2. Sensors Application

Sensors and biosensors are of utmost importance at present for surveillance safety, quality, food traceability and nutritional value. Recently this interest has increased due to their advantages and features especially in the miniaturization, portability, and minimized cost per analysis. For this reason, Mercante et al. [64] developed diverse morphology and composition of multifunctional hybrid electrospun nanofibers ESNFs, by functionalizing the nanofiber surface with a wide range of featured nanomaterials such as (graphene, carbon nanotubes, conjugated polymers and nanoparticles). This is clarified in (Figure. 10), showing its use in applications that serve the platforms of chemical biosensors for analysis of agricultural and food products [65].

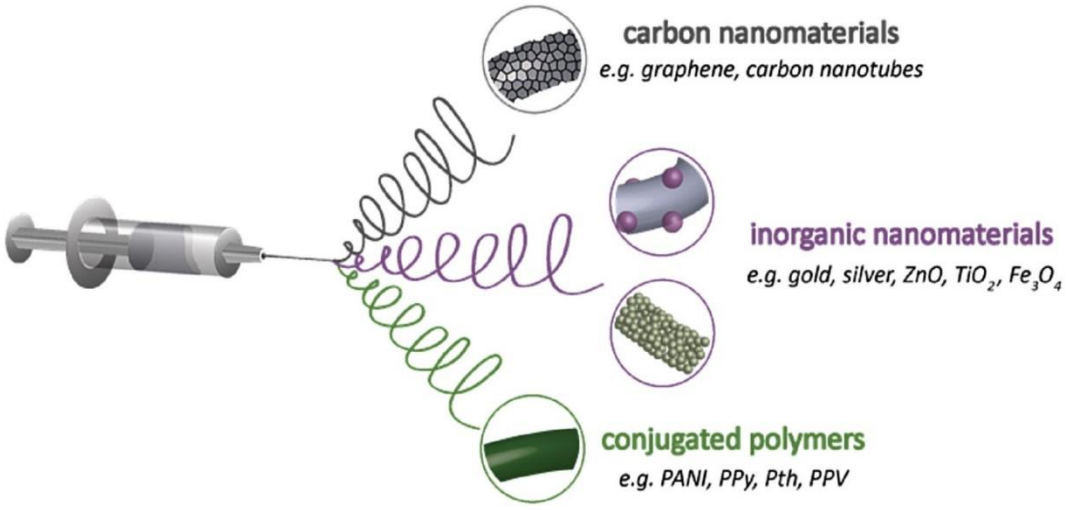

Figure 10. "Multifunctional electrospinning nanofibers containing different materials" [64].

1.5.3. Energy Application

Energy resources are one of the most important endeavors to attract researchers and scientists to develop and improve in a manner that is appropriate to world needs while taking into account the preservation of green environment. Therefore, research in this field is increasing in the push to discover new sources of alternative energy with low cost and high quality, while maintaining low rates of pollution. The energy resources of our time have become limited and this poses a significant risk to our way of life. For example, fossil fuels have been and still are the main source of energy where the global economy depends on it. Because of its depletion and increasing pollution to the environment, it was necessary to work hard to generate renewable sources. The

development of energy technology is essential in order to preserve our air and water resources from pollution. Hence, the importance of using and testing of new nanofibers fabricated by using electrospinning technique, which in return contributed to the production of new materials with high specificity for use in various applications aimed at producing clean energy efficiently and at a high quality. Below are some of these applications of alternative energy production that could one day be a new source of energy and that maintains nature and environment.

1.5.3.1. Dye-sensitized Solar Cells (DSSCs)

Kim et al. [66] synthesized core/shell nanofibers (NFs) composed of poly(acrylonitrile-co-itaconic acid) (PAI) and platinum (Pt) precursor in the shell, by using electrospinning. Following by thermal treatment to convert the materials to carbon nanofibers (CNFs) with platinum nanoparticles (Pt NPs), respectively, bearing a structure of core/shell CNF/Pt hybrids. Polyacrylonitrile (PAN) combined with the itaconic acid (IA) to promote the efficiency of precursor stabilization efficiency through the carbonization operation then graphitization. To grant a huge active area, Kim et al. placed Pt in the shell layer for ameliorating the electrocatalytic activity. More significantly, they applied CNF/Pt hybrids to counter electrodes (CEs) to maintain the unrivaled porous web of the CNFs. The illustration shows that the fabrication of core/shell CNF/Pt hybrid network applied to CE (Figure. 11). Hence, this resulted in successfully converted electrically conductive carbonaceous materials during thermal treatments, which exhibited superior electrocatalytic performance of the carbonization C/Pt CE. Moreover,

the CE manifested resistance of low charge carrier at the interface between electrolyte and CE, evidencing synergistic incorporation of Pt NPs and the CNF. Finally, Kim et al. confirmed the potential of the structure-controlled CNF/Pt hybrid network as a low-cost CE and efficient for DSSCs applications.

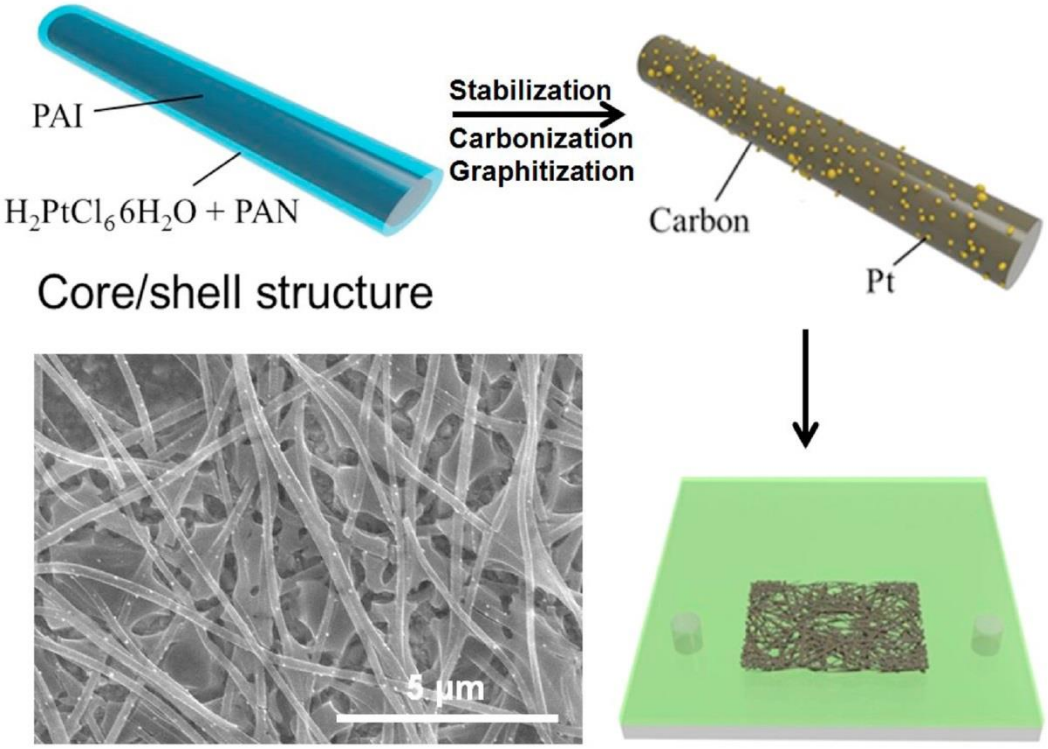

Figure 11. "Fabrication of core/shell CNF/Pt hybrid network applied to CE" [66].

On the other hand, Hwang et al. [67] fabricated TiO_2 nanofibers with different pore size (small, large, and multiscale) by using electrospinning multiscale porous (MSP). (Figure. 12) displays a clarification of the MSP NF-coated films of

TiO_2 nanoparticles (NPs). They observed that the MSP TiO_2 NFs surface area was higher than pristine TiO_2 by a factor of nine, which adsorbed an appropriate amount of dye for light gathering. As well as, MSP TiO_2 NFs exhibited stellar scattering of light. In addition, MSP TiO_2 NFs in large pore size (LPs) provided a venue for electrolyte diffusion for oxidation reactions. Thus, MSP TiO_2 NFs can be utilized for high efficiency DSSCs as an effective material.

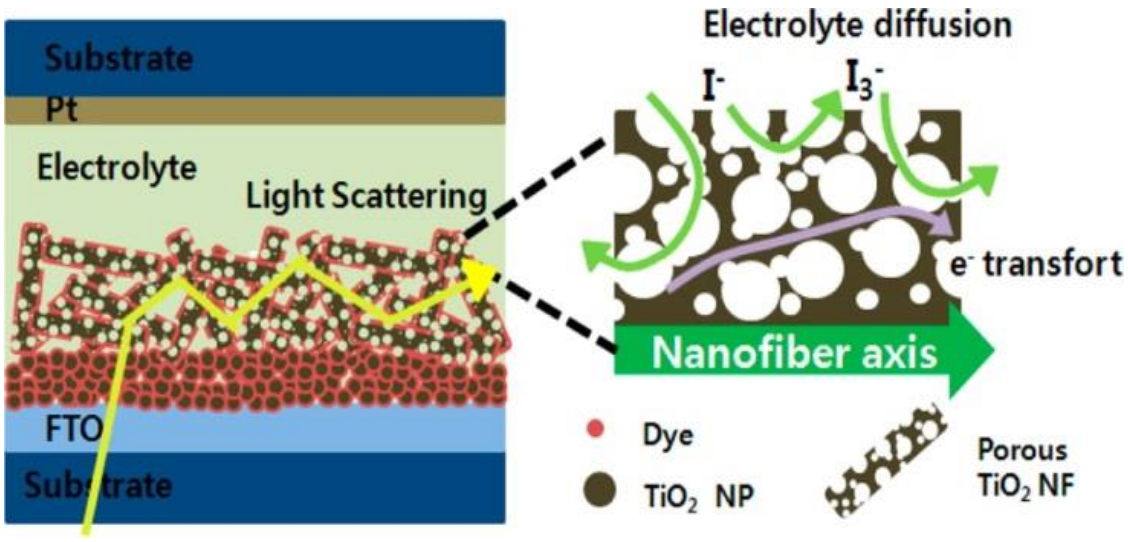

Figure 12. "Clarification of the under layer of the TiO_2 Nanoparticle (NP), the scattering over layer and magnified structure of MSP TiO_2 NFs" [67].

Additionally, Fathy et al. [68] synthesized a membrane of electrospun polymethylacrylate (PMA) nanofibers. They studied the electrospinning operating parameters and the properties of polymer solution Also, they fabricated quasi-

solid-state electrolyte for DSSC utilized PMA nanofibers membrane. They observed uniform morphology of uniform PMA nanofibers with high ionic conductivity and small diameter manifested at room temperature because of the ease of crossing the liquid electrolyte through the membrane pore structure. They utilized electrospun PMA membrane to form quasi-solid-state electrolyte for the first time for dye-sensitized solar cells with electricity conversion efficiency reaching up to 1.4%, and intensity of illumination reaching 100 mW cm^{-2}. Also, the electrospun PMA membrane exhibited the better long life stabilization in comparison with a conventional liquid electrolyte

1.5.3.2. Lithium-Ion Batteries (LIBs)

A case in point, Ning et al. [69] fabricated electrospun polyvinylpyrrolidone (PVP), PAN and zinc acetate dihydrate.($Zn(Ac)_2 2H_2O$) by single-nozzle, followed by a calcination process to acquire a composite of ZnO nanoparticles decorated CNFs as binder-free and self-supported anode material for lithium-ion batteries (LIBs), The illustration in (Figure. 13) explain the visualization in a simplified way. They observed that covered hemispherical ZnO NPs, by amorphous carbon layers sedimented regularly on the surface of CNFs. This immediately served as a binder-free and self-supported anode of LIBs, the ZnO/CNF anode's hierarchical structure expedites the diffusion of Li ions and electrolyte. The steady conductive network created by the criss-cross CNFs includes high-speed electron transmission. The unrivaled coating structures of ZnO NPs wrapped by amorphous carbon layers repair ZnO and prevent its volume amplification through the charge-discharge cycles. Therefore, LIBs collected by binder-free

ZnO/CNFs anode show amended electrochemical performance, comprehensive excellent rate capability, high specific capacity, and enhanced cycling stability. This work provides an effective and simple method to gain self-supported and binder-free anode material for LIBs.

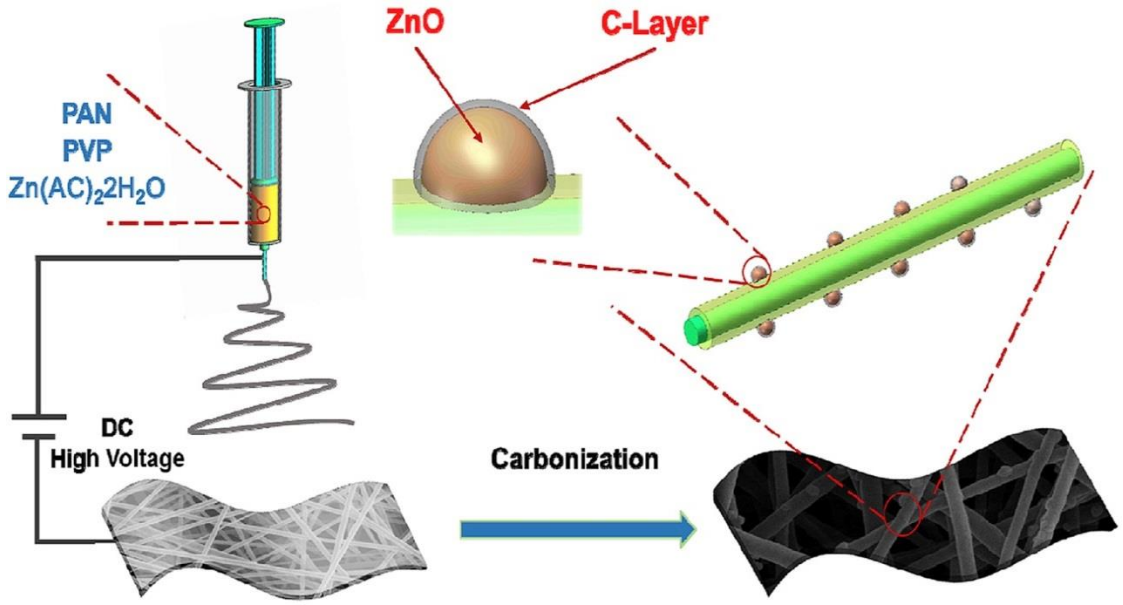

Figure 13. “Fabrication method of composite Zn/CNFs for LIBs” [69].

1.5.3.3. Supercapacitors

Liu et al. [70] introduced a new technique to fabricate microporous carbon nanofibers (MCNFs) by integrating electrospinning and a phase separation process. In particular, they used polyvinylpyrrolidone (PVP) jointly with mixed solvent of dimethylsulfoxide (DMSO) and N,N-dimethylformamide (DMF), to

illustrate the preparation process, see (Figure. 14). They found out that MCNFs exhibited a very high performance of specific capacitance. Also, electrospun PVP along with mixed solvents produced many micro-pores and few meso-pores. Additionally, the surface area of nanofibers increased by phase separation technologies. Therefore, the combination between the two techniques to fabricate MCNFs is promising for the application as supercapacitors with outstanding electrochemical performance and high specific surface area.

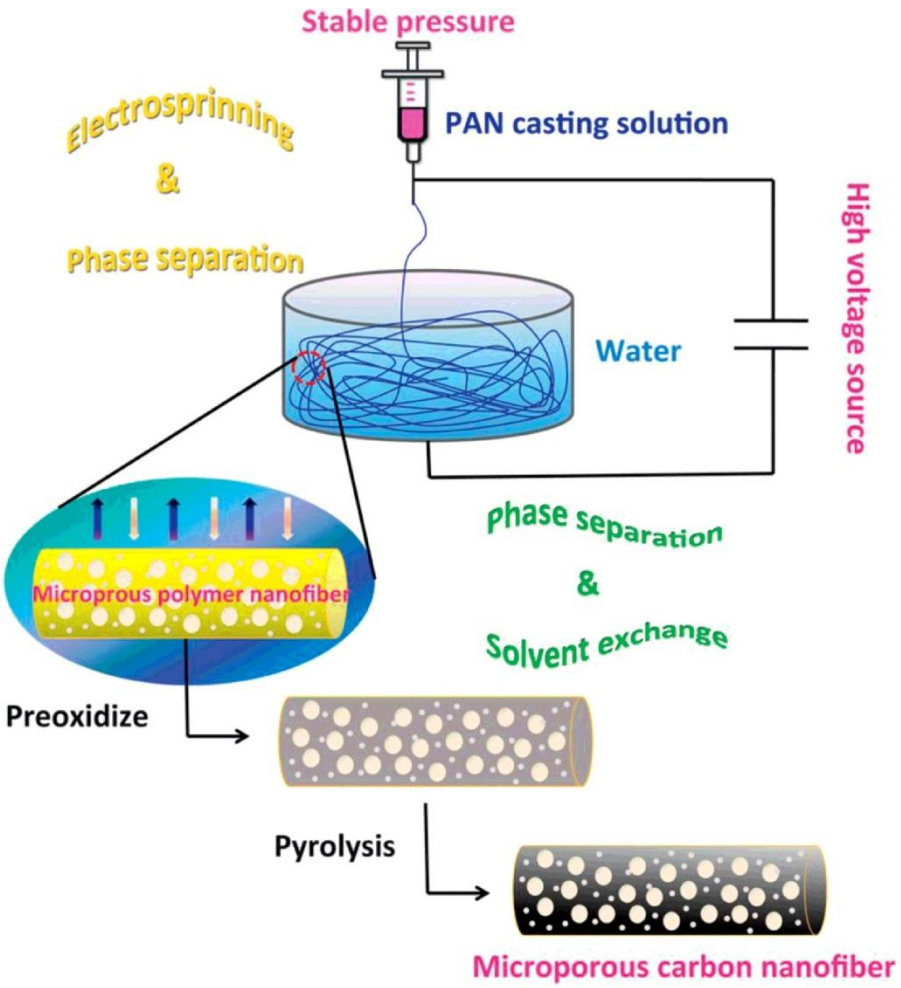

Figure 14. “Schematic clarification of the fabrication process of MCNFs” [70].

Furthermore, Miao et al. [71] synthesized core/shell electrospun polyamic acid (PAA) nanofibers as a matrix with polyaniline (PANi) to form ultimate hollow PANi nanofibers for supercapacitors application, this illustration boosts the procedure of preparation in (Figure. 15). They noticed that a maximum specific capacitance of 601 F g^{-1} had been accomplished at 1 A g^{-1}, which mends the electrochemical performance of hollow PANi nanofibers. Additionally, the flexibility of fiber membranes provided the possibility for fabrication and facile construction of conducting polymers with several hollow structures, which make it highly efficient and promising in various supercapacitors applications and electrochemical devices.

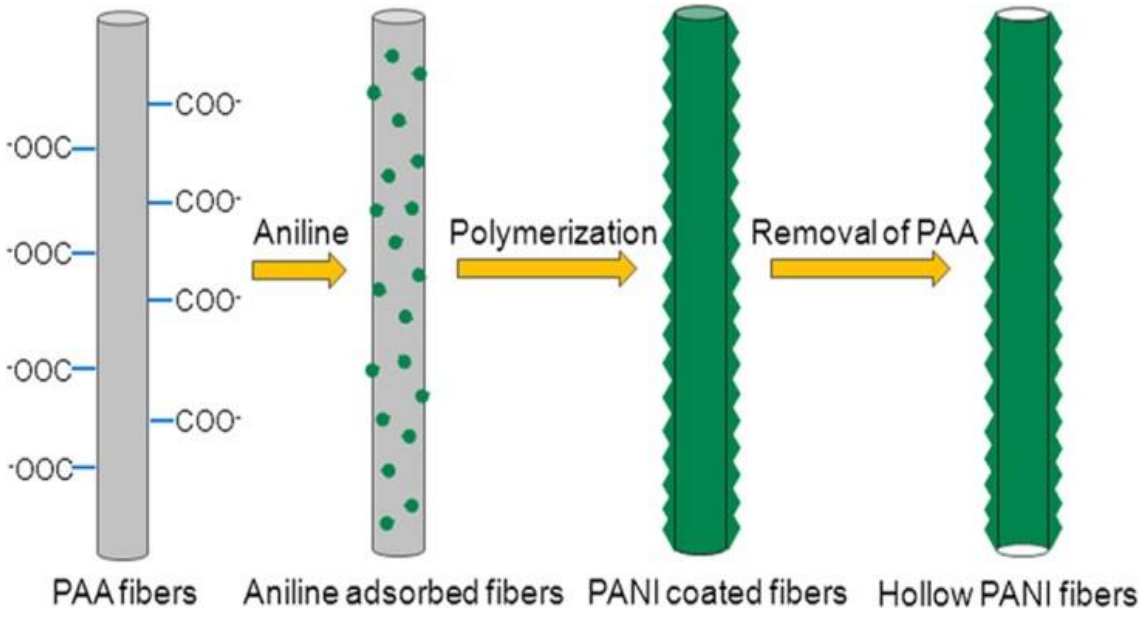

Figure 15. "Fabrication procedure schematic of hollow PANi nanofibers" [71].

On the other hand, Kim et al. [72] fabricated CNFs by carbonization of aligned electrospun PAN nanofibers using high speed rotary collector reaching 2000 rpm to verify possibility to be used as a supercapacitor electrode. They found out the alignment degree of nanofibers while increasing the rotary collector speed, thus enhancing the electrical conductivity and surface properties of CNFs. Consequently, aligned CNFs electrode exhibited obviously amended electrochemical performance making it promising and effective in various supercapacitor applications.

1.5.3.4. Fuel Cells (FCs)

A case in point, Salahuddin et al. [73] studied an innovative survey concerning the integration of carbonized electrospun polyacrylonitrile (PAN) nanofibers into gas diffusion layers (GDLs) of proton exchange membrane fuel cells (PEMFCs), and innovated on those layers a highly hydrophilic and super hydrophobic sections for preferable cathodic water management through the cathodic reaction. For this purpose fabrication of electrospun PAN were sequentially stabilized and carbonized before the super hydrophilization and hydrophobization steps. Also, the new GDL's mechanical, thermal, and electrical characteristics were measured for the PEMFCs application. They found out that GDL performed an increase after the hydrophobization process reaching 58% with superhydrophobic coatings, while reaching a maximum of 162° of water contact angle. Furthermore, they calculated the crystallinity percent from the test of differential scanning calorimetry (DSC) to be 52% with hydrophobic coatings, consequently indicating perfect working conditions. Thereafter, they measured

the electrical resistance for the carbon fibers coated to be 0.1877 Ω/sq., which also exhibit an ideal situation for PEMFCs. As previously reported, the hydrophilic and hydrophobic areas show a highly performance in carbonized GDLs make it promising with PEMFCS.

In addition, Ballengee and Pintauro [74] provided a new approach of electrospun nafion and poly (phenyl sulfone) simultaneously into a dual fiber mat based nanofiber composite fuel cell membranes. They believed that the new process stipulates the following, (i) smooth fabrication, (ii) versatility of morphology "modest hereafter electrospinning treatment steps were advanced to create the two final membrane morphologies", as illustrated by the (Figure. 16), and (iii) a durable structure for future membrane manufacture and design. They observed that the conversion from a dual-fiber mat in any of the two membrane morphologies is straightforward and simple. Also, the structures of both membrane manifested comparable proton conductivity and volumetric/gravimetric water swelling. Contrasted to conventional fuel cell membranes, the nanofiber composite membranes proved better mechanical properties and very low in-plane water swelling. On the other hand, the design of the composite membrane can be widened to manufacture composite films for any dual polymers with sufficient differences. Additionally, they believed it is likely to produce nanofiber composite membrane for more than two various fiber compositions as a new approach of composite ion-exchange membranes.

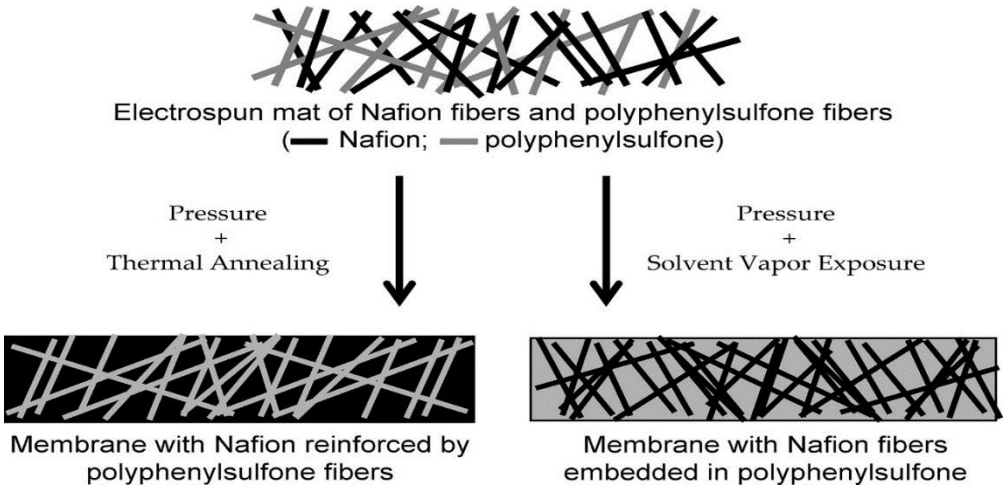

Figure 16. "Fabrication of two nanofiber composite nafion/poly(phenyl sulfone) membrane frameworks from the same dual-fiber mat" [74].

More interestingly, Wei et al. [75] studied incorporating graphene into electrospun polyacrylonitrile (PAN) and polyvinylidene fluoride (PVDF) (GPP) composite nanofiber membrane over gas diffusion layers. Utilizing a co-spinning method, to increase the spinnability of solution. Furthermore, to increase the scarce electrical conductivity, graphene was doped into the co-spinning membrane and subsequently, sprayed on tp a nanofiber membrane platinum (Pt)/C catalyst ink. Consequently, they obtained a conventional catalyst layer of novel membrane electrode assembly (MEA), with a microporous layer thickness. Thus, expected a best of the fuel cell performance utilizing unique MEA with minimum loading of Pt. For the sake of clarity, see illustration (Figure. 17). They noticed that novel hot-pressed (HP) electrospun electrode possesses high electrochemical active surface areas (ECSA) with 2 wt% graphene oxide (GO) comparing with

conventional electrode. In addition, GPP nanofiber electrospun electrodes have shown the highest performance of fuel cell compared to the traditional electrode. The unique electrode structure can be attributed to the improved fuel cell performance. Therefore, the new GPP nanofiber electrospun electrodes under low Pt loading conditions are promising in the application proton exchange membrane fuel cells (PEMFCs) with their high stability and performance.

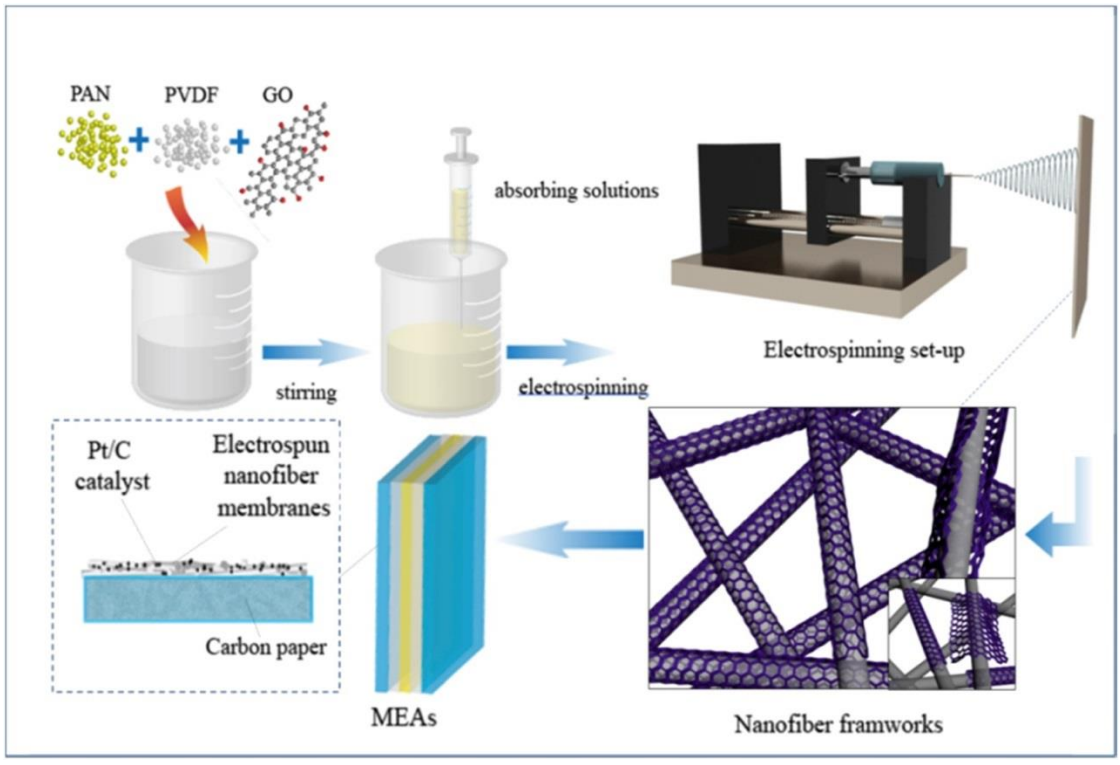

Figure 17. “The artificial path to GO-PAN/PVDF (GPP) nanofibers” [75].

1.6. Carbon Support Materials Based Polymer Fibers

Materials of carbon fiber are attracting technological and scientific interest as catalyst supports with potential and existing commercial applications [76]. The mechanical, thermal properties as well as the electrical conductivities of the produced carbon fibers rely on the preference of a precursor. Polyacrylonitrile (PAN) is used for most of the mercantile carbon fibers as precursors [77], and polyvinyl alcohol (PVA) [78].

1.6.1. Polyacrylonitrile (PAN)

Polyacrylonitrile is a derivative of the acrylate family of polymers, and it is a vinyl polymer. PAN is made from acrylonitrile monomer via free radical vinyl polymerization, as (Figure. 18) shows. For almost a century, PAN has been extensively studied for technological and commercial exploitation. More recently great effort has taken place in an attempt to convert and form it into fibers. PAN is a commonly used polymer, through its diverse precursors for fabricated carbon nanofibers (CNFs), and mostly due to the high yield of carbon resulting through it (up to 56%). It's flexibility in forming the final CNF product structure and the ease of acquisition of more stabilized products, due to the genesis of a ladder body via nitrile polymerization [79]–[82]. PAN chemistry is of significant importance, due to its utilization in different applications as a precursor in the formation of CNFs, an inclusively high surface area with high porosity for energy storage, in electronics applications and as reinforcement filaments of graphite for organic materials in high stiffness and high strength composites. Inagaki et al.[83] Characterized CNF chemistry and applications, restrictive fundamentally to the scientific research

and developments of technology in Japan. Furthermore, Barhate and Ramakrishna [83], studied the filtration troubles and solutions from tiny materials by using nanofibers as a filtering media. Li. et al. [84] published the tendencies in nanofibers, with affirmation on techniques of electrospinning to fabricate nanofibers.

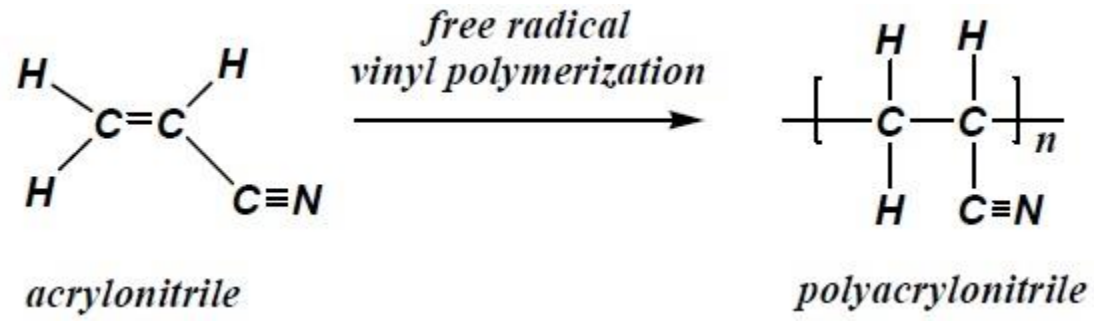

Figure 18. "Acrylonitrile to polyacrylonitrile by free radical vinyl polymerization."

1.6.1.1. Polyacrylonitrile as a Fiber and Carbon Fiber

Although acrylonitrile (AN) has been around since 1893, PAN did not make significant progress in converting into usable fibers until 1925, for the main reason that the difficulty to dissolve it to spin. The PAN homopolymer was sophisticated for industrialization of fibers in 1940, especially after discovering suitable solvent by DuPont [85]. DMSO, DMF, DMAc, tetramethylsulfide, dimethylsulfone and aqueous solution of ethylene carbonate are suitable polar solvents for PAN, as well as some of mineral salts. 25% of PAN dissolved in

DMF to form saturated solution at 50 °C, compared with other solvents it is highly soluble [86]. PAN and its co-polymers are white powders essentially; due to degradation, they become darker up to 250 °C. PAN owning a comparatively high glass transition (Tg), also the thermal plasticity for these polymers are low and cannot be utilized as plastic materials. Furthermore, the PAN crystalline melting point is high and reaches 317 °C. Moreover, the solubility limitation in specific solvents was due to intermolecular strength among the polymer chains, coupled with superior mechanical characteristics of its fibers. The CNF's properties depend fundamentally on the microstructure of the stabilized PAN fibers [87]–[94].

1.6.1.2. Carbon Fiber Formation Mechanism Based PAN

The suggested mechanism of PAN based carbon fiber of cyclization, stabilization and carbonization is shown in (Figure. 19 and 20). The conversion chemistry into carbon fibers based PAN consists of three consecutive phases: begin with cyclization process, the purpose is to transfer the PAN fibers from the linear structure to ring structure. Followed by, PAN stabilization into a ring structure of condensed heterocyclic under 200 °C, Thereafter, heat condensation raised from 200 °C to 800 °C of the intermediate to convert the compound into an aromatic product in the presence of argon gas. Ultimately, when temperature stabilizes at 800 °C and the structure relaxes after N_2 is freed allowing it to produce its graphitic structure.

Figure 19. “The cyclization o PAN nanofibers” [95].

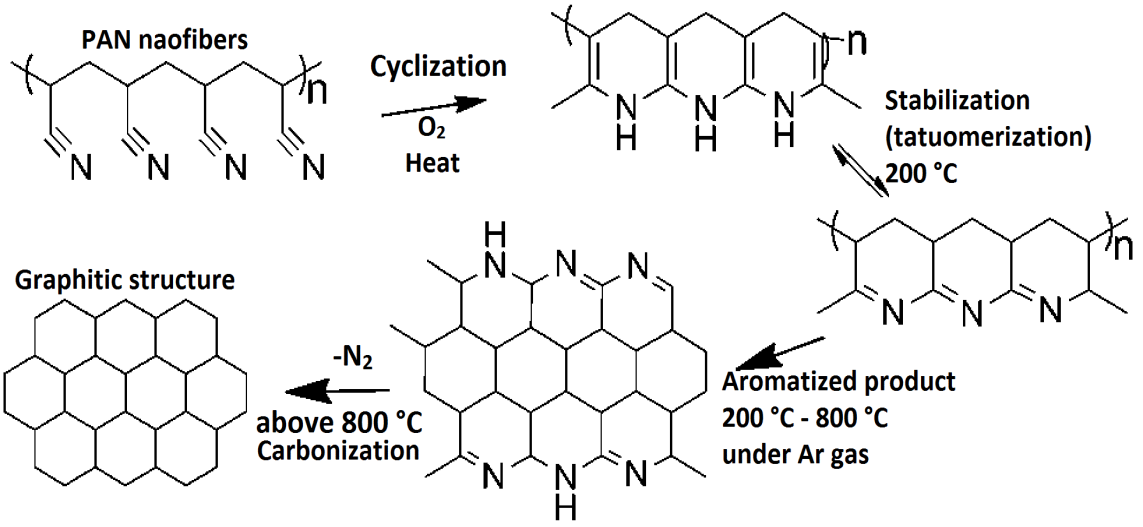

Figure 20. “Carbonization of polyacrylonitrile” [95].

1.6.2. Polyvinyl Alcohol (PVA)

Polyvinyl alcohol (PVA) is a vinyl polymer as well as PAN; vinyl alcohol is the monomer of PVA, as shown in (Figure. 21). PVA is a synthetic polymer derived by partial or full hydrolysis of polyvinyl acetate to strip groups of acetate, exemplary levels of hydrolysis are from 80% to higher than 99%., as shown in (Equation. 1) The hydroxylation amount determines the chemical characteristics,

physical properties and mechanical characteristics of the PVA [96]. The PVA polymer is extremely soluble in water but insoluble in most organic solvents. With increased hydroxylation degree and polymerization of the PVA, the solubility in water will be decreased and the crystallization more difficult [78].

$$[\boldsymbol{CH_2CH(OAc)}]_{\boldsymbol{n}} + \boldsymbol{C_2H_5OH} \rightarrow [\boldsymbol{CH_2CH(OH)}]_{\boldsymbol{n}} + \boldsymbol{C_2H_5OAc}$$

Equation 1. "Synthetic of polyvinyl alcohol from polyvinyl acetate."

PVA was first prepared in 1924 by Herrmann and Haehnel using polyvinyl esters with stoichiometric amounts of caustic soda solution [97]. It is a very common polymer, widely used as it is non-toxic [98], more biologically compatible [99], biodegradable [100], thermally stable in several applications and has superior mechanical characteristics such as: strain, toughness, elastic modulus and flexibility in dry stat [101].

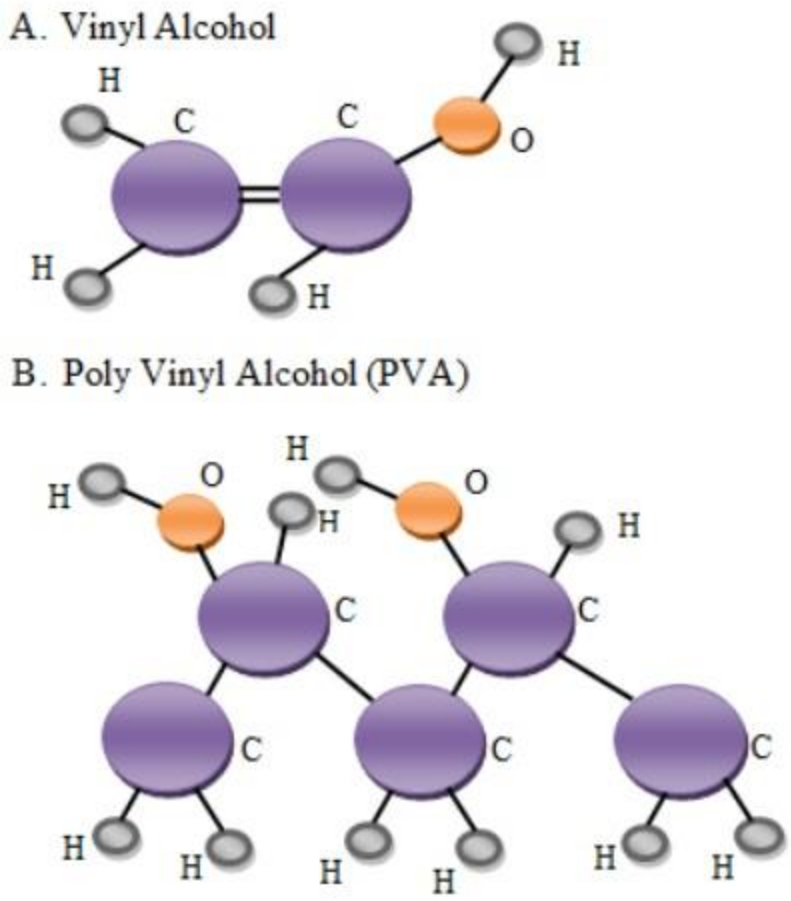

Figure 21. “A. The structure of vinyl alcohol, B. The structure of polyvinyl alcohol (PVA)” [78].

1.6.2.1. Carbon Fiber Formation Mechanism Based PVA

There is no significant difference in the mechanism between polyvinyl alcohol and polyacrylonitrile. The conversion chemistry into carbon fiber based PVA consists of three consecutive phases: it begins with a cyclization process, the purpose of which is to transfer the PVA fibers from the linear structure to a ring structure. Followed by stabilization of PVA into a ring structure of condensed

heterocyclic under 200 °C, Thereafter, heat condensation raised from 200 °C to 800 °C of the intermediate to convert the compound into an aromatic product in the presence argon gas. Ultimately, when the temperature stabilizes at 800 °C and the structure relaxes then N_2 is freed in order to reach graphitic structure.

1.7. Carbon Nanofibers as Catalysts for Electro-Oxidation of Methanol

The invention of imminent energy systems from maintainable energy sources as an alternate for fossil fuels is a major drive of modern studies. The most promising sustainable energy devices in the current age are direct methanol fuel cells (DMFCs) because methanol is easily available, readily stored and transported and inexpensive. Therefore, DMFCs have been attracting an increasing number of researcher's attention because of its low operating temperature, high energy density, comfortable use and environmental friendliness [102]–[106]. Regrettably, the rising cost of manufacturing due to harnessing electrodes of precious metals such as platinum is facing spacious mercantile applications not for DMFCs only but also for all of other fuel cells. Consequently, more endeavors are being made to develop new materials having high catalytic activity and good chemical stability with low cost to substitute platinum [107]–[109].

A case in point, Thamer et al. [110] fabricated catalysts were introduced with cobalt incorporated and nitrogen doped carbon nanofibers Co/N-CNFs) after the carbonization process for electrospun PVA at 850 °C for methanol oxidation as

anode. They revealed advantageous electrocatalytic activity of Co/N-CNFs across methanol oxidation and non-observable impact in alkaline medium particularly at high nitrogen content. Related to the above Co/N-CNFs exhibited advantageous stabilization across methanol oxidation for a prolonged period of time. They expected to create new possibilities to thrust on Co/N-CNFs as an influential non-precious electrocatalyst for oxidation of small organic compounds.

In another study, Mu et al. [111] synthesized cobalt entrenched coal based carbon nanofibers (Co-coal-CNFs) by using electrospinning of PAN, Co and oxidized coal simultaneously, realized by a carbonization process, This is illustrated with the schematic diagram of the preparation process in (Figure. 22). Furthermore, platinum nanoparticles (Pt NPs) used as a support for methanol oxidation reaction (MOR). Also, they compared the catalyst behavior, respectively of Pt/Co-coal-CNFs for MOR with platinum propped without cobalt decoration on CNFs (Pt/CNFs), coal-based CNFs (Pt/coal-CNFs) and platinum Co embedded without coal addition (Pt/Co-CNFs). They found out that reinforced catalytic activity, stabilization of Pt/Co-coal-CNFs referred to the harmonic contribution of cobalt, and coal co-existence will lead to full platinum nanoparticles dispersal and support high graphitization, as well as low resistance of charge transfer. The study provided fuel cell technology with a new idea to style and prepare support materials.

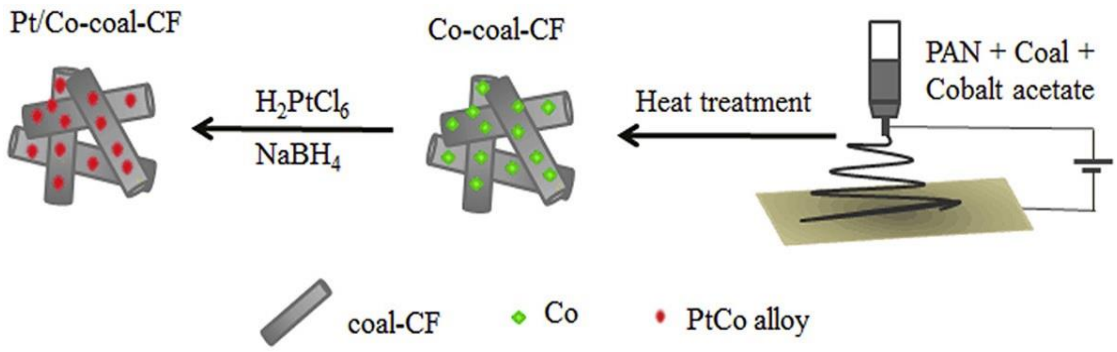

Figure 22. "Synthesized cobalt entrenched coal based carbon nanofibers (Co-coal-CNFs) by electrospinning technique with supported platinum nanoparticles after carbonization" [111].

More interestingly, Abdullah et al. [112] studied increasing doped nitrogen in the carbon nanofiber (CNF) as a catalyst support during nanocomposite matrix changing from electrospun polyacrylonitrile (PAN) or polyvinyl alcohol (PVA) to electrospun polyvinylpyrrolidone (PVP) which drove to a various CNF with a high content of nitrogen, huge surface area and high stability of thermal [113]. Moreover, the calcination temperature effect was studied on the behavior of NiO as a electrocatalyst for direct methanol fuel cells (DMFCs). They confirmed that the CNF/NiO composite in cyclic voltammetry measurement exhibited high electrocatalytic activity towards oxidation of methanol which was attributed to the high content of N of the NiO nanoparticles in the CNF support. Also, increasing of N content enhanced the interaction amidst CNFs and the catalyst, as well as increasing the density of electrons. In addition, the high N content also prevented the agglomeration nanoparticles of the NiO in the methanol solution.

Furthermore, the ideal calcination temperature of the CNF/NiO composite, which was found, resulted in the highest peak currents of MeOH oxidation reaction at 500 °C. Also, the chronoamperometry measurements analysis confirmed the increasing CNF/NiO composite surface area with increasing of calcination temperature, this clarifies the high electrochemical behavior of the composite. The CNF/NiO composite showed high resistivity and stability to the intermediate adsorption and enhanced electrocatalytic properties towards the reaction of methanol oxidation in alkaline medium.

SECTION 2: EXPERIMENTAL WORK

2. Experimental Work

2.1. Chemicals and Reagents

- All chemicals used for work making ready were purchased from SIGMA-ALDRICH as follow:
- Polyacrylonitrile (PAN) – average Mw ~ 150,000 g/mol.
- Polyaniline (PANi) (emeraldine base) – average Mw ~ 20,000 g/mol.
- Graphite – powder, <150 µm, 99.99% trace metals basis.
- Nafion.
- Sulfuric acid (H_2SO_4), 99.999%.
- Sodium nitrate ($NaNO_3$), ACS reagent, ≥ 99.0%.
- Potassium permanganate ($KMnO_4$), ACS reagent, ≥ 99.0%.
- Hydrogen peroxide solution (H_2O_2), contains inhibitor, 35 wt. % in H_2O
- Hydrazine solution (NH_2NH_2), 35 wt. % in H_2O.
- N,N-Dimethylformamide (DMF), ACS reagent, ≥ 99.8%.
- Sodium hydroxide (NaOH), ACS reagent, ≥97.0%, pellets.
- Methyl alcohol (CH_3OH), ACS reagent, ≥99.8%.
- Ethyl alcohol, pure (CH_3CH_2OH), 190 proof, ACS spectrophotometric grade, 95.0%.
- Sodium sulfate (Na_2SO_4), ACS reagent, ≥99.0%, anhydrous, granular.
- Nickel(II) chloride hexahydrate ($NiCl_2.6H_2O$), puriss. p.a., ≥98%.
- Copper(II) chloride dehydrate ($CuCl_2.2H_2O$), ACS reagent, ≥99.0%.

- Cobalt(II) chloride hexahydrate ($CoCl_2.6H_2O$), ACS reagent, 98%.

2.2. Materials Preparation

2.2.1. Graphene Preparation.

Preparation of graphene began with graphene oxide- synthesized by the modified Hummer's method [114]. In brief, 1.0 g of sodium nitrate, and 25 mL of 98% sulfuric acid were mixed with 1.0 g of graphene powder, followed by addition of 5.0 g of potassium permanganate. The reaction was left stirring for 3 hours and maintained at 30 °C, this was followed by the slow addition of 100 mL deionized water at 80 to 90 °C with the resulting solution over 2 hours. After that the reaction was treated with 10 mL of hydrogen peroxide (35% H_2O_2), then washed multiple times with hot deionized water. Particular quantities of the prepared material will be suspended in deionized water, pursued by addendum of hydrazine (30 µL N_2H_4) under stirring, and in the final stage placed in a conventional microwave for 5 cycles, each 30 sec to produce graphene powder.

2.2.2. Polyacrylonitrile, Polyaniline and Graphene Composite Preparation

At room temperature (10 g) of polyacrylonitrile was dissolved in (100 ml) of DMF under stirring. Followed by addition of polyaniline (2 g) and (0.3 g) of graphene to the polymer solution according to (Table. 1) and remain stirring for (8 hours) until reacting uniform precursor suspension of final concentration (12.3 g solid/ 100 ml DMF solvent). The fabrication of electrospun fibers was achieved by electrospinning a uniform suspension with high a voltage DC power supply at

a potential of 20 kV (Spellman-CZE 1000 R, 30 KV, Czech Republic). And also utilizing a syringe pump (scientific-KDS 230-CE, USA) connected to a metallic tip in order to preserve flow rate of 0.5 mL/hour, and suspended at 20 cm from a grounded aluminum collecting drum which was rotated at approximately 120 rpm, (Figure. 23) illustrates the electrospinning settings. Thereafter, fabricated electrospun fibers were extracted from the collector drum and then dried sequentially at room temperature overnight; at 50 °C for 3 hours, and then at 70 °C for 2 hours to ensure complete removal of solvent.

Table 1.

Parameters utilized to fabricate electrospun PAN nanofiber composites

Polymer matrix	**Additive particles**	**Needle size**	**Feed rate**	**Voltage**	**Distance from collector**	**Humidity**
PAN	**Graphene gm**	**Gauge**	**mLh^{-1}**	**KV**	**cm**	**RH%**
5% PANi	0.3	22	0.5	20	20	25±1
10% PANi	0.3	22	0.5	20	20	25±1
15% PANi	0.3	22	0.5	20	20	25±1
20% PANi	0.3	22	0.5	20	20	25±1

+

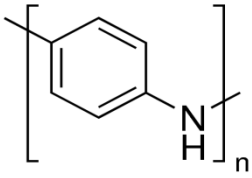

+

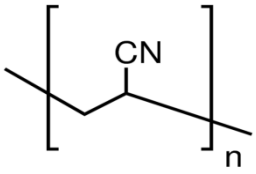

Graphene **Polyaniline** **Polyacrylonitrile**

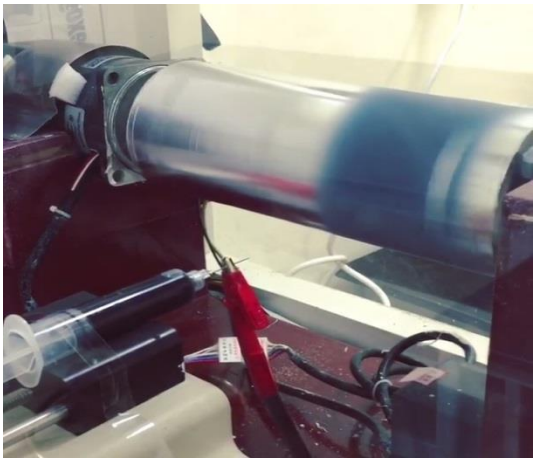

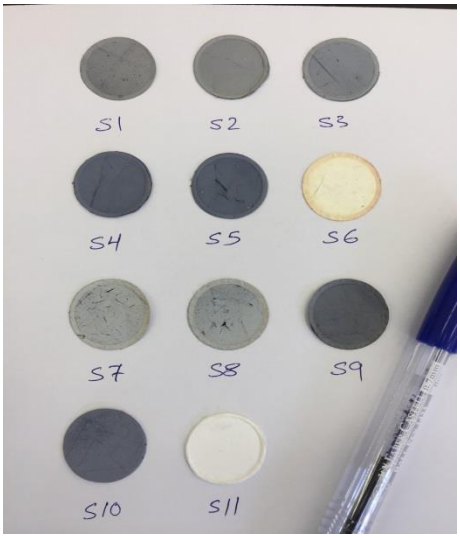

Figure 23. "The electrospinning settings to fabricate electrospun fiber composite."

2.3. Carbon Nanofibers Preparation.

2.3.1. Carbon Nanofibers Based Polyacrylonitrile Preparation.

The fabricated nanofibers were collected and dehydrated overnight at room temperature and then stabilized to 200 °C at 2 °C min^{-1} in atmosphere for two hours. Thereafter, a carbonization step was accomplished by placing in a ceramic crucible a fixed amount of the sample and transferred into a ceramic tube furnace (GSL 1500X-OTF). Eventually, by heat treatment the CNF was

prepared between room temperature and 800 °C and then preserved isothermally at 800 °C for 4 hours (the heating rate was 5 °C min^{-1}) under atmosphere of high purity nitrogen (99.999%), (Figure. 24) illustrates the pyrolysis step.

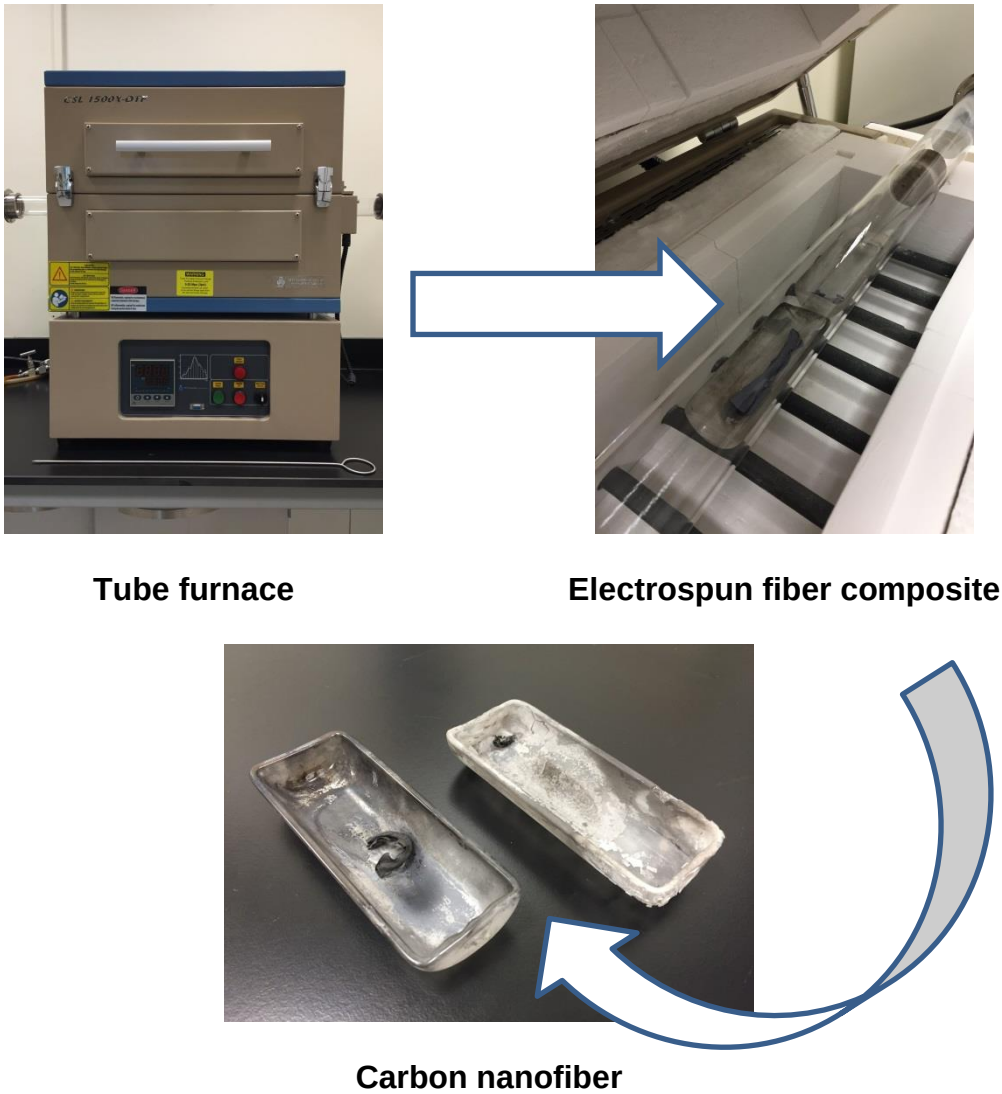

Figure 24. "The pyrolysis step of fiber composite to carbon nanofibers preparation."

2.3.2. Preparation of Carbon Nanofibers Ink Solution Based PAN

The different PAN-CNF fibers were prepared in 1 wt.% Nafion as a solvent. The 1% of Nafion was prepared by dilution of a 5 wt.% Nafion with isopropanol, then 1 mg of CNFs were dispersed in 1 ml of the 1wt.% Nafion and sonicated the solution for 4 hr.

2.3.3. Preparation of Catalyst Based Carbon Nanofibers

Preparation of the metal oxides with the different carbon nanofibers on the glass carbon electrode (GCE) was accomplished in three consecutive steps. First, casting a 5 µL of the suspended ink onto the GCE surface and allowing it to dry for 8 hr. With the same electrolyte that was utilized in the measurement, we flushed the surface in order to emphasize the wettability of the surface, before using an electrolytic cell and introducing the electrode. The second step is the metallic potentiostatic deposition on the working electrode (i.e., CNFs/GCE) from an aqueous solution of 0.1 M sodium sulfate (Na_2SO_4) containing 1 mM of the sulfate salt of each metal ion (i.e. Cu^{2+}, Co^{2+}, Ni^{2+}) at potential of -1 V for 600, 1200, 1800, and 2400 seconds of deposition time. The third step is the mineral deposit passivation in 1 M sodium hydroxide (NaOH) through potential cyclization between 0.2 V and 0.55 V for 15 successive cycles within a scan rate reach to 100 mV s^{-1}.

2.4. Characterization of Samples

2.4.1. X-Ray Diffraction (XRD) Analysis

The of X-ray Diffraction data were compiled on a (PANalytical EMPYREAM Alpha-1), utilizing a source of Cu Kα radiation for the realization of phase and crystalline structure, with 2θ range from 5° to 80°.

"X-ray Diffraction (XRD) PANalytical EMPYREAM Alpha-1"

2.4.2. X-Ray Photoelectron Spectroscopy (XPS) Analysis

The data of X-ray photoelectron spectroscopy (XPS) were collected on a (AXIS ULTRA DLD, Kratos) instrument constructed with a monochromated Al Kα (1486.6 eV) X-ray source at 20 mA emission current and 15 kV anode potential. A full survey has been done at 160 eV passing energy. Moreover, high resolution at 20 or 40 eV passing energy.

"X-ray photoelevtron spectroscopy (XPS) AXIS ULTRA DLD, Kratos"

2.4.2.1. Preparation Samples of X-Ray Photoelectron Spectroscopy (XPS)

Suitable conditions for XPS samples were prepared, as follows. Then 1 mg of carbon fiber based PAN was sonicated for 4 h in 1 mL of 2% Nafion solution. After sonication, a 10 µL of the producing ink was casted over GCE, of an area of 0.5 cm^2, and dried at room temperature for 2 hours, and then transferred into the XPS chamber, as shown in (Figure. 25).

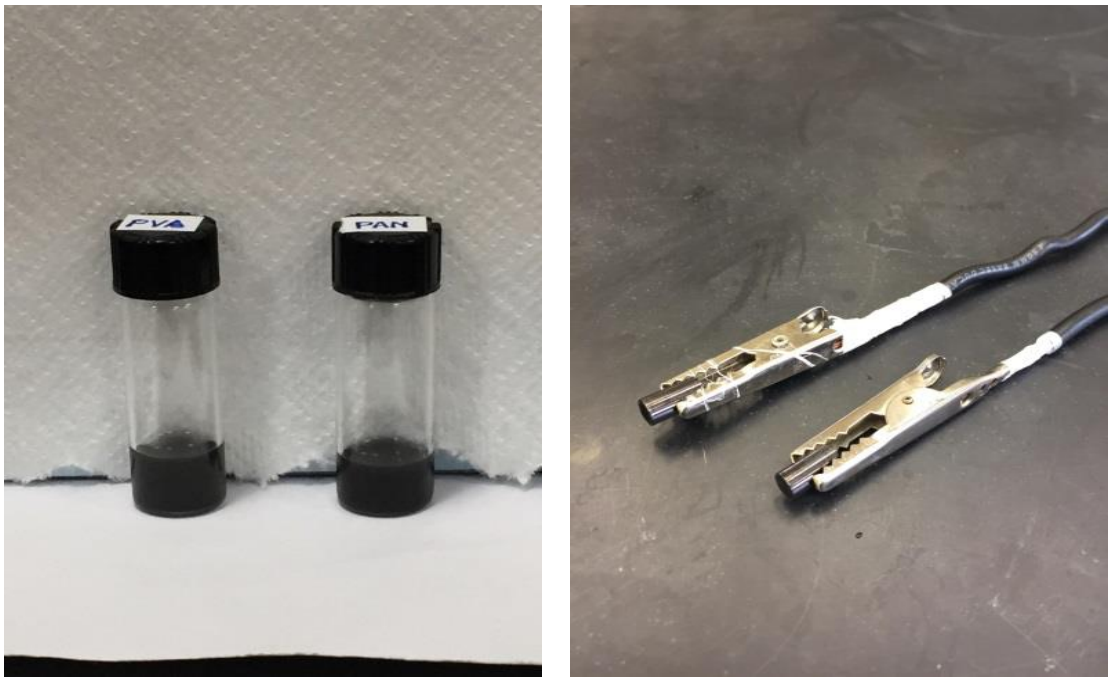

Ink samples **Glass carbon electrodes**

Figure 25. "Illustrations to explaining the XPS samples preparation."

2.4.3. Transmission Electron Microscope (TEM) Analysis

Transmission electron microscopy (TEM) analysis was carried out using (FEI Tecnai G^2 F20 S-TWIN, Czech Republic) at an acceleration voltage of 200 KV. For TEM measurements, samples were primarily sonicated for 5 hours in ethanol, and left to dry overnight. After that the sample was prepared by dropping a highly diluted mixture on the carbon-coated copper grid.

“Transmission electron microscopy (TEM) analysis, FEI Tecnai G2 F20 S-TWIN”

2.4.4. Scanning Electron Microscope (SEM)

Scanning electron microscope (SEM) and energy dispersive X-ray (EDX) mensuration were performed using a (FEI Nova NanoSEM 450 and FEI Quanta 200, Czech Republic) to exhibit the surface morphology and identify the elemental composition of both the nanofibers and nanocomposites. After sputter coating with gold, sample measurements were achieved; the distribution of fiber size was measured randomly by using suitable software.

“Scanning electron microscope (SEM), FEI Nova NanoSEM 450”

“Scanning electron microscope (SEM), FEI Quanta 200”

2.4.5. Electrochemical Technique

Electrochemical behavior of the methanol, ethanol Oxidation and a mixture of both was tested using an electrochemical workstation (GAMRY 3000 potentiostat/galvanostat/ZRA). A GCE was used as a working electrode. Ag/AgCl electrode (3 M KCl) and a platinum wire was used as the counter and reference electrode, successively. The glass carbon electrode was washed by mechanical burnish with aqueous slurries of smooth alumina powder (down to 0.03 μm) respectively and was then cleaned carefully with double distilled water. The electrocatalytic activity for the different catalyst was investigated by CV measurements in 1 M NaOH + (1 M methanol, 1 M ethanol and 0.5 M methanol+ 0.5 M ethanol) from 0 V 1.0 V (vs Ag/AgCl). All the electrochemical tests were achieved at a scan rate of 50 mV s^{-1} for 10 runs. CA measurements were studied in only methanol-contained NaOH solution at different applied voltage based on oxidation peak for 1000 s. All electrolytes were purged with N_2 gas for 30 minutes to remove any dissolved oxygen prior to the measurement.

"GAMRY reference 3000 potentiostat/galvanostat/ZRA"

2.4.5.1. Preparation of Electrode

The electrochemical composite catalyst was synthesized as follows; 1 mg of carbon fiber based PAN was sonicated for 4 h in 1 mL of 2% Nafion solution. After sonication, 5 µL of the producing ink was cast over a GCE (over an area of 0.2 cm^2) and dried at room temperature for 8 hours. With the little electrolyte that is utilized in the measurement the surface was flushed, prior to inserting the electrode in the electrolytic cell (Figure. 26).

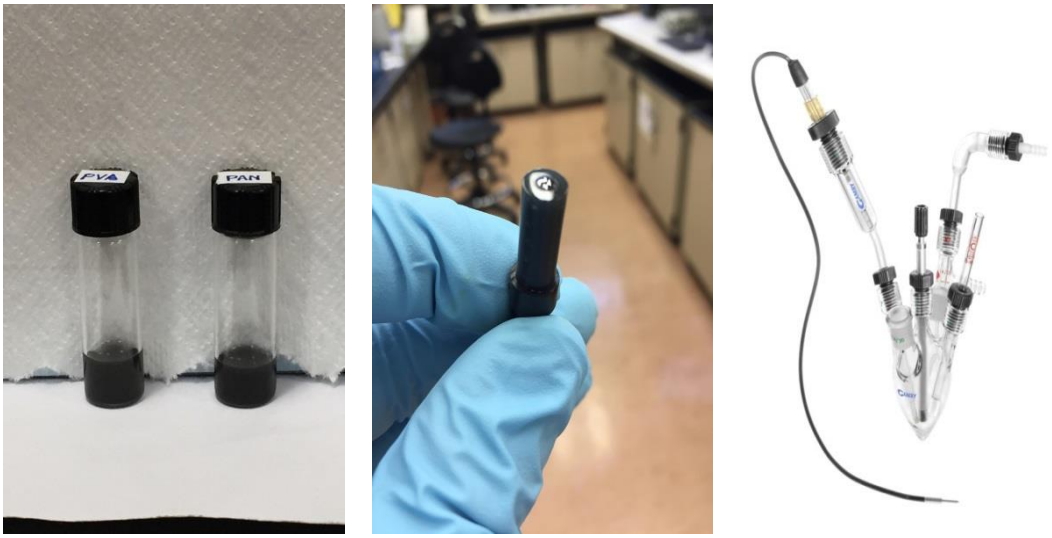

Ink samples **Glass carbon Electrode** **Electrochemical cell**

Figure 26. "Illustrations to explaining electrode preparation."

SECTION 3: RESULTS AND DISCUSSION

PART 3.A: PREPARATION OF ELECTROSPUN FIBERS COMPOSITE

3. Results and Discussion

3.A. Preaparation of Electrospun Fibers Composite

3.A.1. Electrospinning Processing Parameters

Many different parameters affect the produced fiber morphology, elongation and diameter produced by the electrospinning process. In this research, we concentrated on several parameters to include viscosity, concentration, flow rate and the space between needle and collector. According to the literature review, I controlled the electrospinning operation by preserving the optimum variables at constant values, while changing the parameter under continuous investigation and observation. Generally, the optimum parameter values which were used in this research in the production of symmetric, dense, and homogenous and with passable diameters of composite fibers, as shown in the (Table. 2)

Table 2.

Optimum parameters for fabricated electrospun fibers.

Formulations	**PAN**
Based polymers (w/v%)	10
Polyaniline (PANi) (w/w%)	5 10 15 20
Graphene (w/w%)	3
Needle size (Gauge)	22
Feed rate (mLh^{-1})	0.5
Voltage (KV)	20
Distance from collector (cm)	20
Humidity (RH%)	25±1

3.A.1.1. Impact of solution concentration

Molecular weight and viscosity are the most important parameters concerning the concentration of polymer solution. Preserving the continuity of the jet through electrospinning is fundamentally contingent on the polymer solution viscosity and, thus, on its molecular weight [115]. Selecting the appropriate solution concentration with particular viscosity will lead to the suitable entanglement of polymer molecular chains through polymerization solution, once it drops out from the needle tip and through its travel to the collector [116], [117]. The polymer solution at low concentration will lead to the nonhomogeneous fibers formation, and the process becomes electrospraying rather than spinning and fiber

formation will only take place at very low concentrations.

Furthermore, increasing the concentration of polymer solution to a specific extent will commensurately increase the solution viscosity. Consequently, this will lead to a high entanglement of polymer chains within the solution, and will hold the continuity of the jet through electrospinning and may eject the formation of beads or decrease the numbers and size of beads during fiber formation [118]–[124].

In this study, I have prepared a homogenous fiber based PAN at a concentration of 10%, to avoid errors based on a previous study (*Preparation and Characterization of Nano- Composite Materials for Industrial Applications*). Additionally, different concentrations of PANi- 5% to 20%- were prepared and successfully suspended while maintaining the concentration of graphene at 3%, as shown in (Figures. 27-30).

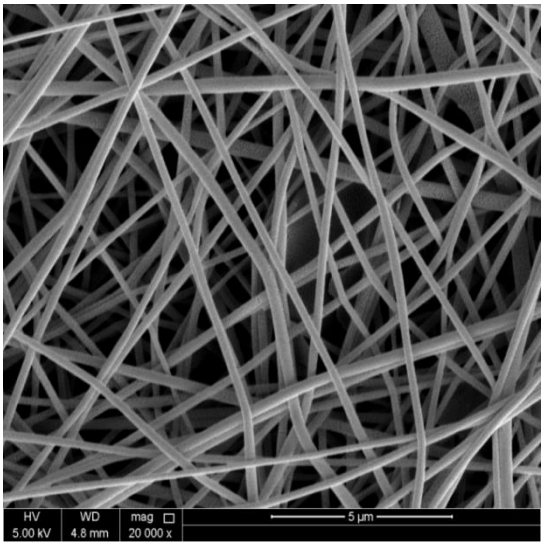

Figure 27. “Scanning electron microscope of the fabricated electrospun fibers based PAN (10% wt/wt), PANi (5% wt/wt) with graphene content of (3% wt/wt).”

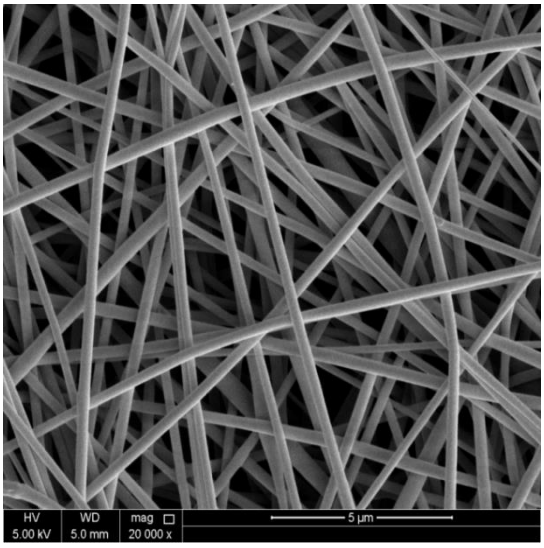

Figure 28. “Scanning electron microscope of the fabricated electrospun fibers based PAN (10% wt/wt), PANi (10% wt/wt) with graphene content of (3% wt/wt).”

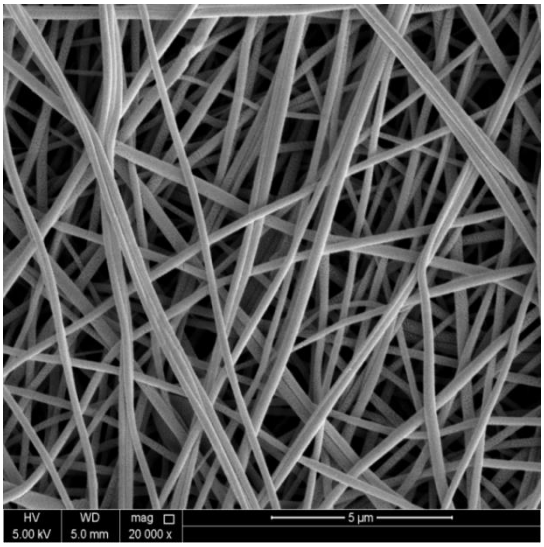

Figure 29. “Scanning electron microscope of the fabricated electrospun fibers based PAN (10% wt/wt), PANi (15% wt/wt) with graphene content of (3% wt/wt).”

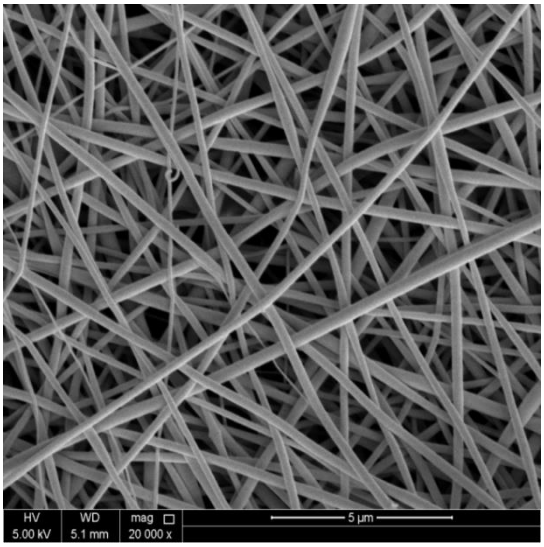

Figure 30. “Scanning electron microscope of the fabricated electrospun fibers based PAN (10% wt/wt), PANi (20% wt/wt) with graphene content of (3% wt/wt).”

3.A.1.2. Impact of Flow Rate

One of the important parameters that dominate the Taylor cone stability of a polymer solution is the feeding rate in the electrospinning technique. Overall, research has shown that a lower flow rate will fabricate fibers with smaller diameter [125]. On other hand, increasing the flow rate will lead to increasing the solution amount on its way out of the needle tip towards the collector and this will make it vulnerable to possible droughts before the fibers reach their desired destination, which leads to the formation of the beads within resulting fibers [126]. The empirical results from the practical experiments confirmed that lowering the flow rate to 0.5 mL.hour^{-1} with decreasing diameter size will display satisfactory results, as shown in (Figures. 31-34).

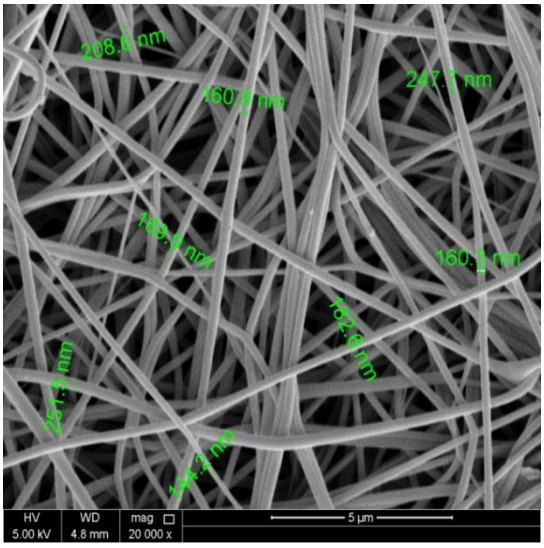

Figure 31. “Scanning electron microscope of the fabricated electrospun fibers based PAN (10% wt/wt), PANi (5% wt/wt) with (3% wt/wt) graphene at flow rate of 0.5 mL/h.”

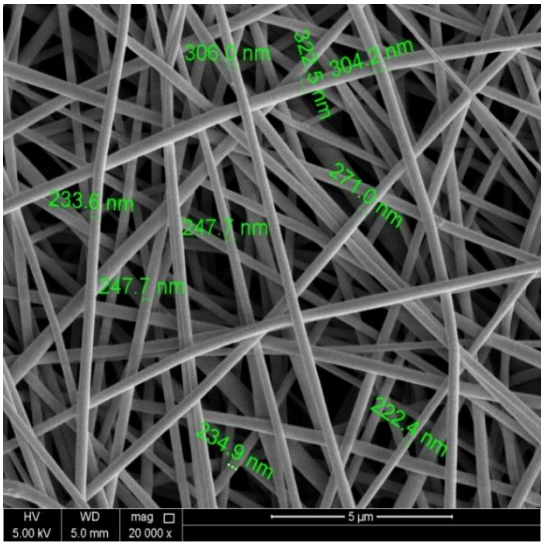

Figure 32. “Scanning electron microscope of the fabricated electrospun fibers based PAN (10% wt/wt), PANi (10% wt/wt) with (3% wt/wt) graphene at flow rate of 0.5 mL/h.”

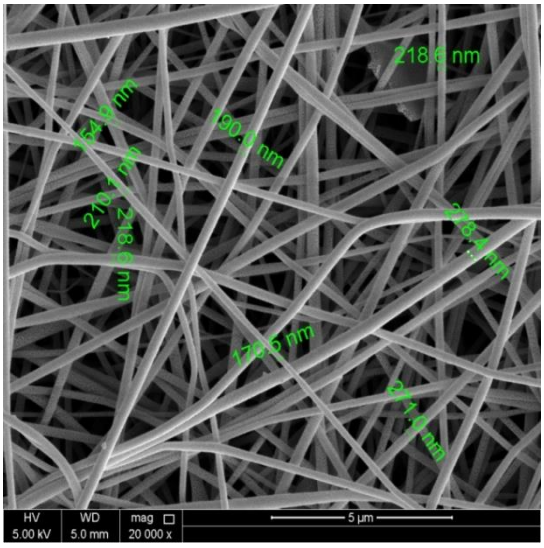

Figure 33. “Scanning electron microscope of the fabricated electrospun fibers based PAN (10% wt/wt), PANi (15% wt/wt) with (3% wt/wt) graphene at flow rate of 0.5 mL/h.”

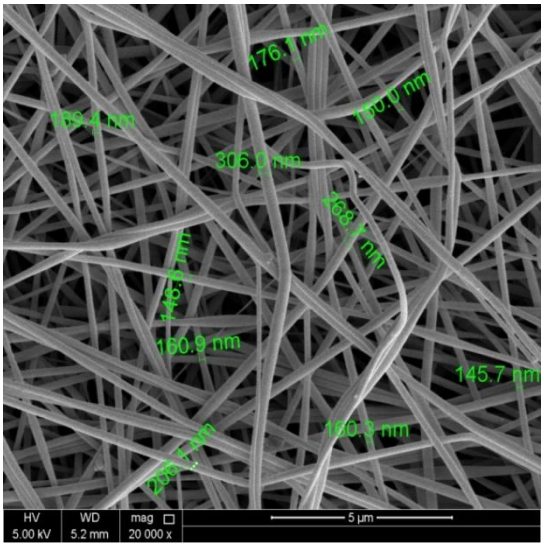

Figure 34. “Scanning electron microscope of the fabricated electrospun fibers based PAN (10% wt/wt), PANi (20% wt/wt) with (3% wt/wt) graphene at flow rate of 0.5 mL/h.”

3.A.1.3. Impact of Distance between Needle and Collector

Researches have exhibited that the distance between the tip of the needle and the collector must be preserved in order to give appropriate time for the fibers to dry before reaching the collector- allowing the solvent to evaporate [127]. The formation of beads within fibers is the result of inappropriate distance between the needle tip and the collector [128]. Nevertheless, no real effect on the morphology of produced fiber was evident on specific polymers, such as polyvinylidene difluoride (PVDF) [129], chitosan [130], gelatin [127], and PVA [126] with regard to changing the distance between the tip of needle and the collector. Instead, by electrospinning a rounder and flatter fiber was produced at different distances between needle and collector of silk-like polymers [116]. Furthermore, with a close distance between the needle tip and collector smaller fibers were obtained for bisophenol-A polysulfone [130]. However, with increased distance and higher required time the fibers will be stretched, before their deposition on the collector [22], [131], [132]. Moreover, at considerable distance between needle tip and collector may lead to non-deposition of fibers [132].

Throughout my study, based on previous work mentioned earlier, I used a distance of 20 cm between needle tip and collector as an optimum distance, because it shows a denser fiber structure, as shown in (Figures. 35-38).

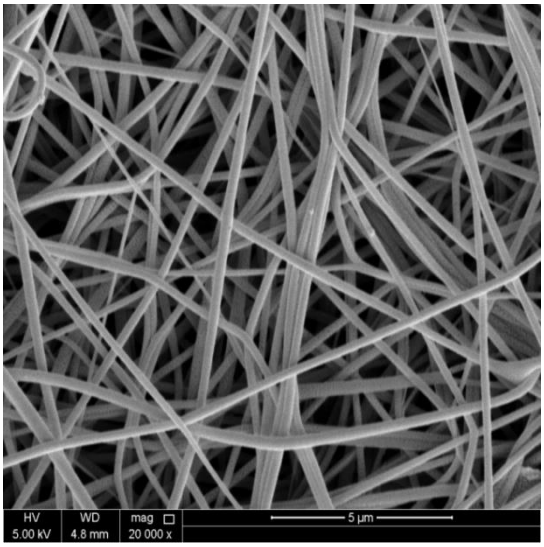

Figure 35. “SEM image of electrospun fibers based PAN (10% wt/wt), PANi (5% wt/wt) with (3% wt/wt) graphene at adjusted distance between tip and collector of 20 cm.”

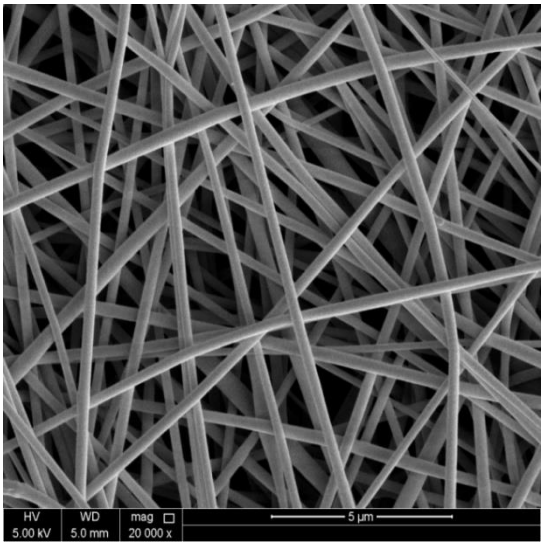

Figure 36. “SEM image of electrospun fibers based PAN (10% wt/wt), PANi (10% wt/wt) with (3% wt/wt) graphene at adjusted distance between tip and collector of 20 cm.”

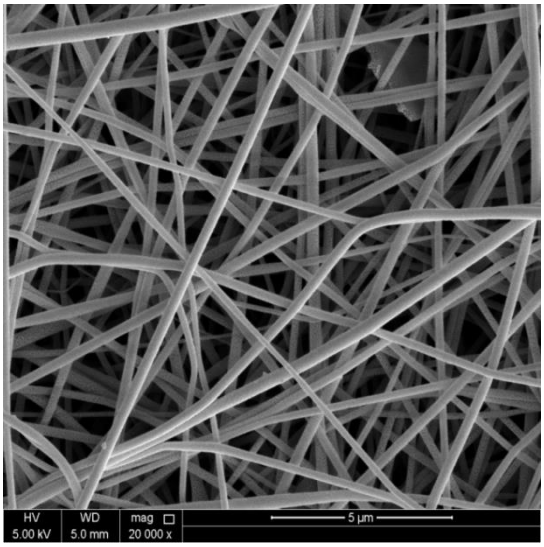

Figure 37. “SEM image of electrospun fibers based PAN (10% wt/wt), PANi (15% wt/wt) with (3% wt/wt) graphene at adjusted distance between tip and collector of 20 cm.”

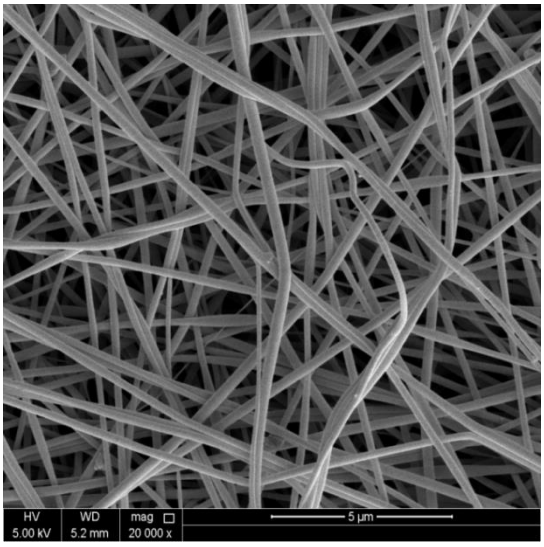

Figure 38. “SEM image of electrospun fibers based PAN (10% wt/wt), PANi (20% wt/wt) with (3% wt/wt) graphene at adjusted distance between tip and collector of 20 cm.”

3.A.1.4. Impact of Graphene Inclusion

The graphene insertion has a high effectiveness on increasing the conductivity of the fabricated fibers. Notwithstanding, to prepare a polymer solution with insertion of a particular amount of graphene to form a homogenous solution is not a simple task. In this work, I have loaded an enough quantity of graphene into the polymer solution by 3% wt/wt. Through scanning electron microscopy **(**SEM) images appeared perfectly homogeneous fibers, as shown in (Figure. 39). Further, this homogeneity is confirmed by transmission electron microscopy (TEM) images, as shown in (Figures. 40-44).

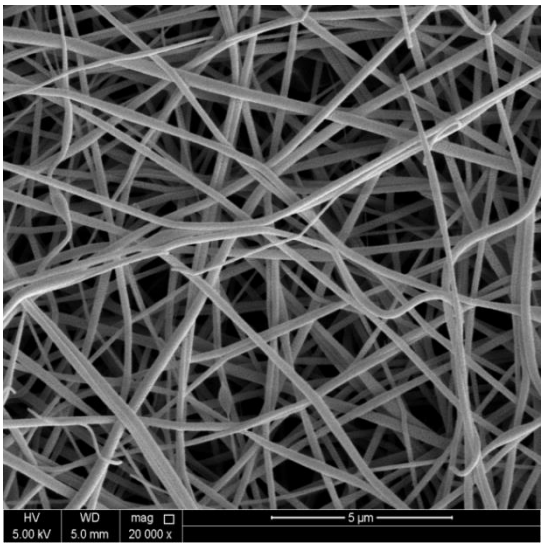

Figure 39. “SEM image of fabricated electrospun fibers based PAN (10% wt/wt) with graphene content of (3% wt/wt).”

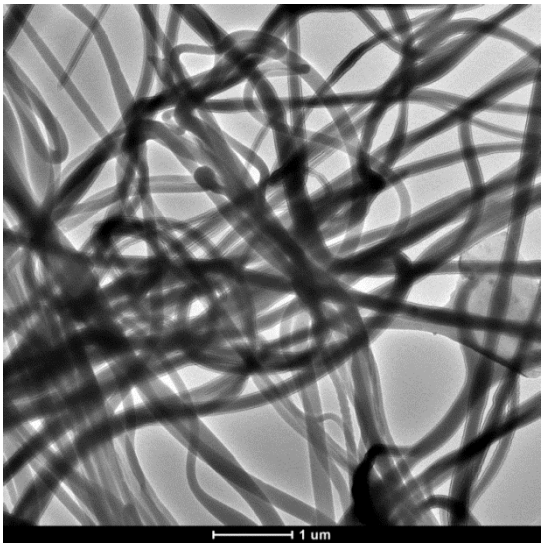

Figure 40. “TEM image of fabricated electrospun fibers based PAN (10% wt/wt), PANi (20% wt/wt) with graphene content of (3% wt/wt) at 1 μm.”

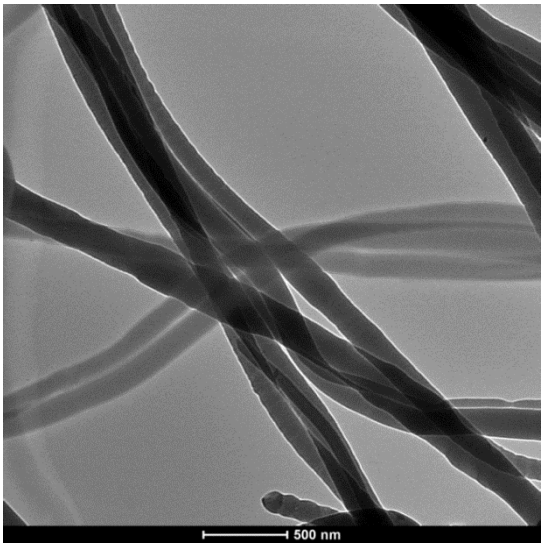

Figure 41. “TEM image of fabricated electrospun fibers based PAN (10% wt/wt), PANi (20% wt/wt) with graphene content of (3% wt/wt) at 500 nm.”

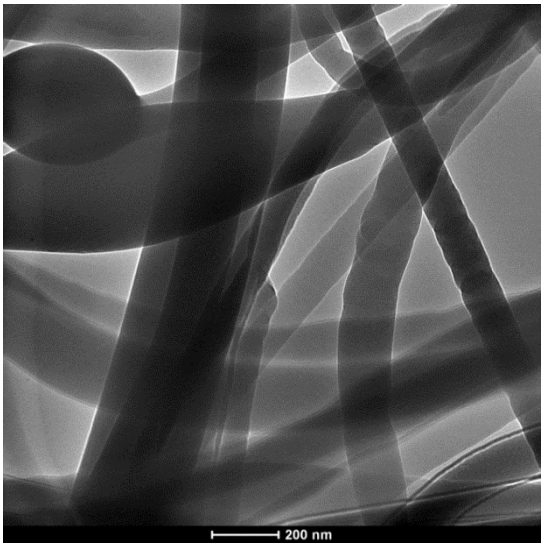

Figure 42. “TEM image of fabricated electrospun fibers based PAN (10% wt/wt), PANi (20% wt/wt) with graphene content of (3% wt/wt) at 200 nm.”

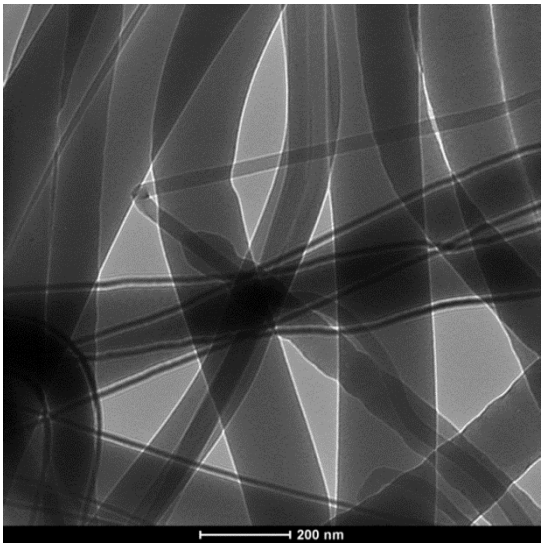

Figure 43. “TEM image of fabricated electrospun fibers based PAN (10% wt/wt), PANi (20% wt/wt) with graphene content of (3% wt/wt) at 200 nm.”

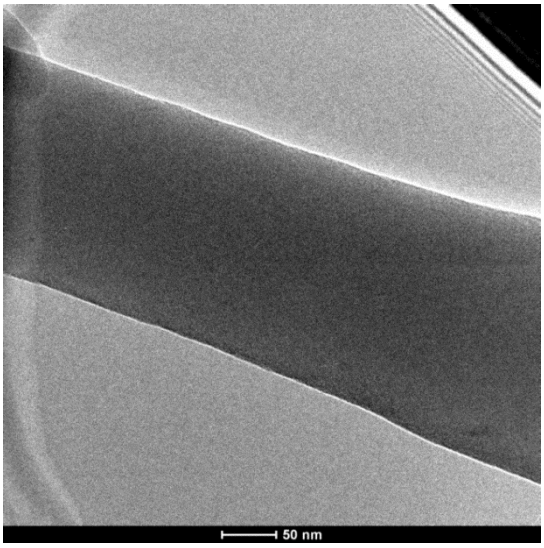

Figure 44. “TEM image of fabricated electrospun fibers based PAN (10% wt/wt), PANi (20% wt/wt) with graphene content of (3% wt/wt) at 50 nm.”

PART 3.B: FIBERS AND CARBON NANOFIBERS COMPOSITE BASED POLYACRYLONITRILE

3.B. Fibers and Carbon Nanofibers Composite Based Polyacrylonitrile

3.B.1. Characterization of Fibers and Carbon Fibers Composite Based Polyacrylonitrile

3.B.1.1. Scanning Electron Microscope (SEM)

We used a Scanning electron microscope (SEM) to examine the external morphological properties (texture) and elemental analysis of the carbon nanofibers surface. As mentioned above, several factors affect the polymer fibers production and therefore carbon nanofibers. (Figure. 45) shows long, uniformly, smooth electrospun polymer fibers based pure PAN, PAN/G, and PAN/PANi/G was fabricated under standard conditions with respect of parameters effect. However, the average diameter of pure PAN is 678 nm as shown in Figure. 45 (a). When graphene is added to the pure PAN polymer solution Figure 45 (b) the average diameter is reduced to 181 nm, which assured us of the successful formation of the blend sought. While mixing PAN and PANi with the polymer solution (Figure 45c) the average diameter is slightly increased compared to PAN/G at 191 nm, which confirmed the existence of PANi mixed with PAN [112]. Additionally, graphene prevented the excessive increasing of the average diameter. However, the transformation process from polymeric electrospun fibers to carbon fibers was the reason of shrinking fibers with an average diameter of 126.1 nm, as shown in (Figure. 46). This could be explained as a result of

stabilization and carbonization process, since various side products are freed, as a conclusion of cyclization mechanism and carbon fibers formation [133], as previously explained in (Figure. 19 and 20).

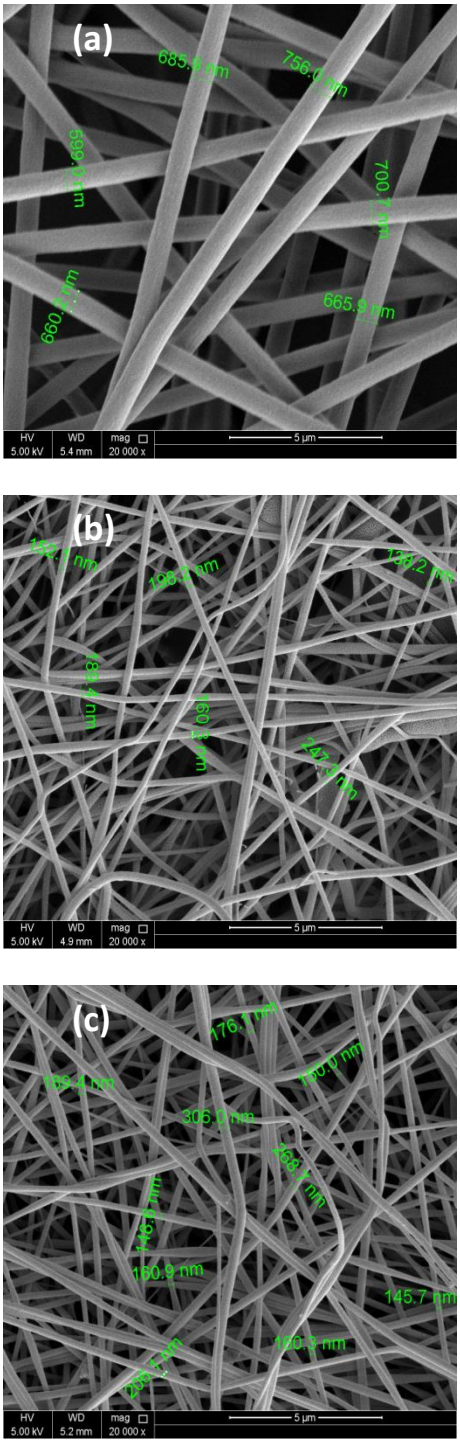

Figure 45. “SEM images of the fabricated electrospun fibers of (a) pure PAN, (b) PAN/G, and (c) PAN/PANi/G.”

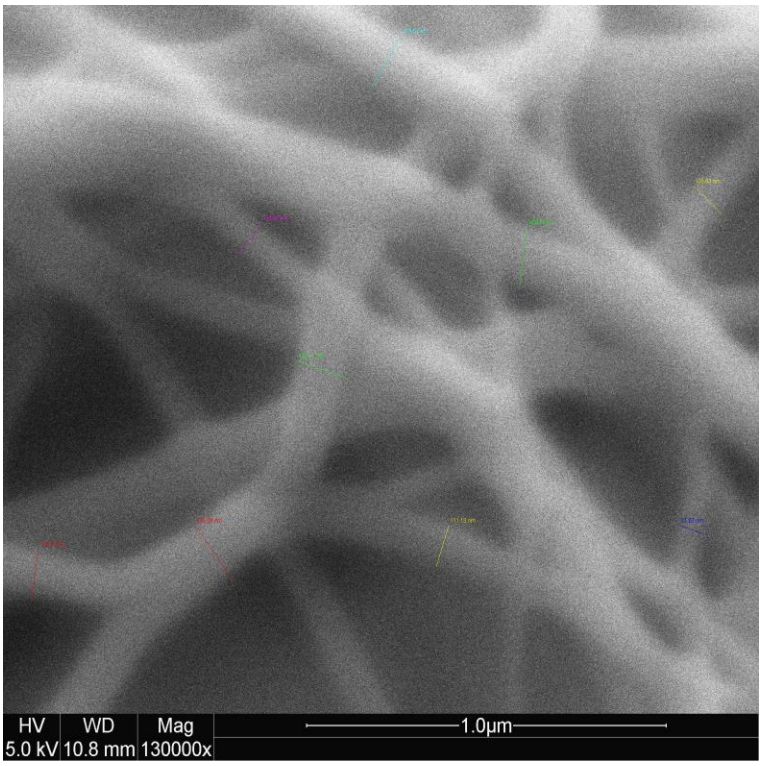

Figure 46. “SEM images for carbon fibers based PAN.”

In (Figure. 47) we can see the SEM images of carbon fibers before and after deposition of catalyst, the difference is obvious between Figure 47 (a) and (b) through the shape of fibers. The first figure shows that the carbon fibers are homogeneous and smooth, while in the second figure it shows the formation of clusters on the fiber, which indicates the successful deposition process.

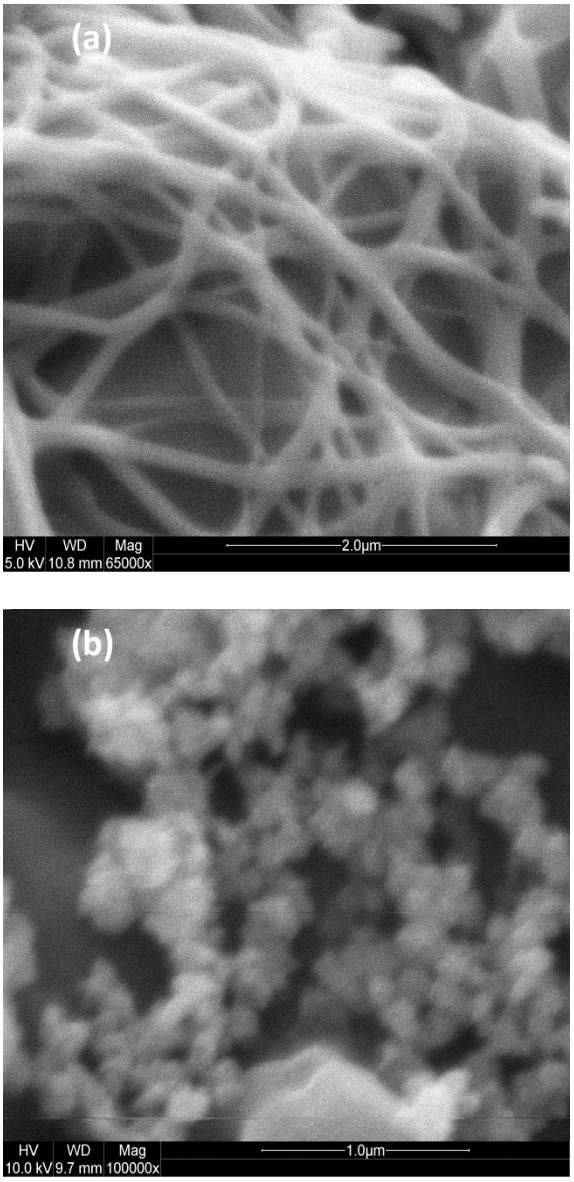

Figure 47. “SEM images of carbon fibers based PAN (a) before catalyst deposition, and (b) after catalyst deposition.”

3.B.1.2. Energy Dispersive X-Ray Spectroscopy (EDX)

Energy dispersive X-ray spectroscopy (EDX) is an analytical technique utilized for elemental analysis or chemical characterization of materials. (Table. 3) describes the determination of carbon and nitrogen for the electrospun fibers in both pure PAN and PAN/20% Polyaniline/3% Graphene composite in (wt.%). The results show that, the content of carbon and nitrogen increased from pure PAN to PAN/PANi/G. The increase of carbon and decrease of nitrogen content may be attributed to the presence of polyaniline.

Table 3.

Energy dispersive X-ray (EDX) of pure electrospun PAN fiber and electrospun PAN/PANi/G composite fiber.

PAN/PANi	%C		%N	
	wt.%	at.%	wt.%	at.%
Blank PAN	66.10	69.10	33.90	30.54
PAN/20% PANi/3% G	70.11	73.23	29.89	26.77

3.B.1.3. X-Ray Diffraction (XRD)

X-ray diffraction spectroscopy (XRD) is one of the most significant implementations to characterize the crystal structure of materials. (Figure. 48) Synopsis is the main structural change exhibited in the XRD spectra. All samples showed major intensity peak and stable at 2Ɵ values between 16° to 17°, which

emphasizes the existence (1 0 0) plane of a hexagonal structure. Another peak with weak diffraction for (1 1 0) plane appeared approximately at 29° of 2Θ value [134]. Moreover, the peak intensity for (1 0 0) and (1 1 0) were significantly influenced with changing PANi loading as is evident in the figure. Note it been has been enhanced and increased crystallization through loaded increasing of PANi which shows at 26.2° and correspond with (2 0 0) crystal plane[135].

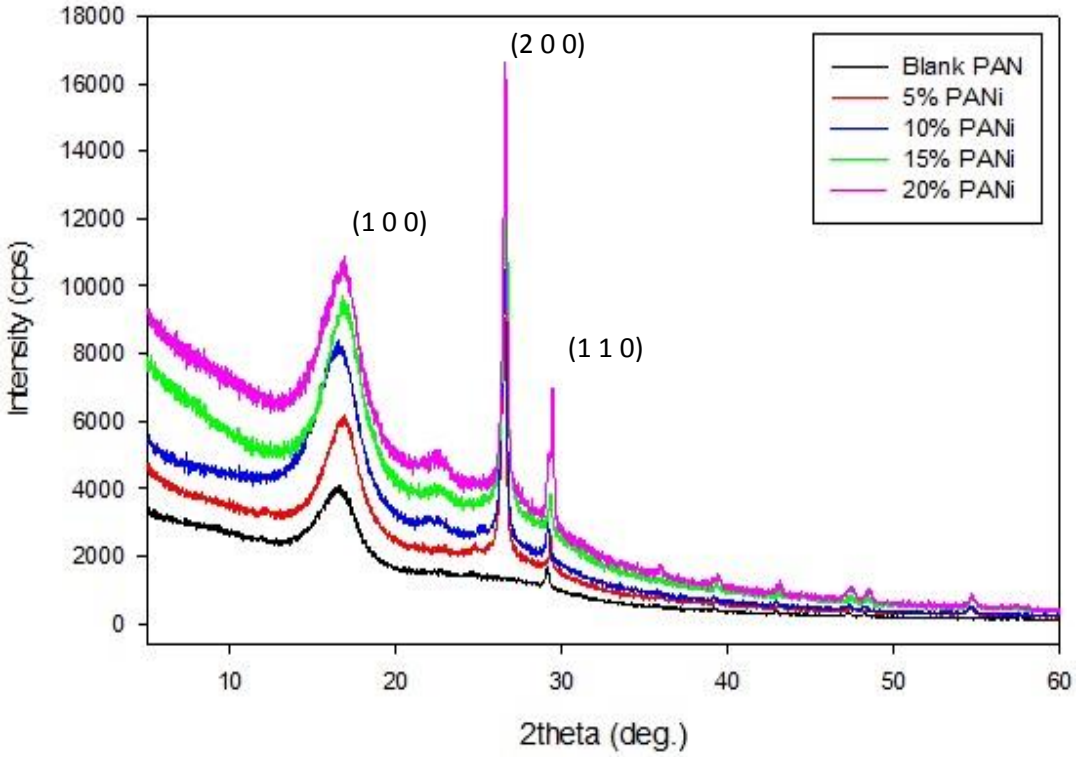

Figure 48. "XRD spectra for PAN with different concentrations of PANi."

3.B.1.4. X-Ray Photoelectron Spectroscopy (XPS)

With the increasing demand for high performance materials, surface engineering is becoming more important. The surface of the material is the point of interaction with the foreign environment and other materials, thus much of the problems related with modern materials can be fixed by the realization of chemical and physical interactions that happen on the surface, or on the interfaces of the layers of the material. Modification of surface can be used to change or improve these properties, so surface analysis is utilized to understand the surface chemistry of the material, and to investigate the effectiveness of surface engineering. Wherefore, X-ray photoelectron spectroscopy (XPS) is one of most important criterion tools for surface characterization.

Through this study, I performed an X-ray photoelectron spectroscopy (XPS) for carbon fiber powder (CFP) and carbon fiber deposited on glass carbon electrode with catalyst contains of (Ni, Co and Cu) based PAN fiber, that's I will call it carbon fiber on electrode (CFE). The XPS spectra for C 1s, N 1s and, O 1s shown in (Figures. 49-51) for carbon fiber powder (CFP) samples with high resolution at 40 passing energy, respectively. In addition, the binding energy are listed in (Table. 4) for CFP. The binding energy of C 1s appears at ~285.0 eV signifies graphitic carbon C-C or represents hydroxyl C-H [136]. However, the main peak of nitrogen N 1s appears at ~400.0 eV split into two peaks, one at ~398 eV signify C=N in the rings, because it was affected by the linear chains produced by the scanty cyclization reactions, and the other at ~401.0 eV indicate graphitic nitrogen in the rings [137], [138]. The O 1s appears at ~532.0 eV which indicates C-O and C=O in the ring structure [139].

Table 4.

The binding energy of the carbon fiber powder based PAN.

	C 1s	N 1s	O 1s
Position BE (eV)	285.000	400.000	532.000

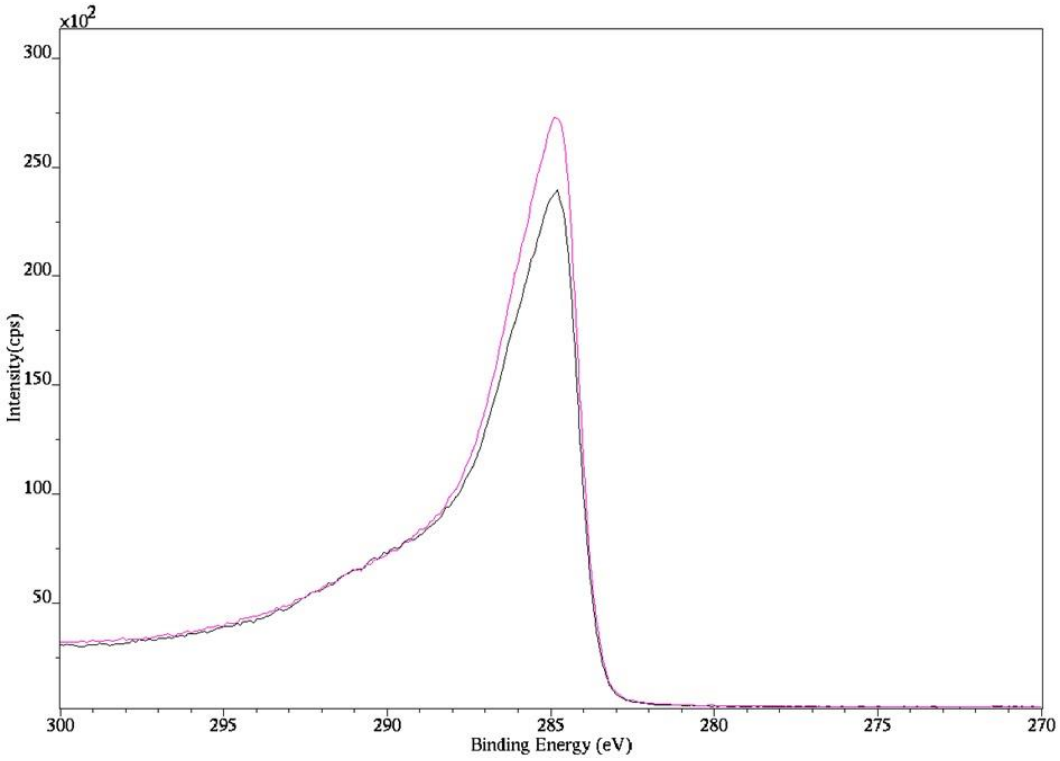

Figure 49. "High resolution XPS spectra (2 spots) for C 1s of the carbon fiber powder based PAN."

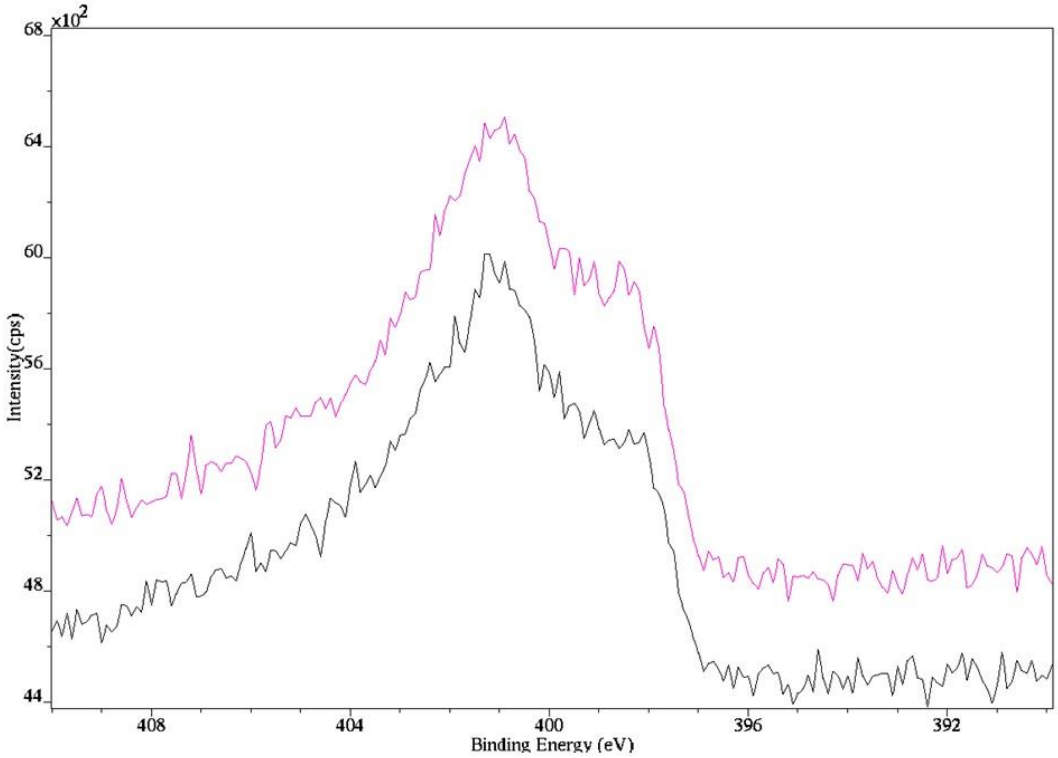

Figure 50. “High resolution XPS spectra (2 spots) for N 1s of the carbon fiber powder based PAN.”

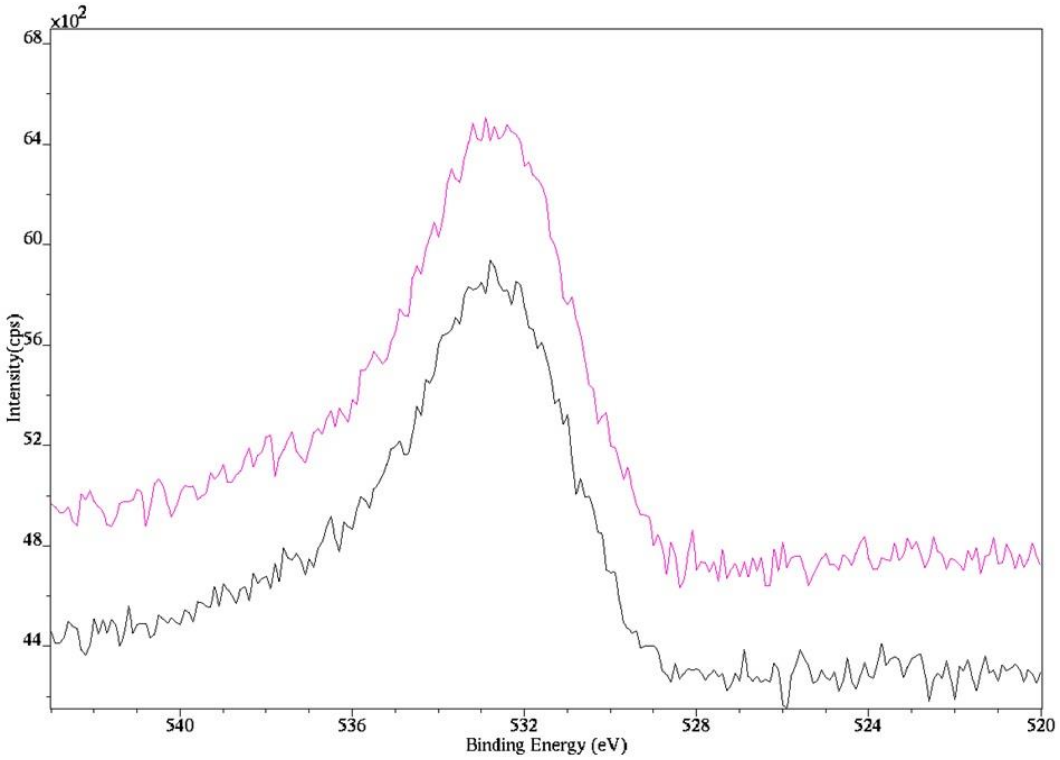

Figure 51. "High resolution XPS spectra (2 spots) for O 1s of the carbon fiber powder based PAN."

Furthermore, (Figure. 52) shows the wide scale of XPS spectrum at 160 passing energy for catalyst deposition on carbon fiber electrode (CFE) based PAN. The results showed that catalysts represented in (Ni, Co and Cu) were successfully loaded on a sample of carbon fiber based PAN. The XPS spectra for C 1s, N 1s and O 1s shown in (Figures. 53-55) for CFE samples with high resolution at 40 passing energy, respectively. Also, the binding energy are listed in (Table. 5) for CFP. In addition, A shifted slightly after catalyst deposition to become C 1s ~283.0 eV, N 1s ~398.0 eV and O 1s ~530.0 eV in the binding energy spectra of

CFE sample. The binding energy of C 1s appears at ~283.0 eV signify graphitic carbon C-C or represent in hydroxyl C-H [136]. Another one of C 1s appears at ~290.6 eV indicates presence of CF_2-CF_2, due to use of Nafion as a solvent for carbon fiber [140]. However, nitrogen N 1s appears at ~398 eV signify C=N in the rings, because it was affected by the linear chains produced by the scanty cyclization reactions [137], [138]. The O 1s appears at ~530.0 eV which indicates metal oxides [141], This confirms that the metals used as catalysts in methanol, ethanol and methanol-ethanol oxidation have been converted into the oxidizing form of the metal. (Figure. 55) also shows a wide and weak peak in the bonding energy of O 1s around ~534.9 eV, this is due to the presence of fluoride produced from Nafion as mentioned above indication of O-F_x.

Table 5.

The binding energy of the carbon fiber after catalyst deposition based PAN.

	C 1s	**N 1s**	**O 1s**	**Ni 2s**	**Co 2s**	**Cu 2s**
Position BE (eV)	283.000	398.000	530.000	860.000	780.000	931.000

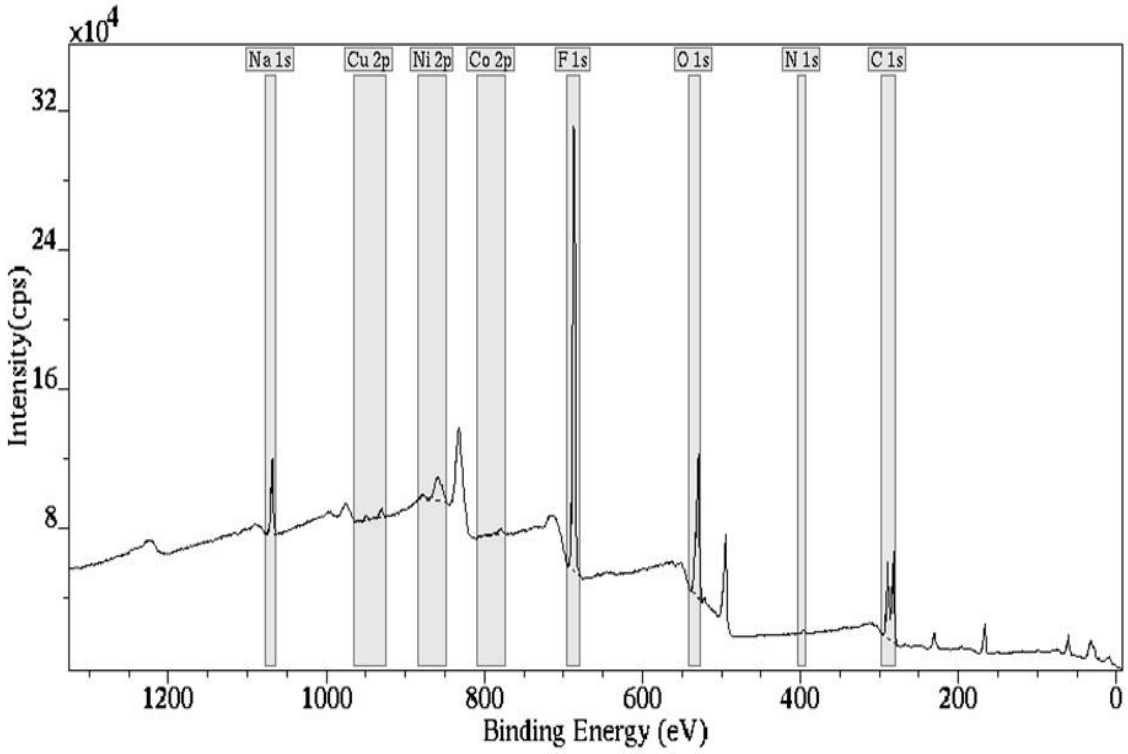

Figure 52. "XPS spectrum wide scale for catalyst deposition on carbon fiber based PAN."

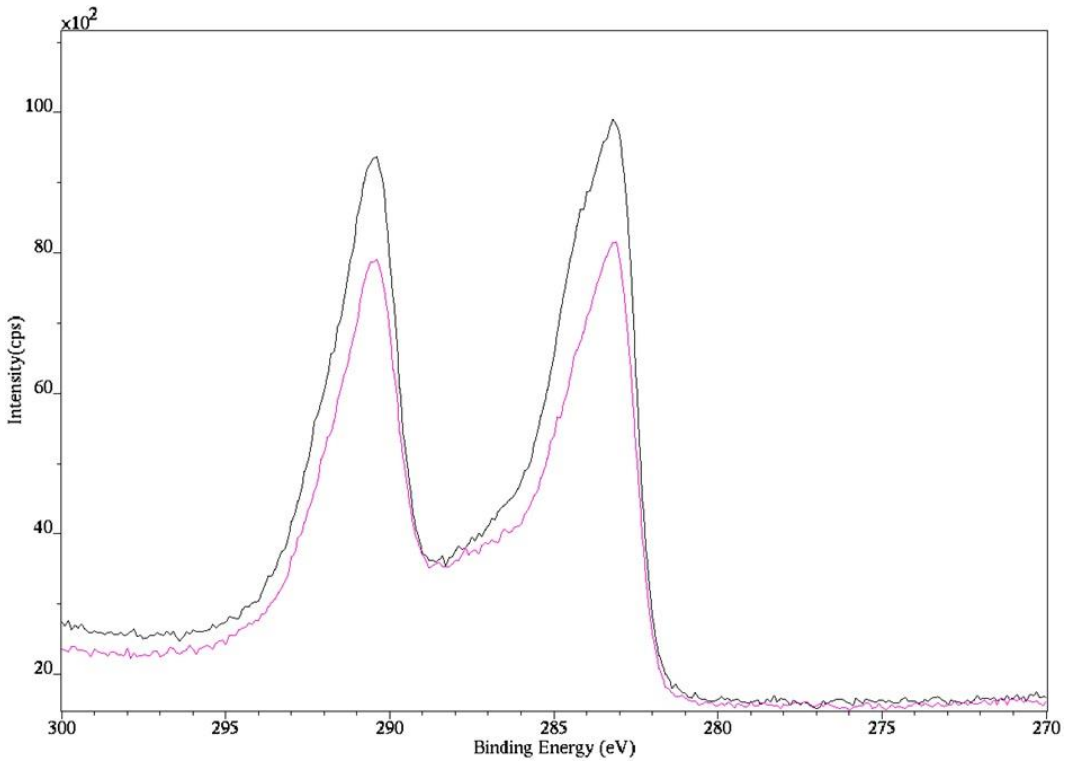

Figure 53. “High resolution XPS spectra (2 spots) for C 1s after catalyst deposition on carbon fiber based PAN.”

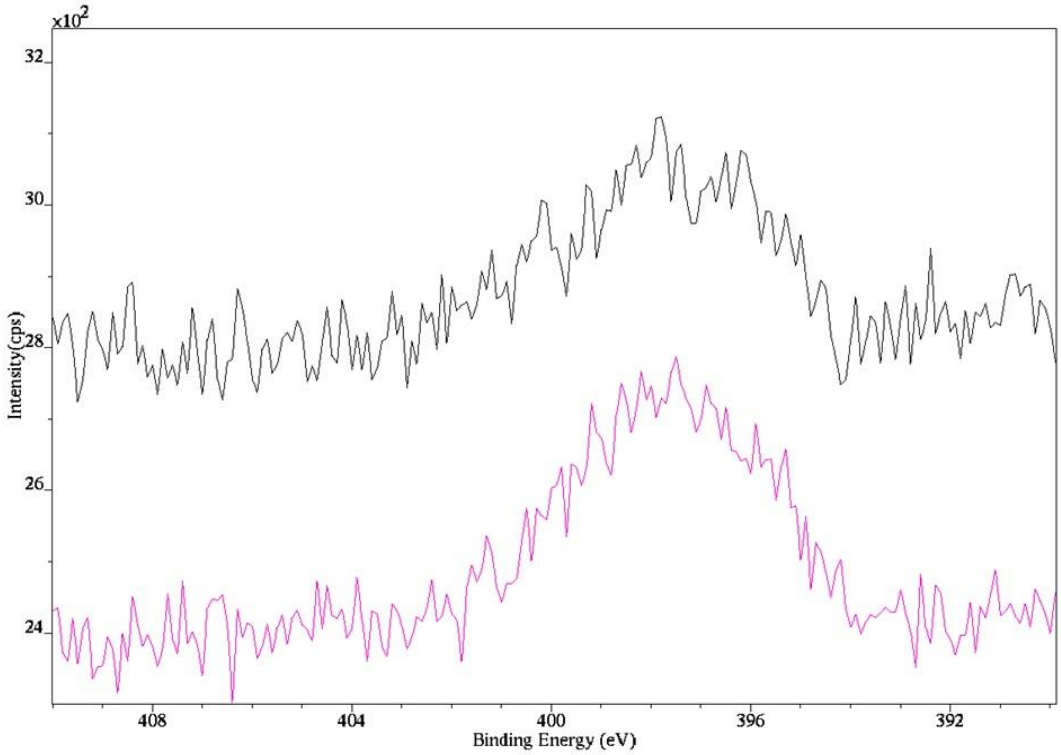

Figure 54. “High resolution XPS spectra (2 spots) for N 1s after catalyst deposition on carbon fiber based PAN.”

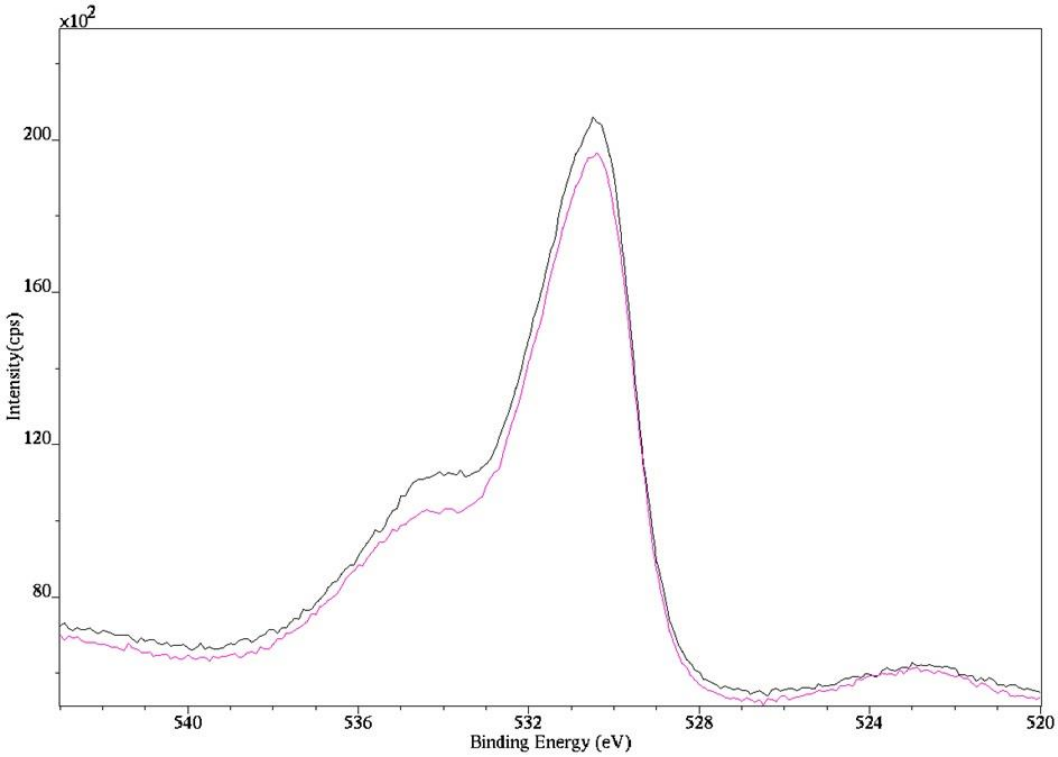

Figure 55. “High resolution XPS spectra (2 spots) for O 1s after catalyst deposition on carbon fiber based PAN.”

PART 3 C: ELECTROCHEMICAL CHARACTERIZATION OF CARBON NANOFIBERS COMPOSITE BASED POLYACRYLONITRILE

3.C. Electrochemical Characterization for Carbon Nanofibers Composite Based Polyacrylonitrile

(Figure 56) shows the cyclic voltammograms (CVs) at a scan rate of 50 mV S^{-1} in 1 M NaOH + 1 M methanol solution using PAN-CNF/GC with Ni-Co-Cu nanocatalysts. The nanocatalysts were deposited using different times of electrodeposition (0, 600, 1200, 1800 and 2400 s) 1 at -1 V Vs RHE. This figure shows the effect of electrodeposition time of the electrocatalytic behavior of the CNF/nanocatalyst. It is clear the increase of the anodic oxidation peak currents with increasing the electrodeposition time where the anodic peak current increased to 3.3 mA cm^{-2} at the 2400 s of electrodeposition time. The reason for the increase of the current is attributed to the increase of the surface area of the nanocatalyst as the loading percentage increases with the increase in the time of electrodeposition. (Figure. 57) shows the current transient for Ni-Co-Cu at PAN-CNF/GCE which are deposited on the PAN-CNF/GC at different times of electrodeposition (600, 1200, 1800 and 2400 Seconds) in 1 M NaOH + 1 M methanol solution. It shows the stability of the electrode over long time. Furthermore, the poisoning of the electrode is checked by using the same electrodes used in the current transients shown in (Figure. 57) to measure their CVs again in 1M methanol + 1 M NaOH solution. (Figure. 58) shows the CVs for PAN-CNF/GC with electrodeposited Ni-Co-Cu at different times of electrodeposition (600, 1200, 1800 and 2400 s) on glassy carbon electrode in 1

M NaOH + 1 M methanol solution before and after the corresponding current time (IT) transients shown in (Figure. 57). It is clear that there is a poisoning of the electrode by about 50% as the current is reduced to half of its initial values. This indicates the adsorption of CO on the surface of the Cu-Co-Ni during the electro oxidation of methanol.

The prepared nanocatalysts on the PAN-CNF/GC electrode was tested towards the electrooxidation of a mixture of C1 and C2 fuels (methanol + ethanol). Surprisingly, the electrocatalytic behavior of the Cu-Co-Ni nanocatalyst supported by PAN-CNF towards this fuel mixture was much higher than that for methanol or ethanol alone. (Figure. 59) shows the CVs for PAN-CNF with electrodeposited Ni-Co-Cu at 1200 s in different electrolytes (1 M NaOH + 1 M methanol), (1 M NaOH + 1 M ethanol) and (1 M NaOH + 0.5 M methanol + 0.5 M ethanol). As can be seen the anodic oxidation peak current for the mixture of fuel is almost doubled in presence of methanol or ethanol alone. The reason for this may be attributed to the autocatalytic reactions that occur between the intermediates that are formed and adsorbed on the surface of the nanocatalyst. A further investigation is needed using spectroelectrochemistry to study the intermediates during the electro-oxidation of this mixture of fuels.

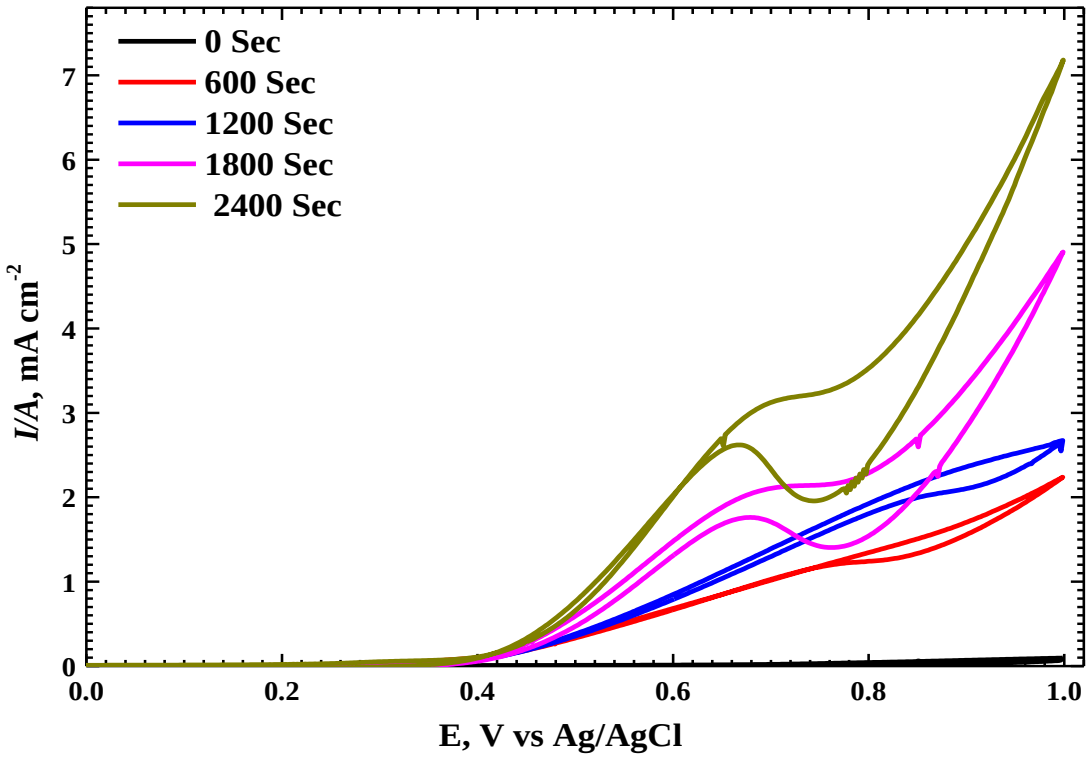

Figure 56. "Cyclic voltammogram (CV) curves for PAN-CNF with electrodeposited Ni-Co-Cu at different deposited time on glassy carbon electrode in 1 M NaOH + 1 M methanol solution."

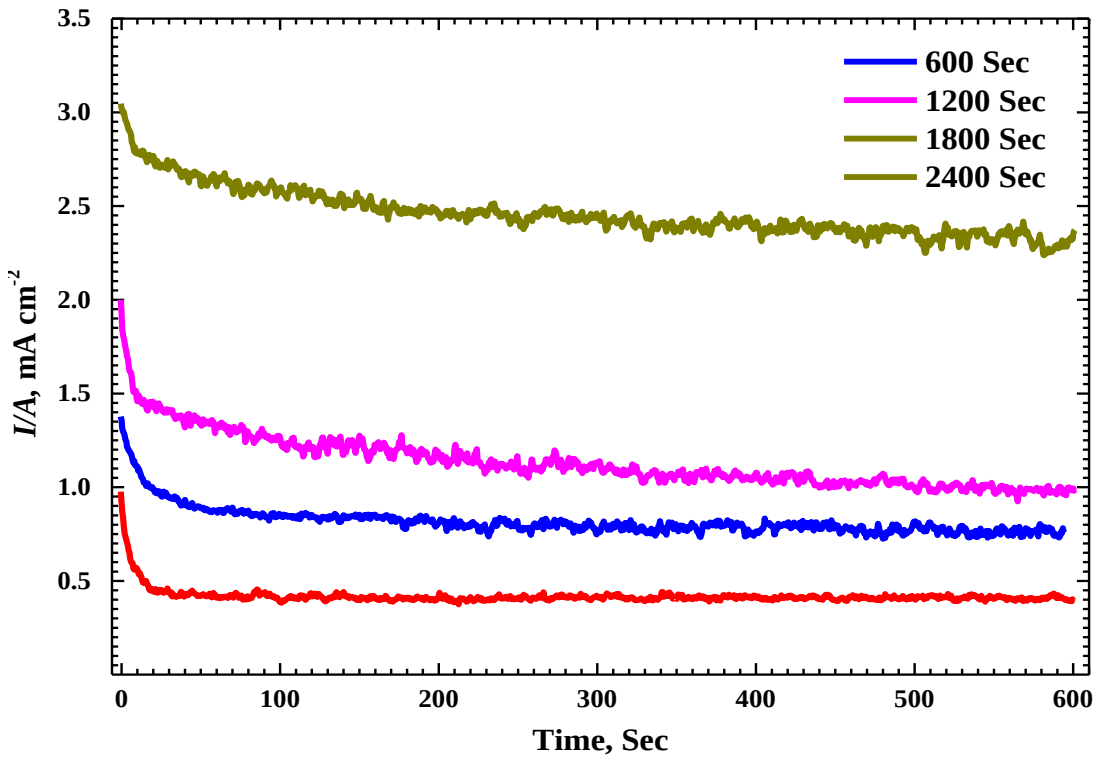

Figure 57. "Current transients for PAN-CNF/GC with electrodeposited Ni-Co-Cu at different electrodeposition time (600, 1200, 1800 and 2400 s) in 1 M NaOH + 1 M methanol solution."

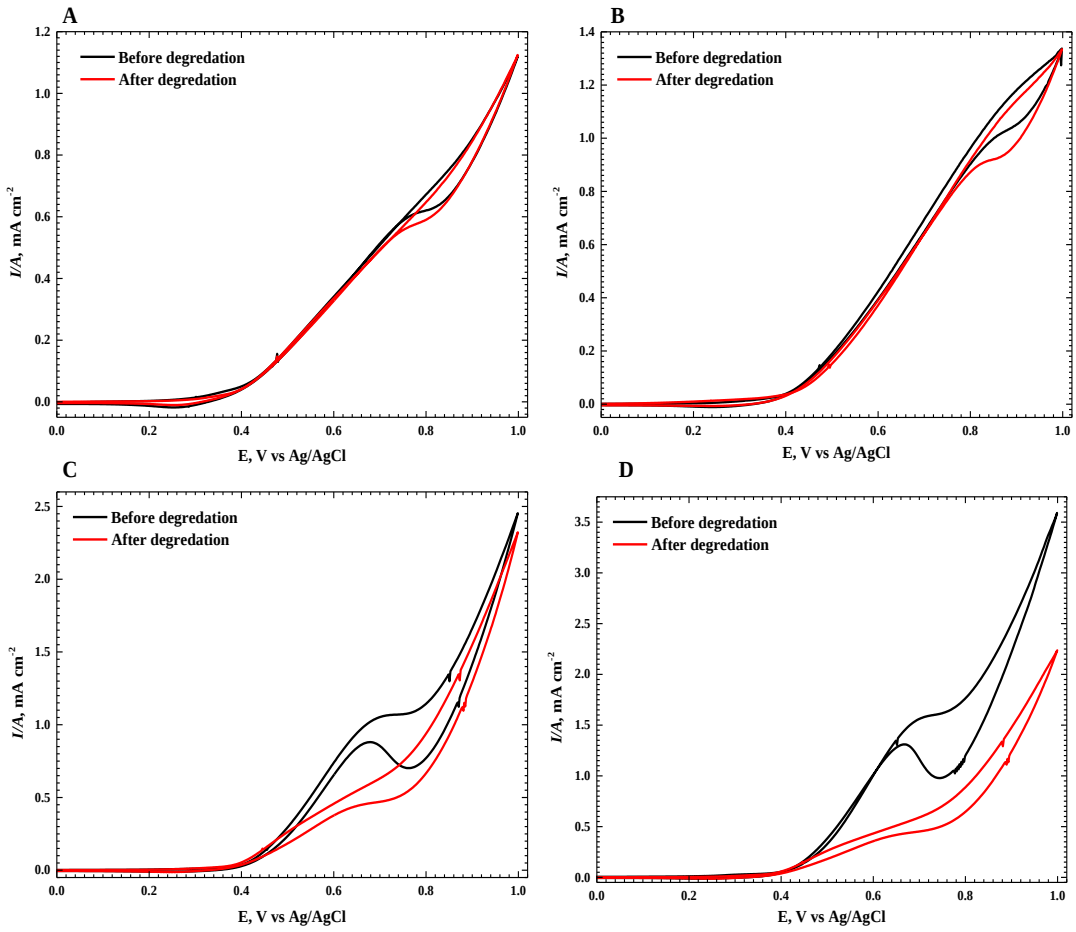

Figure 58. "CV curves for PAN-CNF with electrodeposited Ni-Co-Cu at different times of electrodeposition (600, 1200, 1800 and 2400 s) on glassy carbon electrode in 1 M NaOH + 1 M methanol solution before and after the corresponding IT transients shown in (Figure 54)."

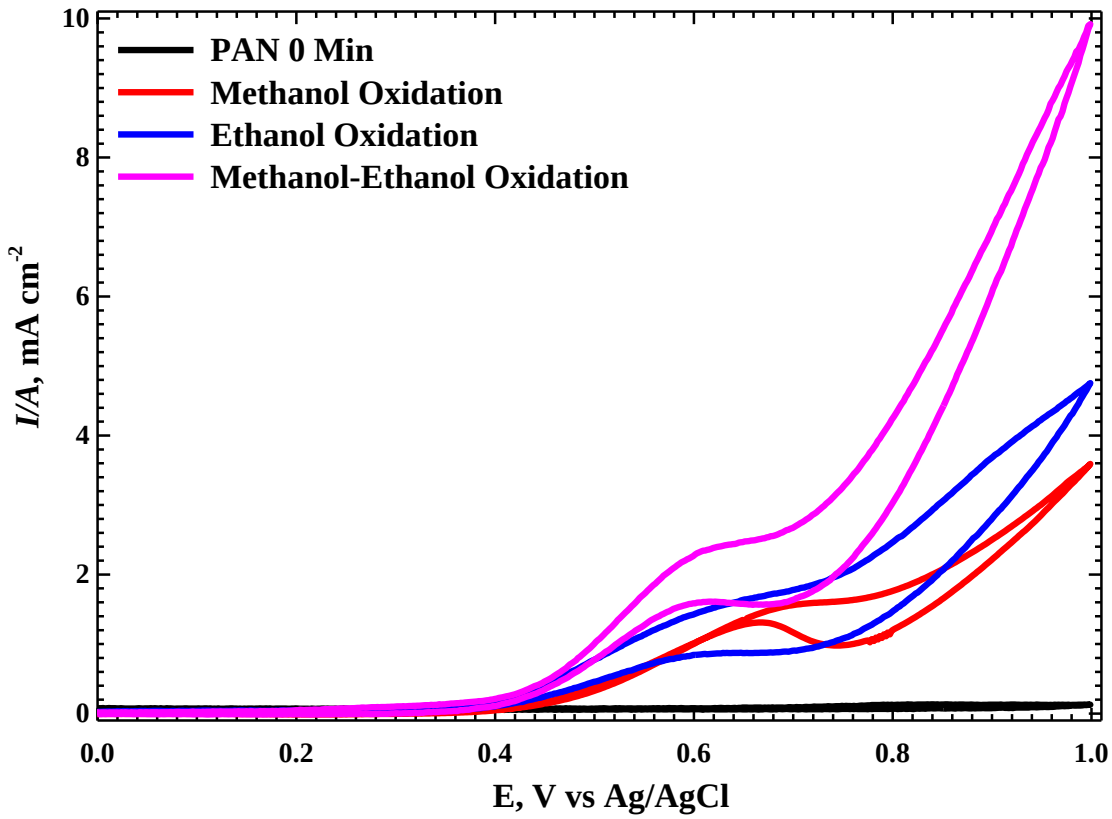

Figure 59. "CV curves for PAN-CNF with electrodeposited Ni-Co-Cu at 1200 s deposited time on glassy carbon electrode in different electrolyte 1 M NaOH + 1 M methanol, 1 M NaOH + 1 M ethanol and 1 M NaOH + 0.5 M methanol + 0.5 M ethanol."

SECTION 4: CONCLUSION

4. Conclusion

In this work, we successfully sophisticated a novel nanostructure material of a low cost non-precious effective catalyst. It consisted of Ni, Co and Cu deposited by an electrochemical reaction on modified carbon nanofibers to be used towards the electrooxidation of methanol, ethanol and their mixtures in alkaline mediums within DMFCs. Electrospinning technique was utilized to fabricate the nitrogen doped carbon fibers with a few nanometer diameter as an efficient and inexpensive method to produce influential catalyst based nanocomposite material for utilization in FC application.

The operation was based on polyacrylonitrile (PAN) as the polymer material doped with nitrogen using polyaniline (PANi) as a nitrogen source, with various concentrations of PANi to fabricate the nanofiber in addition to a proportion of graphene (G) to improve the conductivity properties. The fabricated polymer nanofibers were treated thermally via two steps. The first step involves stabilization in air and the second step is carbonization in a nitrogen gas atmosphere to transfer the polymer nanofibers to carbon nanofibers (CNFs). The fabricated composites were characterized by transmission electron microscopy (TEM), scanning electron microscopy (SEM), X-ray photoelectron spectroscopy (XPS), Energy dispersive X-ray spectroscopy (EDX), and X-ray diffraction (XRD). The SEM results showed that the synthesized nitrogen-doped PAN-CNFs has

uniform, continuous and bead free fibers with an average diameter of 126.1 nm. Also noted were cluster formations of nanoparticles on the PAN-CNFs after electrodeposition.

The structural and chemical properties of the resulting nitrogen-doped PAN-CNFs observed increasing crystallization with increasing in PANi concentration, as well as that of the nitrogen doped. This signifies as pyridone-like at ~398 eV and graphite-like at ~401.0 eV form into the CNF networks.

The electrodeposition for the ternary metal oxides on the nitrogen-doped PAN-CNFs surface was successfully accomplished via electrochemical deposition on GCE using different times of electrodeposition (0, 600, 1200, 1800 and 2400 s). The electrochemical results exhibited long durability and excellent electrocatalytic activity for electrooxidation of methanol. It is clear the increase of the anodic oxidation peak currents with the increasing of electrodeposition time where the anodic peak current increased to 3.3 mA cm^{-2} at the 2400 s of electrodeposition time. However, it was observed after current transient that there is a poisoning of the electrode by about 50% as the current is reduced to half of its initial values. The fuel mixture on electrochemical oxidation is almost double that in the presence of methanol or ethanol alone and can attributed to the autocatalytic reactions that occur between the intermediates that are formed and adsorbed on the surface of the nanocatalyst.

In view of the low cost and effectiveness of this, the fabricated nitrogen-doped PAN-CNF which have unique structure and excellent electrical properties held promising electrocatalyst for DMFCs.

5. Future Work

The main goal of this study was to investigate the development of a new more cost effective catalyst for fuel cells.

More experiments will be designed in the future to try a new combination of transition metals and to investigate thier catalytic activation on methanol, ethanol and different combination. In addition to that, we will try to use different techniques to activate carbon fibers support materials.

6. References

[1] A. Greiner and J. H. Wendorff, “Electrospinning: A fascinating method for the preparation of ultrathin fibers,” *Angewandte Chemie - International Edition*, vol. 46, no. 30. pp. 5670–5703, 2007.

[2] L. Wang and A. J. Ryan, “Introduction to electrospinning,” in *Electrospinning for Tissue Regeneration*, Elsevier, 2011, pp. 3–33.

[3] P. McClellan and W. J. Landis, “Recent Applications of Coaxial and Emulsion Electrospinning Methods in the Field of Tissue Engineering,” *Biores. Open Access*, vol. 5, no. 1, pp. 212–227, 2016.

[4] J. Zeleny, “The electrical discharge from liquid points, and a hydrostatic method of measuring the electric intensity at their surfaces,” *Phys. Rev.*, vol. 3, no. 2, pp. 69–91, 1914.

[5] J. Zeleny, “Instability of electrified liquid surfaces,” *Phys. Rev.*, vol. 10, no. 1, pp. 1–6, 1917.

[6] W. J. Morton, “Apparatus for electrically dispersing fluids,” vol. 7, no. 692, 1902.

[7] W. J. Morton, “Method of dispersing fluids,” no. 705, pp. 3–6, 1902.

[8] A. Formhals, “Process and apparatus for preparing artificial threads,” 1934.

[9] A. Formhals, “Production of artificial fibers,” p. 1919, 1919.

[10] A. Formhals, “Artificial Fiber Construction,” pp. 1–28, 1956.

[11] A. Formhals, “Method and apparatus for the production of fibers_1,” 1936.

[12] A. Formhals, “Method and apparatus for the production of fibers_2,” 1936.

[13] A. Formhals, “Method of producing artificial fibers,” 1939.

[14] A. Formhals, “Method and apparatus for the production of artificial fibers,” pp. 1–8, 1939.

[15] A. Formhals, “Artificial thread and method of producing same,” 1940.

[16] A. Formhals, “Production of artificial fibers from fiber forming liquids,” 1943.

[17] A. Formhals, “Method and apparatus for spinning_1,” 1939.

[18] A. Formhals, “Method and apparatus for spinning_2,” 1944.

[19] R. Society and P. Sciences, “The Oscillations of the Atmosphere Author (s): G . I . Taylor Source : Proceedings of the Royal Society of London . Series A , Mathematical and Physical Published by : Royal Society Stable URL : http://www.jstor.org/stable/96596,” vol. 156, no. 888, pp. 318–326, 2017.

[20] B. L. and J. W. D. Annis, A. Bornat, O. Edwards, A. Higham, “An elastomeric vascular prosthesis.” 1978.

[21] D. H. Reneker and A. L. Yarin, “Electrospinning jets and polymer nanofibers,” *Polymer (Guildf).*, vol. 49, no. 10, pp. 2387–2425, 2008.

[22] D. H. Reneker, A. L. Yarin, H. Fong, and S. Koombhongse, “Bending instability of electrically charged liquid jets of polymer solutions in electrospinning,” *J. Appl. Phys.*, vol. 87, no. 9, pp. 4531–4547, 2000.

[23] P. Bébin and R. E. Prud’Homme, “Flat polymer ribbons and other shapes by electrospinning,” *J. Polym. Sci. Part B Polym. Phys.*, vol. 39, no. 1, pp. 2363–2377, 2001.

[24] C. J. Thompson, G. G. Chase, A. L. Yarin, and D. H. Reneker, “Effects of parameters on nanofiber diameter determined from electrospinning model,” *Polymer (Guildf).*, vol. 48, no. 23, pp. 6913–6922, 2007.

[25] Y. Qin, “Some fascinating phenomena in electrospinning processes and applications of electrospun nanofibers,” *Polym. Int.*, vol. 57, no. April, pp. 171–180, 2008.

[26] J. J. Feng, “The stretching of an electrified non-Newtonian jet: A model for electrospinning,” *Phys. Fluids*, vol. 14, no. 11, pp. 3912–3926, 2002.

[27] D. Lukas, A. Sarkar, and P. Pokorny, “Self-organization of jets in electrospinning from free liquid surface: A generalized approach,” *J. Appl. Phys.*, vol. 103, no. 8, pp. 1–7, 2008.

[28] A. H. Nurfaizey, J. Stanger, N. Tucker, N. Buunk, A. Wallace, and M. P. Staiger, “Manipulation of electrospun fibres in flight: The principle of superposition of electric fields as a control method,” *J. Mater. Sci.*, vol. 47, no. 3, pp. 1156–1163, 2012.

[29] C. Vaquette and J. Cooper-White, “The use of an electrostatic lens to enhance the efficiency of the electrospinning process,” *Cell Tissue Res.*, vol. 347, no. 3, pp. 815–826, 2012.

[30] N. Bhardwaj and S. C. Kundu, “Electrospinning: A fascinating fiber fabrication technique,” *Biotechnology Advances*, vol. 28, no. 3. pp. 325–347, Jan-2010.

[31] D. Liang, B. S. Hsiao, and B. Chu, “Functional electrospun nanofibrous scaffolds for biomedical applications,” *Adv. Drug Deliv. Rev.*, vol. 59, no.

14, pp. 1392–1412, 2007.

[32] T. J. Sill and H. A. von Recum, “Electrospinning: Applications in drug delivery and tissue engineering,” *Biomaterials*, vol. 29, no. 13, pp. 1989–2006, 2008.

[33] S. Chew, Y. Wen, Y. Dzenis, and K. Leong, “The Role of Electrospinning in the Emerging Field of Nanomedicine,” *Curr. Pharm. Des.*, vol. 12, no. 36, pp. 4751–4770, 2006.

[34] G. Taylor, “Electrically Driven Jets,” *Proc. R. Soc. A Math. Phys. Eng. Sci.*, vol. 313, no. 1515, pp. 453–475, 1969.

[35] A. L. Yarin, S. Koombhongse, and D. H. Reneker, “Bending instability in electrospinning of nanofibers,” *J. Appl. Phys.*, vol. 89, no. 5, pp. 3018–3026, 2001.

[36] E. Adomavičiūtė, “The Influence of Applied Voltage on Poly (vinyl alcohol) (PVA) Nanofibre Diameter,” *Europe*, vol. 15, no. 5, pp. 69–72, 2007.

[37] S. Kidoaki, I. K. Kwon, and T. Matsuda, “Mesoscopic spatial designs of nano- and microfiber meshes for tissue-engineering matrix and scaffold based on newly devised multilayering and mixing electrospinning techniques,” *Biomaterials*, vol. 26, no. 1, pp. 37–46, 2005.

[38] Y. A. Wang, X. Yu, P. M. Silverman, R. L. Harris, and H. Edward, “Microintegrating smooth muscle cells into a biodegradable, elastomeric fiber matrix,” vol. 385, no. 1, pp. 22–29, 2010.

[39] J. Doshi and D. H. Reneker, “Electrospinning process and applications of electrospun fibers,” *Conf. Rec. 1993 IEEE Ind. Appl. Conf. Twenty-Eighth*

IAS Annu. Meet., vol. 35, pp. 151–160, 1993.

[40] J. S. Kim and D. H. Reneker, “Mechanical properties of composites using ultrafine electrospun fibers,” *Polym. Compos.*, vol. 20, no. 1, pp. 124–131, 1999.

[41] V. M. Tysseling-mattiace *et al.*, “Self-Assembling Nanofibers Inhibit Glial Scar Formation and Promote Axon Elongation after Spinal Cord Injury,” *J Neurosci*, vol. 28, no. 14, pp. 3814–3823, 2009.

[42] K. C. Gupta, A. Haider, Y. Choi, and I. Kang, “Nanofibrous scaffolds in biomedical applications,” *Biomater. Res.*, vol. 18, no. 1, p. 5, 2014.

[43] A. Haider, S. Haider, and I. K. Kang, “A comprehensive review summarizing the effect of electrospinning parameters and potential applications of nanofibers in biomedical and biotechnology,” *Arabian Journal of Chemistry*, King Saud University, 2015.

[44] A. Haider, K. C. Gupta, and I. K. Kang, “Morphological effects of HA on the cell compatibility of electrospun HA/PLGA composite nanofiber scaffolds,” *Biomed Res. Int.*, vol. 2014, 2014.

[45] R. Vasita and D. S. Katti, “Nanofibers and their applications in tissue engineering,” *International Journal of Nanomedicine*, vol. 1, no. 1. pp. 15–30, 2006.

[46] W. J. Li, C. T. Laurencin, E. J. Caterson, R. S. Tuan, and F. K. Ko, “Electrospun nanofibrous structure: A novel scaffold for tissue engineering,” *J. Biomed. Mater. Res.*, vol. 60, no. 4, pp. 613–621, 2002.

[47] B. Sun *et al.*, “Advances in three-dimensional nanofibrous macrostructures

via electrospinning," *Progress in Polymer Science*, vol. 39, no. 5. pp. 862–890, 2014.

[48] M. Moffa *et al.*, "Microvascular endothelial cell spreading and proliferation on nanofibrous scaffolds by polymer blends with enhanced wettability," *Soft Matter*, vol. 9, no. 23, p. 5529, 2013.

[49] E. R. Kenawy *et al.*, "Release of tetracycline hydrochloride from electrospun poly(ethylene-co-vinylacetate), poly(lactic acid), and a blend," *J. Control. Release*, vol. 81, no. 1–2, pp. 57–64, 2002.

[50] P. Tipduangta *et al.*, "Electrospun Polymer Blend Nanofibers for Tunable Drug Delivery: The Role of Transformative Phase Separation on Controlling the Release Rate," *Mol. Pharm.*, vol. 13, no. 1, pp. 25–39, 2016.

[51] S. Mitragotri, P. A. Burke, and R. Langer, "Overcoming the challenges in administering biopharmaceuticals: formulation and delivery strategies," *Nat. Rev. Drug Discov.*, vol. 13, no. 9, pp. 655–672, 2014.

[52] W. Liu, S. Thomopoulos, and Y. Xia, "Electrospun nanofibers for regenerative medicine," *Adv. Healthc. Mater.*, vol. 1, no. 1, pp. 10–25, 2012.

[53] T. M. Allen, "Drug Delivery Systems: Entering the Mainstream," *Science (80-.).*, vol. 303, no. 5665, pp. 1818–1822, 2004.

[54] D. G. Yu, X. Y. Li, X. Wang, J. H. Yang, S. W. A. Bligh, and G. R. Williams, "Nanofibers Fabricated Using Triaxial Electrospinning as Zero Order Drug Delivery Systems," *ACS Appl. Mater. Interfaces*, vol. 7, no. 33, pp. 18891–

18897, 2015.

[55] W. Li, T. Luo, Y. Yang, X. Tan, and L. Liu, “Formation of controllable hydrophilic/hydrophobic drug delivery systems by electrospinning of vesicles,” *Langmuir*, vol. 31, no. 18, pp. 5141–5146, 2015.

[56] P. Martin, “Wound Healing--Aiming for Perfect Skin Regeneration,” *Science (80-.).*, vol. 276, no. 5309, pp. 75–81, 1997.

[57] Y. Gao, Y. B. Truong, Y. Zhu, and I. Louis Kyratzis, “Electrospun antibacterial nanofibers: Production, activity, and in vivo applications,” *J. Appl. Polym. Sci.*, vol. 131, no. 18, pp. 9041–9053, 2014.

[58] A. GhavamiNejad *et al.*, “Mussel-Inspired Electrospun Nanofibers Functionalized with Size-Controlled Silver Nanoparticles for Wound Dressing Application,” *ACS Appl. Mater. Interfaces*, vol. 7, no. 22, pp. 12176–12183, 2015.

[59] N. M. Aruan, I. Sriyanti, D. Edikresnha, T. Suciati, M. M. Munir, and K. Khairurrijal, “Polyvinyl Alcohol/Soursop Leaves Extract Composite Nanofibers Synthesized Using Electrospinning Technique and their Potential as Antibacterial Wound Dressing,” *Procedia Eng.*, vol. 170, pp. 31–35, 2017.

[60] A. Dwevedi, *Enzyme immobilization: Advances in industry, agriculture, medicine, and the environment*. 2016.

[61] Z. G. Wang, L. S. Wan, Z. M. Liu, X. J. Huang, and Z. K. Xu, “Enzyme immobilization on electrospun polymer nanofibers: An overview,” *Journal of Molecular Catalysis B: Enzymatic*, vol. 56, no. 4. pp. 189–195, 2009.

[62] M. R. El-Aassar, “Functionalized electrospun nanofibers from poly (AN-co-MMA) for enzyme immobilization,” *J. Mol. Catal. B Enzym.*, vol. 85–86, pp. 140–148, 2013.

[63] C. Tang, C. D. Saquing, S. W. Morton, B. N. Glatz, R. M. Kelly, and S. A. Khan, “Cross-linked polymer nanofibers for hyperthermophilic enzyme immobilization: Approaches to improve enzyme performance,” *ACS Appl. Mater. Interfaces*, vol. 6, no. 15, pp. 11899–11906, 2014.

[64] L. A. Mercante, V. P. Scagion, F. L. Migliorini, L. H. C. Mattoso, and D. S. Correa, “Electrospinning-based (bio)sensors for food and agricultural applications: a review,” *Trends Anal. Chem.*, vol. 91, p. 2017, 2017.

[65] R. Rapini and G. Marrazza, “Biosensor Potential in Pesticide Monitoring,” *Compr. Anal. Chem.*, vol. 74, pp. 3–31, 2016.

[66] G. H. Kim, S. H. Park, M. S. Birajdar, J. Lee, and S. C. Hong, “Core/shell structured carbon nanofiber/platinum nanoparticle hybrid web as a counter electrode for dye-sensitized solar cell,” *J. Ind. Eng. Chem.*, vol. 52, pp. 211–217, 2017.

[67] S. H. Hwang, C. Kim, H. Song, S. Son, and J. Jang, “Designed architecture of multiscale porous TiO 2 nanofibers for dye-sensitized solar cells photoanode,” *ACS Appl. Mater. Interfaces*, vol. 4, no. 10, pp. 5287–5292, 2012.

[68] M. Fathy, A. B. Kashyout, J. El Nady, S. Ebrahim, and M. B. Soliman, “Electrospun polymethylacrylate nanofibers membranes for quasi-solid-state dye sensitized solar cells,” *Alexandria Eng. J.*, vol. 55, no. 2, pp.

1737–1743, 2016.

[69] H. Ning *et al.*, “Electrospinning ZnO/carbon nanofiber as binder-free and self-supported anode for Li-ion batteries,” *J. Alloys Compd.*, vol. 722, pp. 716–720, 2017.

[70] C. Liu *et al.*, “Microporous carbon nanofibers prepared by combining electrospinning and phase separation methods for supercapacitor,” *J. Energy Chem.*, vol. 25, no. 4, pp. 587–593, 2016.

[71] Y. E. Miao, W. Fan, D. Chen, and T. Liu, “High-performance supercapacitors based on hollow polyaniline nanofibers by electrospinning,” *ACS Appl. Mater. Interfaces*, vol. 5, no. 10, pp. 4423–4428, 2013.

[72] M. Kim *et al.*, “Electrochemical improvement due to alignment of carbon nanofibers fabricated by electrospinning as an electrode for supercapacitor,” *Carbon N. Y.*, vol. 99, pp. 607–618, 2016.

[73] M. Salahuddin, M. N. Uddin, G. Hwang, and R. Asmatulu, “Superhydrophobic PAN nanofibers for gas diffusion layers of proton exchange membrane fuel cells for cathodic water management,” *Int. J. Hydrogen Energy*, pp. 1–9, 2017.

[74] J. B. Ballengee and P. N. Pintauro, “Composite fuel cell membranes from dual-nanofiber electrospun mats,” *Macromolecules*, vol. 44, no. 18, pp. 7307–7314, 2011.

[75] M. Wei, M. Jiang, X. Liu, M. Wang, and S. Mu, “Graphene-doped electrospun nanofiber membrane electrodes and proton exchange

membrane fuel cell performance," *J. Power Sources*, vol. 327, pp. 384–393, 2016.

[76] A. D. Taylor, M. Michel, R. C. Sekol, J. M. Kizuka, N. A. Kotov, and L. T. Thompson, "Fuel cell membrane electrode assemblies fabricated by layer-by-layer electrostatic self-assembly techniques," *Adv. Funct. Mater.*, vol. 18, no. 19, pp. 3003–3009, 2008.

[77] Z. Zhou *et al.*, "Development of carbon nanofibers from aligned electrospun polyacrylonitrile nanofiber bundles and characterization of their microstructural, electrical, and mechanical properties," *Polymer (Guildf).*, vol. 50, no. 13, pp. 2999–3006, 2009.

[78] C. E. Schildknecht, "Polyvinyl alcohol, properties and applications, C. A. Finch, Wiley, New York, 1973. 622 pp. $37.50," *J. Polym. Sci. Polym. Lett. Ed.*, vol. 12, no. 2, pp. 105–106, Feb. 1974.

[79] Y. Liang *et al.*, "Preparation and electrochemical characterization of ionic-conducting lithium lanthanum titanate oxide/polyacrylonitrile submicron composite fiber-based lithium-ion battery separators," *J. Power Sources*, vol. 196, no. 1, pp. 436–441, 2011.

[80] M. S. A. Rahaman, A. F. Ismail, and A. Mustafa, "A review of heat treatment on polyacrylonitrile fiber," *Polym. Degrad. Stab.*, vol. 92, no. 8, pp. 1421–1432, 2007.

[81] and N. A. K. K. E. Perepelkin, N. V. Klyuchnikova, "Experimental evaluation of man-made fibre brittleness," no. 2, pp. 36–37, 2000.

[82] A. D. Litmanovich and N. Platé, "Alkaline hydrolysis of polyacrylonitrile. On

the reaction mechanism," *Macromol. Chem. Phys.*, vol. 201, no. 16, pp. 2176–2180, 2000.

[83] M. Inagaki, K. Kaneko, and T. Nishizawa, "Nanocarbons - Recent research in Japan," *Carbon N. Y.*, vol. 42, no. 8–9, pp. 1401–1417, 2004.

[84] D. Li, J. T. McCann, and Y. Xia, "Use of electrospinning to directly fabricate hollow nanofibers with functionalized inner and outer surfaces," *Small*, vol. 1, no. 1, pp. 83–86, 2005.

[85] H. D. Johnson, "Synthesis , Characterization , Processing and Physical Behavior of Melt-Processible Acrylonitrile Co- and Terpolymers for Carbon Fibers : Effect of Synthetic Variables on Copolymer Structure," p. 108, 2006.

[86] F. Publications, "correlating plastic shrinkage cracking potential of fiber reinforced cement composites with its early-age constitutive response in tension," vol. 24, no. April, pp. 80–94, 2014.

[87] A. M. Sarmadi, C. J. Noel, and J. B. Birch, "Effects of heat treatment on dyeability, glass transition temperature, and tensile properties of polyacrylonitrile fibers.," *Ind. Eng. Chem. Res.*, vol. 29, no. 8, pp. 1640–1646, 1990.

[88] R. B. Mathur, J. Mittal, O. P. Bahl, and N. K. Sandle, "Characteristics of KMnO4-modified PAN fibres-its influence on the resulting carbon fibres' properties," *Carbon N. Y.*, vol. 32, no. 1, pp. 71–77, 1994.

[89] F. Application *et al.*, "Carbon fibers and non-woven fabrics," vol. 35, no. 7, pp. 886–890, 1985.

[90] D. D. Edie, “The effect of processing on the structure and properties of carbon fibers,” *Carbon N. Y.*, vol. 36, no. 4, pp. 345–362, 1998.

[91] J. Mittal, R. B. Mathur, and O. P. Bahl, “Post spinning modification of PAN fibres — a review,” *Carbon N. Y.*, vol. 35, no. 12, pp. 1713–1721, 1997.

[92] C. Guo, L. Zhou, and J. Lv, “Investigating the jet stretch in the wet spinning of PAN fiber,” *Polym. Polym. Compos.*, vol. 21, no. 7, pp. 449–456, 2013.

[93] B. Rand, S. P. Appleyar, and M. F. Yardim., *Carbon fiber processing and structure/property relations*. .

[94] T. Kobashi and S. Takao, “High strength polyacrylonitrile fiber and method of producing the same,” no. 19, pp. 1–4, 1985.

[95] S.-J. Park, *Carbon Fibers*, vol. 210. 2015.

[96] R. K. Tubbs, “Sequence distribution of partially hydrolyzed poly(vinyl acetate),” *J. Polym. Sci. Part A-1 Polym. Chem.*, vol. 4, no. 3, pp. 623–629, Mar. 1966.

[97] H. O. F. Adhesives, *Poly(Vinyl Alcohol) for Adhesives*. .

[98] E. Da Silva, L. Lebrun, and M. Métayer, “Elaboration of a membrane with bipolar behaviour using the semi-interpenetrating polymer networks technique,” *Polymer (Guildf).*, vol. 43, no. 19, pp. 5311–5320, 2002.

[99] J. Wang, X. Wang, C. Xu, M. Zhang, and X. Shang, “Preparation of graphene/poly(vinyl alcohol) nanocomposites with enhanced mechanical properties and water resistance,” *Polym. Int.*, vol. 60, no. 5, pp. 816–822, 2011.

[100] T. S. Gaaz *et al.*, “Properties and applications of polyvinyl alcohol,

halloysite nanotubes and their nanocomposites," *Molecules*, vol. 20, no. 12, pp. 22833–22847, 2015.

[101] S. V.P, S. T. P, S. K.I, S. V, R. M.P, and R. Stephen, "Thermal properties of poly (vinyl alcohol)(PVA)/halloysite nanotubes reinforced nanocomposites," *Int. J. Plast. Technol.*, vol. 19, no. 1, pp. 124–136, 2015.

[102] R. Othman, A. L. Dicks, and Z. Zhu, "Non precious metal catalysts for the PEM fuel cell cathode," *Int. J. Hydrogen Energy*, vol. 37, no. 1, pp. 357–372, 2012.

[103] N. A. M. Barakat, M. A. Abdelkareem, A. Yousef, S. S. Al-Deyab, M. El-Newehy, and H. Y. Kim, "Cadmium-doped cobalt/carbon nanoparticles as novel nonprecious electrocatalyst for methanol oxidation," *Int. J. Hydrogen Energy*, vol. 38, no. 8, pp. 3387–3394, 2013.

[104] Z. Wen, J. Liu, and J. Li, "Core/shell Pt/C nanoparticles embedded in mesoporous carbon as a methanol-tolerant cathode catalyst in direct methanol fuel cells," *Adv. Mater.*, vol. 20, no. 4, pp. 743–747, 2008.

[105] N. Tsiouvaras, M. a Pen, J. L. G. Fierro, and F. Sa, "Novel Synthesis Method of CO-Tolerant PtRu - MoO x Nanoparticles : Structural Characteristics and Performance for Methanol Electrooxidation," no. 5, pp. 4249–4259, 2008.

[106] Y. H. Kwon, S. C. Kim, and S. Y. Lee, "Nanoscale phase separation of sulfonated poly(arylene ether sulfone)/poly(ether sulfone) semi-IPNs for DMFC membrane applications," *Macromolecules*, vol. 42, no. 14, pp. 5244–5250, 2009.

[107] H. An *et al.*, “Synthesis and performance of palladium-based catalysts for methanol and ethanol oxidation in alkaline fuel cells,” *Electrochim. Acta*, vol. 102, pp. 79–87, 2013.

[108] N. V. Long, Y. Yang, C. Minh Thi, N. Van Minh, Y. Cao, and M. Nogami, “The development of mixture, alloy, and core-shell nanocatalysts with nanomaterial supports for energy conversion in low-temperature fuel cells,” *Nano Energy*, vol. 2, no. 5, pp. 636–676, 2013.

[109] N. A. M. Barakat, M. A. Abdelkareem, and H. Y. Kim, “Ethanol electro-oxidation using cadmium-doped cobalt/carbon nanoparticles as novel non precious electrocatalyst,” *Appl. Catal. A Gen.*, vol. 455, pp. 193–198, 2013.

[110] B. M. Thamer, M. H. El-Newehy, S. S. Al-Deyab, M. A. Abdelkareem, H. Y. Kim, and N. A. M. Barakat, “Cobalt-incorporated, nitrogen-doped carbon nanofibers as effective non-precious catalyst for methanol electrooxidation in alkaline medium,” *Appl. Catal. A Gen.*, vol. 498, pp. 230–240, 2015.

[111] X. Mu, Z. Xu, Y. Xie, H. Mi, and J. Ma, “Pt nanoparticles supported on Co embedded coal-based carbon nanofiber for enhanced electrocatalytic activity towards methanol electro-oxidation,” *J. Alloys Compd.*, vol. 711, pp. 374–380, 2017.

[112] R. S. Anwane, S. B. Kondawar, and D. J. Late, “Bessel’s polynomial fitting for electrospun polyacrylonitrile/polyaniline blend nanofibers based ammonia sensor,” *Mater. Lett.*, 2018.

[113] A. M. Al-Enizi *et al.*, “Synthesis and electrochemical properties of nickel oxide/carbon nanofiber composites,” *Carbon N. Y.*, vol. 71, pp. 276–283,

2014.

[114] W. S. Hummers and R. E. Offeman, “Preparation of Graphitic Oxide,” *J. Am. Chem. Soc.*, vol. 80, no. 6, p. 1339, 1958.

[115] D. H. Reneker and L. Chun, “Nanometre diameters of polymer, produced by electrospinning,” *Nanotechnology*, vol. 7, pp. 216–223, 1996.

[116] C. J. Uchko, L. C. Chen, Y. Shen, and D. C. Martina, “Processing and microstructural characterization of porous biocompatible\rprotein polymer thin films,” *Polymer (Guildf).*, vol. 40, pp. 7397–7407, 1999.

[117] K. H. Lee, H. Y. Kim, H. J. Bang, Y. H. Jung, and S. G. Lee, “The change of bead morphology formed on electrospun polystyrene fibers,” *Polymer (Guildf).*, vol. 44, no. 14, pp. 4029–4034, 2003.

[118] P. Supaphol, C. Mit-Uppatham, and M. Nithitanakul, “Ultrafine electrospun polyamide-6 fibers: Effect of emitting electrode polarity on morphology and average fiber diameter,” *J. Polym. Sci. Part B Polym. Phys.*, vol. 43, no. 24, pp. 3699–3712, 2005.

[119] C. M. Hsu and S. Shivkumar, “Nano-sized beads and porous fiber constructs of Poly(ε-caprolactone) produced by electrospinning,” *J. Mater. Sci.*, vol. 39, no. 9, pp. 3003–3013, 2004.

[120] T. Jarusuwannapoom *et al.*, “Effect of solvents on electro-spinnability of polystyrene solutions and morphological appearance of resulting electrospun polystyrene fibers,” *Eur. Polym. J.*, vol. 41, no. 3, pp. 409–421, 2005.

[121] H. Fong, I. Chun, and D. H. Reneker, “Beaded nanofibers formed during

electrospinning," *Polymer (Guildf).*, vol. 40, no. 16, pp. 4585–4592, 1999.

[122] J. . Deitzel, J. Kleinmeyer, D. Harris, and N. . Beck Tan, "The effect of processing variables on the morphology of electrospun nanofibers and textiles," *Polymer (Guildf).*, vol. 42, no. 1, pp. 261–272, 2001.

[123] M. M. Demir, I. Yilgor, E. Yilgor, and B. Erman, "Electrospinning of polyurethane fibers," *Polymer (Guildf).*, vol. 43, no. 11, pp. 3303–3309, 2002.

[124] P. K. Baumgarten, "Electrostatic spinning of acrylic microfibers," *J. Colloid Interface Sci.*, vol. 36, no. 1, pp. 71–79, 1971.

[125] X. Zong, K. Kim, D. Fang, S. Ran, B. S. Hsiao, and B. Chu, "Structure and process relationship of electrospun bioabsorbable nanofiber membranes," *Polymer (Guildf).*, vol. 43, no. 16, pp. 4403–4412, 2002.

[126] C. Zhang, X. Yuan, L. Wu, Y. Han, and J. Sheng, "Study on morphology of electrospun poly(vinyl alcohol) mats," *Eur. Polym. J.*, vol. 41, no. 3, pp. 423–432, 2005.

[127] C. S. Ki, D. H. Baek, K. D. Gang, K. H. Lee, I. C. Um, and Y. H. Park, "Characterization of gelatin nanofiber prepared from gelatin-formic acid solution," *Polymer (Guildf).*, vol. 46, no. 14, pp. 5094–5102, 2005.

[128] J. S. Lee *et al.*, "Role of molecular weight of atactic poly(vinyl alcohol) (PVA) in the structure and properties of PVA nanofabric prepared by electrospinning," *J. Appl. Polym. Sci.*, vol. 93, no. 4, pp. 1638–1646, 2004.

[129] Z. Zhao, J. Li, X. Yuan, X. Li, Y. Zhang, and J. Sheng, "Preparation and properties of electrospun poly(vinylidene fluoride) membranes," *J. Appl.*

Polym. Sci., vol. 97, no. 2, pp. 466–474, 2005.

[130] Q. P. Pham, U. Sharma, and A. G. Mikos, “Electrospinning of Polymeric Nanofibers for Tissue Engineering Applications: A Review,” *Tissue Eng.*, vol. 0, no. 0, p. 60509065116001, 2006.

[131] S. Ramakrishna, “INTRODUCTION TO ELECTROSPINNING AND NANOFIBERS,” in *Electrospinning for Tissue Regeneration*, Elsevier, 2005, pp. 3–33.

[132] S. Zhao, X. Wu, L. Wang, and Y. Huang, “Electrospinning of ethyl-cyanoethyl cellulose/tetrahydrofuran solutions,” *J. Appl. Polym. Sci.*, vol. 91, no. 1, pp. 242–246, 2004.

[133] A. M. Al-Enizi, A. A. Elzatahry, A. M. Abdullah, A. Vinu, H. Lwai, and S. S. Al-Deyab, “Preparation and Characterization of Nano-Composite Materials for Industrial Applications,” 2013.

[134] H. K. Shin, M. Park, H. Y. Kim, and S. J. Park, “Influence of orientation on ordered microstructure of PAN-based fibers during electron beam irradiation stabilization,” *J. Ind. Eng. Chem.*, vol. 32, pp. 120–122, 2015.

[135] F. Miao *et al.*, “Flexible solid-state supercapacitors based on freestanding electrodes of electrospun polyacrylonitrile@polyaniline core-shell nanofibers,” *Electrochim. Acta*, vol. 176, pp. 293–300, 2015.

[136] X. Qian, R. Zou, Q. OuYang, X. Wang, and Y. Zhang, “Surface structural evolvement in the conversion of polyacrylonitrile precursors to carbon fibers,” *Appl. Surf. Sci.*, vol. 327, pp. 246–252, 2015.

[137] R. X. Zhao *et al.*, “Influence of heating procedures on the surface structure

of stabilized polyacrylonitrile fibers," *Appl. Surf. Sci.*, vol. 433, pp. 321–328, 2018.

[138] X. Mu, Z. Xu, Y. Ma, Y. Xie, H. Mi, and J. Ma, "Graphene-carbon nanofiber hybrid supported Pt nanoparticles with enhanced catalytic performance for methanol oxidation and oxygen reduction," *Electrochim. Acta*, vol. 253, pp. 171–177, 2017.

[139] A. Sharma and B. K. Lee, "Photocatalytic reduction of carbon dioxide to methanol using nickel-loaded TiO2supported on activated carbon fiber," *Catal. Today*, vol. 298, no. November 2016, pp. 158–167, 2017.

[140] T. V. Reshetenko *et al.*, "Multianalytical Study of the PTFE Content Local Variation of the PEMFC Gas Diffusion Layer," *J. Electrochem. Soc.*, vol. 160, no. 11, pp. F1305–F1315, 2013.

[141] M. Rethinasabapathy *et al.*, "Ternary PtRuFe nanoparticles supported N-doped graphene as an efficient bifunctional catalyst for methanol oxidation and oxygen reduction reactions," *Int. J. Hydrogen Energy*, vol. 42, no. 52, pp. 30738–30749, 2017.